

Grant Agreement Number:
641185

Action acronym:
CEMCAP

Action full title:
CO₂ capture from cement production

Type of action:
H2020-LCE-2014-2015/H2020-LCE-2014-1

Starting date of the action: 2015-05-01
Duration: 42 months

D12.3
**Calcium Looping CO₂ capture for the cement industry –
Demonstration of fluidized bed CaL at 200 kW scale and
research on entrained flow CaL**

Due delivery date: 2017-12-31
Actual delivery date: 2017-12-15

Organization name of lead participant for this deliverable:
University of Stuttgart

| Project co-funded by the European Commission within Horizon2020 | | |
|---|---|---|
| Dissemination Level | | |
| PU | Public | X |
| CO | Confidential , only for members of the consortium (including the Commission Services) | |

| | |
|----------------------------|---|
| Deliverable number: | D12.3 |
| Deliverable title: | Calcium Looping CO ₂ capture for the cement industry – Demonstration of fluidized bed CaL at 200 kW scale and research on entrained flow CaL |
| Work package: | WP 12 Calcium looping (CaL) capture |
| Lead participant: | USTUTT |

| Author(s) | | |
|----------------------|--------------|--|
| Name | Organisation | E-mail |
| Matthias Hornberger* | USTUTT | matthias.hornberger@ifk.uni-stuttgart.de |
| Borja Arias | CSIC | borja@incar.csic.es |
| Sandra Turrado | CSIC | s.turrado@incar.csic.es |
| Carlos Abanades | CSIC | abanades@incar.csic.es |
| Reinhold Spörl | USTUTT | reinhold.spoerl@ifk.uni-stuttgart.de |

*Lead author

| Keywords |
|---|
| Calcium Looping, CO ₂ capture, CaL, semi industrial scale, fluidized bed, entrained flow, cement, CCS, demonstration |

| Abstract |
|--|
| <p>In this report, the findings of experimental research regarding Calcium Looping CO₂ capture for the cement industry are presented. The Calcium Looping process using the fluidized bed technology was demonstrated at semi-industrial scale at USTUTT's 200 kW_{th} Calcium Looping pilot facility investigating comprehensively a field of operation conditions relevant to the technology's application in the clinker production process, such as high make-up ratios up to 1 mol_{CaO}/mol_{CO₂}, CO₂ concentrations up to 33 vol%_{wet}, carbonator temperatures between 600 to 710 °C, looping ratios up to 20 mol_{CaO}/mol_{CO₂}, two different reactor configurations (CFB-CFB and BFB-CFB) and two limestone qualities. CO₂ capture applying an alternative Calcium Looping concept using entrained flow reactors has been investigated at CSIC's electrically heated drop tube reactor.</p> <p>High CO₂ capture rates in the carbonator (up to 98 %) have been demonstrated at industrially relevant conditions (TRL6). The high make-up ratios that are feasible when applying the Calcium Looping technology to the cement industry result in increased bed activity which enhances the CO₂ capture performance. The high make-up feed rates of uncalcined material require however the provision of an increased thermal power in the calciner compared to Calcium Looping systems for power plant application. This needs to be addressed by a suitable calciner design. Carbonator CO₂ capture rates of 90 % and above were achieved at carbonator temperatures below 650 °C and looping ratios above 8 mol_{CaO}/mol_{CO₂} for make-up ratios around 0.7 mol_{CaCO₃}/mol_{CO₂}. To reach the same capture rate with a make-up ratio of 0.2 mol_{CaCO₃}/mol_{CO₂}, a looping ratio of 10.5 mol_{CaO}/mol_{CO₂} was estimated.</p> <p>Regarding the experimental testing of CO₂ capture by CaO carbonation under entrained flow reactor conditions, CSIC has completed additional test campaigns measuring the extent of carbonation conversion in gas-solid contact time scales between 1-6 seconds at different concentrations of CO₂, carbonation temperatures, initial activity of the material and different types of CaO precursors. It has been confirmed that the carbonation reaction follows a pseudo-</p> |

homogeneous kinetic model, first order in respect to CO_2 , with a small positive effect of water vapour in the gas. The rate of reactions are shown to be linearly dependent of the CO_2 carrying capacity of the material, X_{ave} , irrespective of the nature of the calcined material. A first screening of calcination conditions in a TG apparatus, regarding this new important aspect identified during the CEMCAP project, was included in D12.2. The results in EF conditions presented in this report confirm that, in order to understand the progress of carbonation reaction in integrated CaL systems, it will be essential to anticipate the value of X_{ave} resulting after calcination, taking into account the competitive reactions (i.e. belite formation) that are present during calcination of cement raw meals and that tend to reduce X_{ave} .

Please cite this report as: *Hornberger, Matthias, Arias Borja, Turrado Sandra, Abanades Carlos, Spörl Reinhold, 2017. Calcium Looping CO₂ capture for the cement industry – Demonstration of fluidized bed CaL at 200 kW scale and research on entrained flow CaL (D12.3).*

Refer to the [CEMCAP community in Zenodo.org](https://zenodo.org/communities/CEMCAP) for citation with DOI.

TABLE OF CONTENTS

| | Page |
|--|------|
| 1 EXECUTIVE SUMMARY | 2 |
| 2 CALCIUM LOOPING CO ₂ CAPTURE..... | 5 |
| 3 EXPERIMENTAL FACILITIES | 7 |
| 3.1 USTUTT's fluidized bed pilot facility | 7 |
| 3.1.1 Measurement instrumentation | 9 |
| 3.1.2 Fuel and sorbent Properties | 10 |
| 3.1.3 Design of experiments | 12 |
| 3.2 CSIC's entrained flow facility..... | 13 |
| 4 EXPERIMENTAL RESULTS AND DISCUSSION..... | 15 |
| 4.1 Calcium Looping CO ₂ capture performance | 15 |
| 4.2 Demonstration of Calcium Looping CO ₂ capture under cement specific operation conditions | 17 |
| 4.2.1 Hydrodynamics..... | 19 |
| 4.2.2 Calciner operation..... | 22 |
| 4.2.3 Carbonator operation | 23 |
| 4.3 Characterization of Calcium Looping CO ₂ capture..... | 25 |
| 4.3.1 Influence of make-up rate | 25 |
| 4.3.2 Influence of looping ratio | 26 |
| 4.3.3 Influence of CO ₂ concentration in the flue gas..... | 28 |
| 4.3.4 Influence of Calcination temperature | 29 |
| 4.3.5 Influence of Carbonation temperature | 29 |
| 4.3.6 Sorbent CO ₂ carrying capacity | 30 |
| 4.3.7 Sorbent attrition | 31 |
| 4.3.8 Sorbent deposition | 32 |
| 4.4 Results on entrained flow carbonation conducted at CSIC | 34 |
| 4.4.1 Effect of average CO ₂ carrying capacity | 36 |
| 4.4.2 Effect of steam..... | 37 |
| 4.4.3 Effect of CO ₂ concentration..... | 38 |
| 5 SUMMARY AND CONCLUSIONS..... | 41 |
| 6 REFERENCES | 43 |

LIST OF ABBREBIATION

| | |
|------|-------------------------------|
| ASU | air separation unit |
| BFB | bubbling fluidized bed |
| CaL | Calcium Looping |
| CFB | circulating fluidized bed |
| TFB | turbulent fluidized bed |
| TIC | total inorganic carbon |
| TOC | total organic carbon |
| NDIR | nondispersive infrared sensor |
| LOI | loss on ignition |
| PSD | particle size distribution |

Chemical

| | |
|---------------------|-------------------|
| C | Carbon |
| CaO | Calcium oxide |
| CaCO ₃ | Calcium carbonate |
| Ca(OH) ₂ | Calcium hydroxide |
| CO | Carbon monoxide |
| CO ₂ | Carbon dioxide |
| H | Hydrogen |
| H ₂ O | Water / steam |
| MgCO ₃ | Magnesium oxide |
| N | Nitrogen |
| NO _x | Nitrogen oxides |
| O | Oxygen |
| O ₂ | Oxygen (moleular) |
| S | Sulfur |
| SiO ₂ | Silicon dioxide |
| SO ₂ | Sulfur dioxide |

Symbols

| | |
|----------------|-------------------------------------|
| H _i | lower heating value |
| Q ₃ | cumulative volume/mass distribution |
| q ₃ | volume/mass distribution density |

1 EXECUTIVE SUMMARY

Within WP12, two different Calcium Looping process schemes for CO₂ capture from clinker manufacturing have been developed and investigated. The so called tail-end option in which a standalone post-combustion Calcium Looping CO₂ capture unit is employed after the preheater tower of the clinker production plant and a so called integrated Calcium Looping option in which the Calcium Looping process is installed directly after the rotary kiln. In the tail-end option, a share of CaCO₃ required for clinker production serves as the sorbent in the Calcium Looping process. The purge (spent sorbent) in this configuration is then cooled, milled, mixed with the other raw meal components and then fed to the cement plant's preheater tower. In this and other CEMCAP reports, the term integration level is used in this context to describe the share of CaCO₃ being fed to the Calcium Looping system in respect to the total amount of CaCO₃ required for clinker manufacturing.

The integrated Calcium Looping option calcines the complete amount of CaCO₃ required for clinker production. Therefore, two thirds of the cement plants CO₂ emissions are directly captured in the Calcium Looping's oxy-fuel calciner and the carbonator treats only the kiln flue gas. Clinker production requires the raw meal/raw material particles to be relatively finely milled, to allow for a good mixing of solid particles and an efficient formation of clinker phases. If the Calcium Looping process can be operated with such fine materials, additional requirements for cooling, milling and reheating of the material exiting the Calcium Looping system before being sent to the rotary kiln can be avoided. For utilization of materials with such a small particle size in the integrated Calcium Looping configuration, particularly entrained flow reactor systems may be suitable. However, also fluidized bed reactor systems may be applied, potentially requiring an additional cooling and milling step if particle sizes are too coarse for direct utilization in the clinker burning process.

With increasing integration level, the sorbent activity will improve and simultaneously the flue gas CO₂ concentration will reduce since a larger share of the raw meal is already calcined by the Calcium Looping process and does therefore reduce the requirement for raw meal calcination in the conventional clinker manufacturing process. While the tail-end option is relatively easy to retrofit to an existing clinker production plant, its energetic efficiency of the CO₂ capture is reduced compared to the integrated Calcium Looping configuration that is more challenging to implement into an existing cement plant [1].

Within the activities of CEMCAP's work package 12, the experimental facilities at CSIC and USTUTT have been modified to meet the requirements for investigation of the Calcium Looping process under cement specific conditions. Furthermore, at CSIC the electrically heated Calcium Looping test facility was restructured to investigate CO₂ capture under entrained flow conditions and in particular, a suitable dosing system for fine particles has been developed and commissioned. Experimental studies on Calcium Looping application to the clinker manufacturing process are reported in this and two other deliverable reports (D12.1 and D12.2). This report (D12.3) summarizes the Calcium Looping research conducted by USTUTT in pilot scale, but also includes experimental work conducted by CSIC after the completion of D12.2. The following shall give an orientation about the experimental activities at different facilities and scales at both institutes and the available research reports: Calcium Looping using fluidized bed technology has been investigated at CSIC's 30 kW facility, screening various parameters relevant to the Calcium Looping application in clinker manufacturing. At USTUTT's Calcium Looping pilot plant, this fluidized bed process has been demonstrated at semi-industrial scale over a wide range of operational parameters. This work is summarized in this deliverable report (D12.3). The entrained flow Calcium Looping configuration was investigated using two different electrically heated facilities at USTUTT (entrained flow oxy-fuel calcination) and CSIC (entrained flow

carbonation). Furthermore, TGA experiments were conducted by CSIC to analyze different limestone and raw meal qualities with respect to their CO₂ capture performance after calcination. All activities were supported by and interacting with process modelling and simulation studies conducted by Politecnico di Milano (PoliMi) (see also D12.4). The results regarding the fluidized bed experiments conducted by CSIC in a 30 kW facility, were already reported in D12.1. In addition to that, deliverable D12.2 covers TGA analyses of different limestone and raw meal qualities as well as first experiments conducted by CSIC on entrained flow carbonation. Research on entrained flow oxy-fuel calcination by USTUTT are reported in Deliverable 8.2.

In the fluidized bed Calcium Looping demonstration activities in a semi-industrial scale 200 kW_{th} pilot plant of USTUTT, five experimental campaigns were conducted. These test campaigns covered the field of operational conditions relevant to the Calcium Looping technology's application in the clinker production process comprehensively, investigating parameters such as high make-up ratios up to 1 mol_{CaO}/mol_{CO₂}, CO₂ concentrations up to 33 vol%_{wet}, carbonator temperatures between 600 to 710 °C, and looping ratios up to 20 mol_{CaO}/mol_{CO₂}. Two different reactor configurations, a CFB carbonator coupled with a CFB calciner as well as a BFB carbonator coupled with a CFB calciner were tested. These experiments demonstrate that CO₂ capture from the clinker production process by Calcium Looping using fluidized bed reactors is a very promising configuration for this CO₂ capture process, with high CO₂ capture rates (up to 98 %) that have been demonstrated in pilot scale. The high make-up ratios that are feasible when applying the Calcium Looping technology to the cement industry result in an increased bed activity that enhanced the CO₂ capture performance. The sorbent's CO₂ carrying capacity increased up to 4 times when the make-up ratio was increased from 0.25 mol_{CaCO₃}/mol_{CO₂} to 0.7 mol_{CaCO₃}/mol_{CO₂}.

The high make-up feed rates of uncalcined material require the provision of an increased thermal power in the Calcium Looping calciner compared to Calcium Looping systems for power plant application. This needs to be addressed by a suitable calciner design allowing for higher thermal power of this unit or at a fixed calciner geometry by adjusting the calciner operation conditions. For the conducted pilot scale experiments this issue was addressed by increasing the oxygen content of the calciner's fluidization gas up to 53 vol%_{wet}. The plant could be safely operated without temperature peaks along the calciner height that would cause excessive sorbent deactivation and without other operational problems under these conditions. Also an operation with even higher oxygen concentrations may be feasible, additionally reducing the recycle line's size and energy consumption.

During the pilot scale tests, a significant reduction of fluidization gas flow rate in the carbonator was observed when operating with increased CO₂ flue gas concentration, that needs to be considered when designing this kind of reactors for back-end Calcium Looping systems to be used in clinker production plants. This reduction of volumetric flow is caused by the CO₂ capture that removes up to about one third of the flue gas flow of typical cement plants which is much more than in power plant Calcium Looping applications (approx. 15 % volume reduction). Therefore, the carbonator reactor design should be tailored precisely to the flue gases' CO₂ content, since a lack of fluidization gas effects the entrainment of solids and consequently the Calcium Looping process operation and performance.

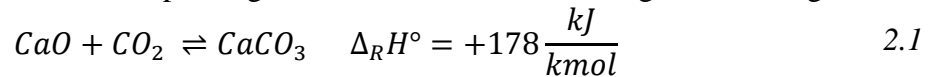
During USTUTT's 200 kW_{th} pilot scale tests, sorbent attrition has been assessed using two different limestone qualities. Loss of sorbent by attrition did not affect the Calcium Looping operation negatively. Moreover, increased sorbent attrition would be tolerable or in certain limits even beneficial to a Calcium Looping system applied to a clinker manufacturing process, since this can be compensated by an increase in the make-up feed rate and the utilization of the attrited fines in the clinker production. The results obtained through USTUTT's research will also be published in an open-access scientific journal paper.

Experiments (in addition to the ones reported in D12.2) on an entrained flow Calcium Looping reactor concept were conducted by CSIC in an electrically heated drop tube reactor/carbonator. In these tests, the extent of carbonation conversion in time scales for gas-solid contact between 1-6 seconds at different concentrations of CO₂, different carbonation temperatures and initial activities of the material and different types of CaO precursors was studied. The results obtained from these tests conducted at CSIC's 30 kW_{th} entrained flow carbonator indicate that the carbonation reaction in that system follows a pseudo-homogeneous kinetic model, first order in respect to CO₂, with a small positive effect of steam in the gas. The rate of reactions are shown to be linearly dependent on the CO₂ carrying capacity of the sorbent (X_{ave}), irrespective of the nature of the calcined material. Apparent reaction rate constants have been calculated (referring to the active fraction of the material only) which are consistent with the lower range of values reported in the literature for other CaL applications, probably reflecting on some gas-solid contact inefficiencies in the lab scale experimental set up. Overall, it is concluded that the X_{ave} resulting after calcination, taking into account the competitive reactions that are present during calcination of raw meals and mixtures of Si and Ca compounds (i.e. belite formation), is the crucial parameter that has to be evaluated for the process specific calcination conditions in an integrated CaL system. The remaining variables affecting carbonation rates remain roughly identical to those present in other CaL systems. An open access scientific journal paper is planned to disclose these results.

Within the CEMCAP project the Calcium Looping technology for CO₂ capture from cement plants using fluidized bed reactors has been demonstrated at industrially relevant conditions over a wide range of parameters, yielding very high CO₂ capture efficiencies (up to 98%). Thus, for this Calcium Looping process configuration, a TRL of 6 is reached. The less mature Calcium Looping concept using entrained flow reactors proved to be a promising technology. However, further research is required (e.g. in respect to the CO₂ capture activity of calcined raw meal based sorbent materials) to increase the maturity level of this technology before its commercial application for CO₂ capture from clinker manufacturing.

2 CALCIUM LOOPING CO₂ CAPTURE

The Calcium Looping process is a high temperature carbon capture process based on the cyclic calcination and carbonation of a calcium containing sorbent – generally limestone (CaCO₃). The process is based on the reversible reaction of calcium oxide (CaO) and carbon dioxide (CO₂) to calcium carbonate (CaCO₃) (cf. eq. 2.1). By means of cyclic carbonation and calcination (or regeneration) of the sorbent a CO₂ depleted gas stream and a CO₂ enriched gas stream is generated.



A general scheme of the Calcium Looping CO₂ capture process is shown in Figure 2.1. CO₂ is captured in the so called carbonator by the forward exothermic reaction (carbonation reaction) depleting the entering flue gas from CO₂. By the means of a circulating solid the CO₂ is transported into a second reactor (calciner or regenerator) where the loaded sorbent is regenerated by the backward endothermic reaction (calcination reaction). Usually, the Calcium Looping process is operated in a dual fluidized bed system due to the good gas solid contact of fluidized bed reactors. However, entrained flow reactors may also be applied. The operation conditions of the Calcium Looping process are specified by the calcination carbonation equilibrium (shown in Figure 2.2). In order to produce a high concentrated CO₂ stream the calciner is operated under oxy-fuel conditions e.g. high CO₂ partial pressure. To ensure proper calcination or regeneration of the sorbent temperatures above 900 °C are required (red range). The energy required for the endothermic calcination is provided by the combustion of an auxiliary fuel. Whereas, high capture rates in the carbonator e.g. low CO₂ partial pressure require temperature at least below 700 °C (blue range).

One of the main advantages of the Calcium Looping process is its energy efficiency. Due to the high reactor temperatures of 650 °C and 920 °C respectively the required energy can be recuperated by an efficient critical steam cycle commonly applied in power plant applications.

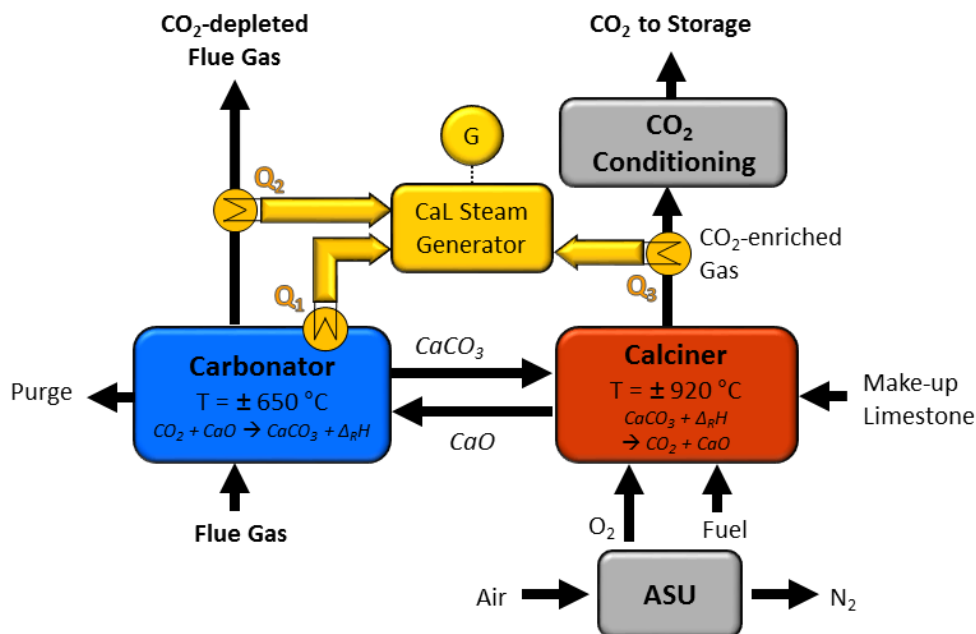


Figure 2.1: General scheme of the Calcium Looping CO₂ capture process.

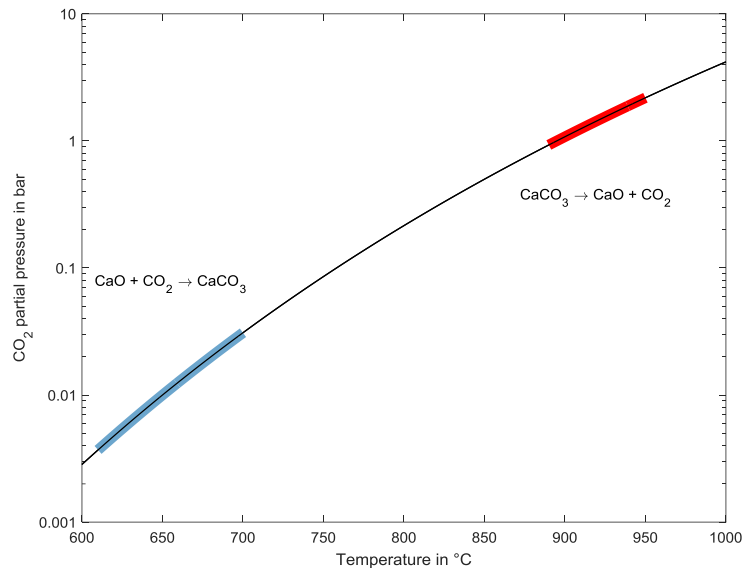


Figure 2.2 Calcination-Carbonation equilibrium of CaCO_3/CaO derived from the work of Baker [2] and Hill & Winter [3].

During the repetitive cycles the sorbent's CO_2 carrying capacity decays. Therefore, spent sorbent must be purged from the system and replaced by fresh amount of sorbent (make-up) to maintain an active bed/sorbent. In case of Calcium Looping CO_2 capture from power plants the amount of make-up or purge respectively is minimized to reduce cost and disposal effort. However, synergies between the clinker manufacturing and the Calcium Looping CO_2 capture process arise due to the share of the common feedstock CaCO_3 and the integration/utilization of the steam or electricity provided by the Calcium Looping steam cycle in the cement plants auxiliaries.

Two different Calcium Looping CO_2 capture process schemes have been developed within WP12. The first so called tail-end option is a standalone Calcium Looping CO_2 capture process that captures CO_2 from the flue gas exiting the cement plant's preheater tower. A part of the cement plant's share of CaCO_3 is fed to the Calcium Looping unit as make-up. With increasing share of CaCO_3 being fed to the Calcium Looping system the CO_2 concentration of the flue gas leaving the preheater tower is reduced since calcination is partly moved to the Calcium Looping calciner and captured. The second so called integrated option treats the complete raw meal. Therefore, two thirds of the cement plants CO_2 emissions are captured in the Calcium Looping calciner. The carbonator solely captures the CO_2 emission from the kiln. With increasing integration level the sorbent performance will improve, simultaneously the flue gas CO_2 concentration will be reduced since a larger share of the raw meal is already calcined by the Calcium Looping process. While the tail-end option is easy to retrofit the energy efficiency is reduced compared to the integrated option that is more challenging to implement into an existing cement plant [1].

3 EXPERIMENTAL FACILITIES

The experiments presented in section 4.2 and section 4.3 of this report were conducted at the 200 kW_{th} fluidized bed calcium looping pilot facility of the Institute of Combustion and Power Plant Technology (IFK) at University of Stuttgart (USTUTT). The experiments conducted at CSIC's electrically heated entrained flow facility are presented in section 4.4.

The experimental work includes preparative work such as preparation of fuels and sorbent, installation of additional not permanently installed measurement devices, modification of the experimental facility for the respective experiments as well as construction work to be able to operate under conditions typical for Calcium Looping for cement application. Furthermore, in order to keep the pilot facility operational continuous maintenance work such as verification and calibration of permanently installed measurement equipment, cleaning of the experimental facility, disposal of utilized materials, and repair of damaged equipment is required.

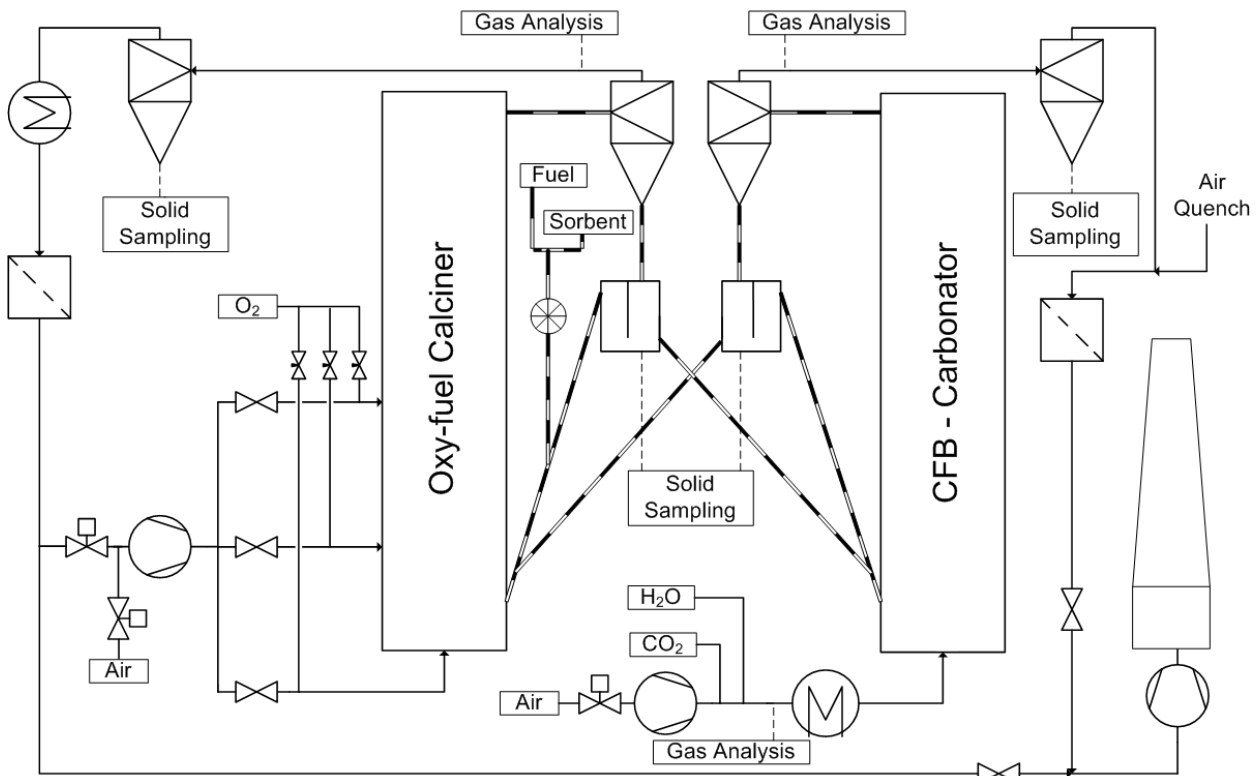
3.1 USTUTT's fluidized bed pilot facility

USTUTT's Calcium Looping pilot plant consist of three refractory lined fluidized bed reactors. Two of the three reactors can be operated in circulating fluidized bed (CFB) mode. Both CFB reactors are 10 m in height and have an inner diameter of approx. 20 cm. The third reactor is 6 m in height and has an inner diameter of approx. 33 cm and can be operated from bubbling mode (BFB) to circulating mode (CFB). The reactors can be variously coupled resulting in a CFB-CFB configuration and a CFB-TFB configuration. For both configurations the calciner is operated as circulating fluidized bed while the carbonator is operated either in CFB mode or TFB mode. A flow sheet of both configurations is given in Figure 3.1.

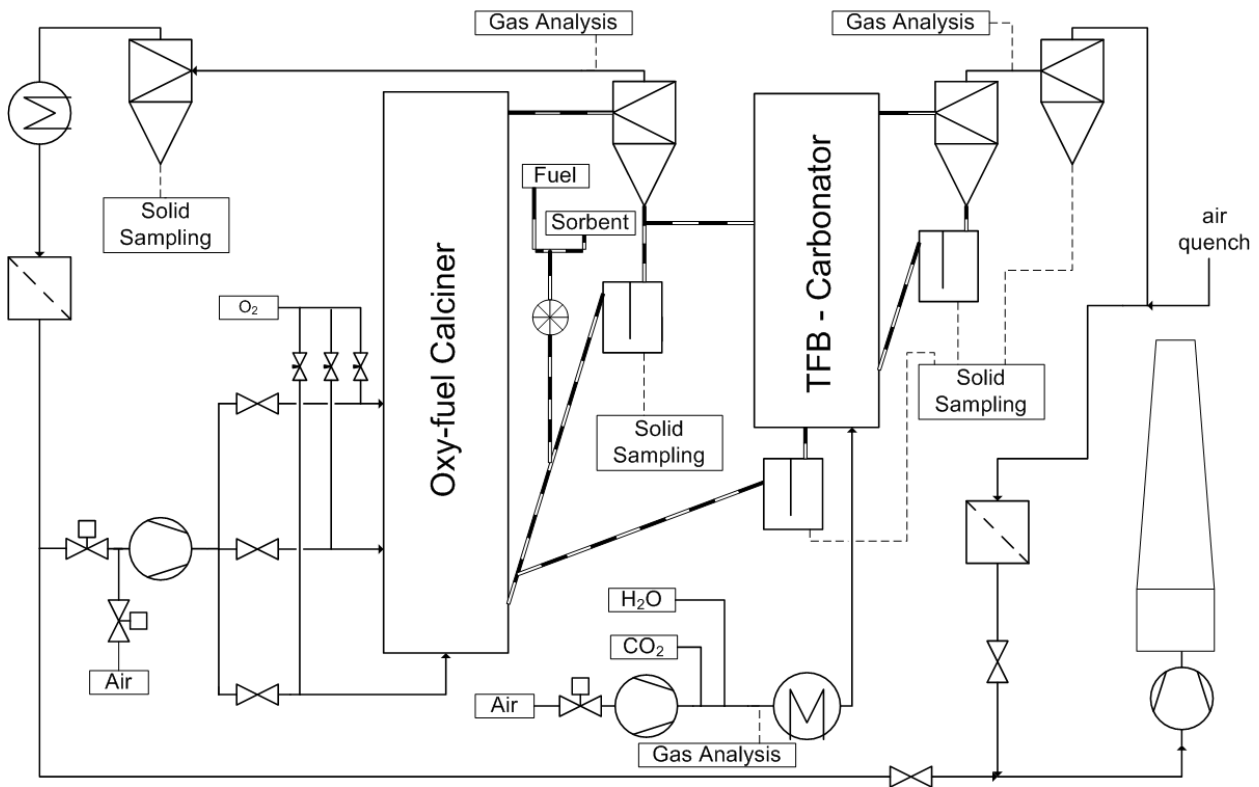
The CFB carbonator as well as the BFB carbonator are fluidized with synthetic flue gas which is generated by mixing air, CO₂ and H₂O. The calciner is fluidized with hot recirculation gas to which oxygen is added according to the required oxygen demand. The fluidization gas (oxidation gas respectively) is feed in stages to the calciner to enhance the burnout of fuel in the calciner and to homogenize the temperature profile along the reactor. CO₂ and O₂ is supplied by liquid tanks, whereas steam is generated by a 36 kW steam generator.

Solids are dosed by screw feeders and fed via a rotary valve into the calciner. Each reactor's exhaust line is equipped with a protective (secondary) cyclone and a bag filter to avoid particle emission into the environment.

In case of the CFB-CFB configuration solid circulation is adjusted by two cone valve. Solids are purged at the bottom of the carbonator in order to maintain a constant bed inventory. However, in case of the CFB-TFB configuration solid circulation between the reactors is controlled by a conveyer screw and solids are purged from the calciner's loop seal. Internal and external circulation of solids is monitored by microwave sensors that are manually controlled and calibrated during the operation of the pilot facility.



(a)



(b)

Figure 3.1 Flow sheet of USTUTT's Calcium Looping pilot plant facility (a) CFB-CFB configuration (b) CFB-TFB configuration.

3.1.1 Measurement instrumentation

All reactors are equipped with multiple thermocouples and pressure transducers along the height, recirculation section and the exhaust gas line. Gas concentration are continuously measured with online gas analyzers at the carbonator's gas supply line and after the primary cyclones of both carbonator and calciner/regenerator reactors. The gas analyzers are calibrated before the experimental campaign and their calibrations are verified every 24 h and recalibrated if required. The gas measurement port is frequently cleaned from accumulating solids in order to ensure proper gas measurement. A summary of the measured gas components with their respective measurement point and their measurement principle is given in Table 3.1.

Table 3.1: Summary of gas measurement techniques.

| Measurement Point | Measured Component | Measurement Principle |
|-------------------|--------------------|---------------------------|
| Calciner outlet | CO ₂ | NDIR |
| | CO | NDIR |
| | O ₂ | paramagnetic |
| | NO _x | chemiluminescence |
| | SO ₂ | NDIR |
| | H ₂ O | (Impact jet) psychrometer |
| Carbonator inlet | CO ₂ | NDIR |
| | CO | NDIR |
| | O ₂ | paramagnetic |
| Carbonator outlet | CO ₂ | NDIR |
| | CO | NDIR |
| | O ₂ | paramagnetic |

Besides the gas measurement solid samples are taken at various points depending on the pilot plant configuration. If experiments are conducted utilizing the CFB-CFB configuration (cf. Figure 3.1a) solid samples are taken from the loop seals and the secondary cyclone. Whereas, solid samples are taken from the calciner's loop seal and secondary cyclone as well as the carbonator's bottom loop seal, internal circulation loop seal and its secondary cyclone if the CFB-TFB configuration is used (cf. Figure 3.1b). Selected representative solid samples are analyzed with respect to their chemical composition as well as total inorganic carbon (TIC) and total organic carbon (TOC) and their Calcium Looping characteristics.

3.1.2 Fuel and sorbent Properties

Two different Colombian coals have been used for the Calcium Looping CO₂ capture experiments. The coals were tried to a moisture content below 7 wt% and crushed to a particle size below 4 mm. Their fuel properties as well as chemical composition is shown in Table 3.2. The average PSD of the utilized Columbian coals is presented in Figure 3.2

Table 3.2 Elemental analysis of coals used for the Calcium Looping demonstration tests.

| Coal | C | H | O* | N | S | ash | H _i |
|--------------|---------|-----|----|-----|-----|-----|----------------|
| | wt%, wf | | | | | | MJ/kg |
| Columbian I | 73 | 4.4 | 11 | 1.7 | 0.6 | 9.6 | 28.98 |
| Columbian II | 71 | 4.8 | 13 | 1.4 | 1.0 | 9.1 | 28.09 |

* calculated by difference

Two different limestone qualities from western Germany were used within the CEMCAP project. One with a mass-median diameter of approx. 637 μm and a limestone with finer particle size distribution and a mass-median diameter of approx. 213 μm. The PSD of the used limestones are presented in Figure 3.3 and Figure 3.4.

Table 3.3 Chemical composition of limestone used for the Calcium Looping demonstration tests.

| Limestone | PSD | CaCO ₃ | MgCO ₃ | Others* | LOI |
|-----------------|-----------|-------------------|-------------------|---------|------|
| | μm | wt%, ar | | | % |
| Western Germany | 100 – 300 | 98.6 | 0.2 | 1.2 | 43.6 |
| | 300 – 700 | 97.1 | 0.9 | 2.0 | 40.5 |

* calculated by difference

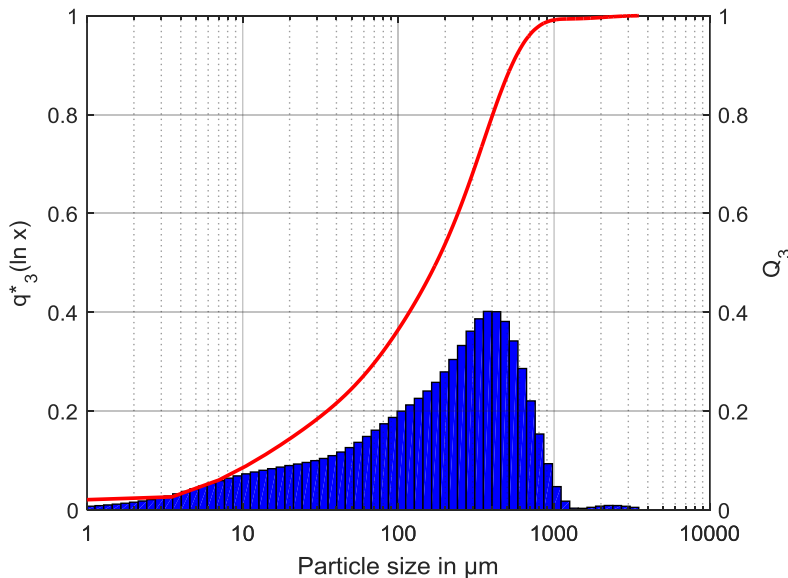


Figure 3.2 Average particle size distribution of the utilized Columbian coals.

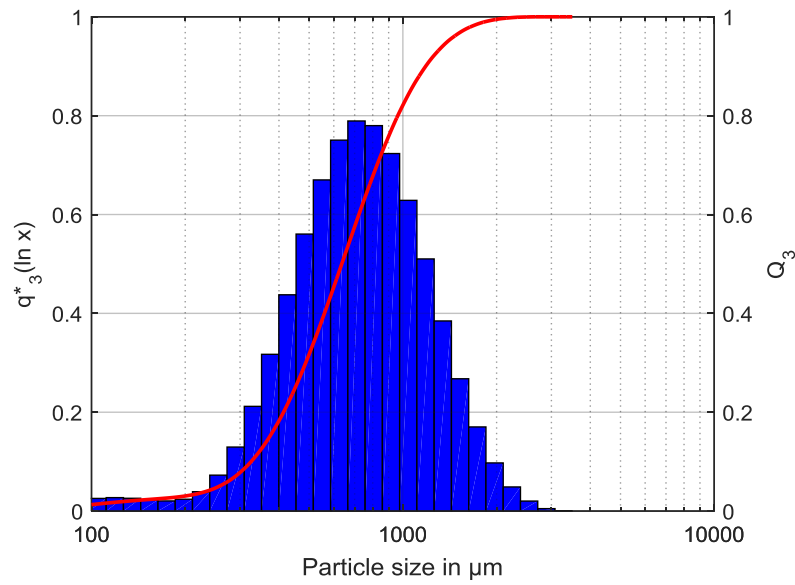


Figure 3.3 Particle size distribution of the 300-700 µm Limestone quality – volume distribution density and cumulative volume distribution.

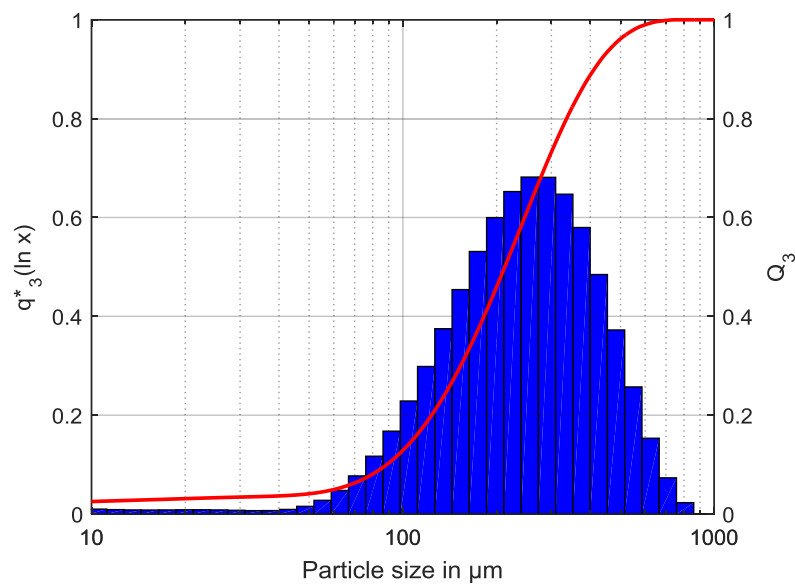


Figure 3.4 Particle size distribution of the 100-300 µm Limestone quality – volume distribution density and cumulative volume distribution.

3.1.3 Design of experiments

Synergies between Calcium Looping CO₂ capture and cement production have been theoretically assessed in the literature. To confirm the suitability of Calcium Looping CO₂ capture for the cement industry various integration methods have been developed during the CEMCAP project (see milestone MS12.1) and investigated experimentally.

The first experimental campaigns were dedicated to demonstrate CO₂ capture from an highly integrated Calcium Looping clinker manufacturing system in which the raw material's carbonates are calcined within the Calcium Looping CO₂ capture process resulting in comparatively low CO₂ flue gas concentrations (15 vol%) and high specific make-up flows of fresh CaCO₃ (up to 4 mol_{CaCO₃}/mol_{CaO}) since two thirds of the cement plants CO₂ emissions are captured by the Calcium Looping calciner and do not need to be treated by the Calcium Looping carbonator.

Further experimental campaigns' objectives were to demonstrate Calcium Looping CO₂ capture for less integrated Calcium Looping systems resulting in higher CO₂ flue gas concentration and lower specific make-up flows since only a part of the cement plant's raw materials are fed to the Calcium Looping system.

Initially Calcium Looping experiments with raw meal were considered. However, due to the outcome of the sorbent characterization carried out at CSIC within Task 12.1 and Task 12.2 these tests have been discarded. Whereas additional experiments were carried out to investigate a wider range of operation conditions of the two integration methods using limestone as sorbent.

3.2 CSIC's entrained flow facility

As discussed in more detail in D12.2, the entrained bed carbonation tests have been carried out by retrofitting high temperature reactors available at INCAR-CSIC for circulating fluidized CaL systems. Thus, one of the 6 m long risers has been refurbished to operate as an entrained reactor (eventually resembling a drop-tube furnace). Since this kind of lab scale reaction length (about 5.5 m achieved of flat temperature profile) is small compared to the 40-100 m expected in industrial applications, it is not possible to fully reproduce gas and solid residence time and contact mode of an industrial system. Therefore, a certain sacrifice is compulsory on some key operating variables (gas velocity, gas/solid ratios etc). As in other G/S reaction systems, this kind of set up allows to access experimental information on detailed reaction kinetics and other reaction phenomena in very short gas solid contact times (few seconds) that are not easily accessible from other experimental set ups (i.e. thermogravimetric analysis).

Figure 3.5 shows a scheme and picture of the entrained carbonator reactor. The operation of the carbonator reactor in such entrained mode, with very low solid loading to allow differential conditions in respect to the gas, requires a very careful control of temperature profiles in the reactor. The carbonator was equipped with five ovens with an individual capacity of 3.0 kW_e installed in the first 2.5 m of the reactor. Four additional heating elements with 1.5 kW_e were installed in the upper part. Moreover, the insulation of this part was improved by installing new ceramic refractory fibres. This has allowed carrying out the experiments with a controlled axial temperature profile along the reaction zone.

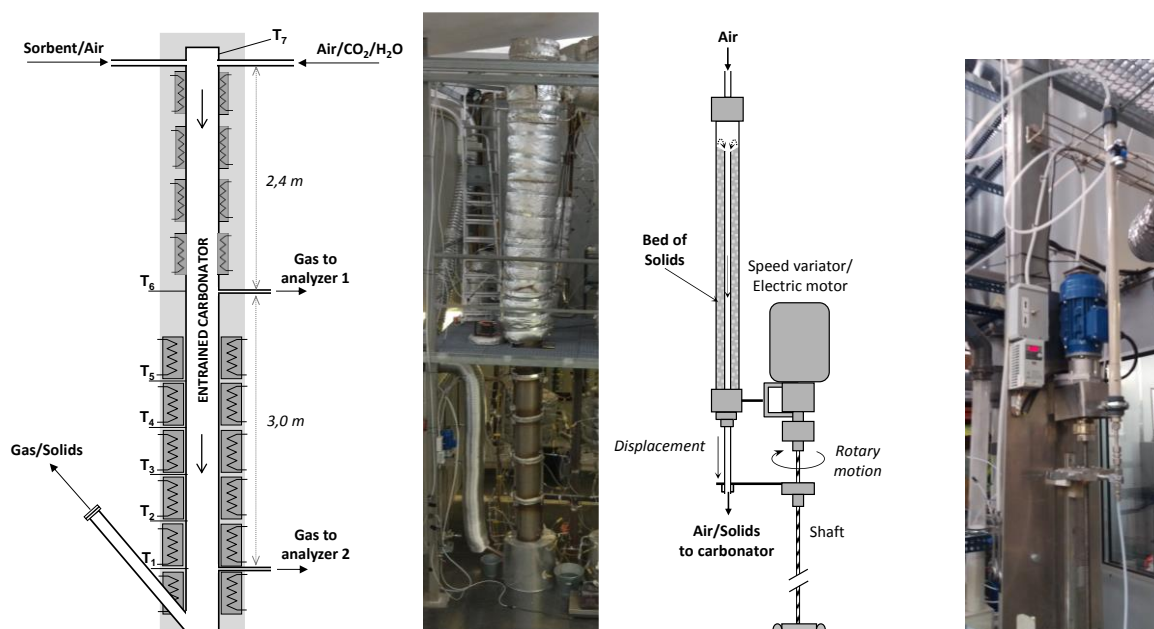


Figure 3.5 Left: Scheme and picture of the down-flow carbonator reactor set up used during carbonation test in entrained mode (gas and solids moving downwards). Right: detail of the solid feeding system. (See D12.2 for more details).

In this reactor, gas and solids are injected at the top of the carbonator and move downwards. The feeding system shown in Figure 3.5, consists in a cylindrical reservoir where the fine solids are loaded at the beginning of each experiment.

Inserted in the bed of solids, there is a drain tube that can be moved downwards in order to remove the solids from the reservoir. This is connected to a mechanical system to control the rate of displacement. This device allows for solids feeding rate up to 8 kg/h. Air is fed at the top of the reservoir in order to disperse and transport the solids to the inlet of the carbonator.

The simulated flue gas is generated by mixing air, CO₂ and steam. Air and CO₂ flow rates are adjusted using mass flow controllers to generate a synthetic combustion flue gas. A small steam generator has also been installed to produce the continuous flow of steam. In the down flow configuration shown in the Figure 3.5 the mixture of air/CO₂/H₂O is pre-heated at temperatures around 250-300 °C before being fed into the entrained carbonator by using the second riser of the 30 kW_{th} pilot facility.

The gas composition can be measured at two heights (at 2.4 m and 5.4 m from the solids injection point) using two gas analyzers (ABB EL3020, ABB AO2000). Each gas sampling port is equipped with a particulate filter and a gas sampling dryer system in order to protect the analyzers from the sorbent particles and moisture (in the case of the experiments carried out with steam). Seven ports along the reactor are used to measure the temperature profile. Each oven has its own independent controller in order to adjust the temperature in each zone of the reactor. All the electric signals from the thermocouples, pressure transducers, gas analyzers, and mass flow controllers are collected in a computer using a data logger.

The methodology to carry out the experiments in the entrained bed carbonator was presented in a previous report (D12.2) and the new results are detailed in the Appendix C. To facilitate data analysis and scalability of results, these tests were carried out in “differential conditions” with respect to the gas. This means that only modest changes in CO₂ concentration are allowed during the carbonation test, so that all particles entering the reactor will experience, ideally, a similar, controlled and measurable reaction environment. Due to the difficulties found to take representative solid samples from the reactor, it was decided to use the measurement of the CO₂ concentration in the gas phase as method to calculate the conversion of the sorbent. This approach was proven to be successful by ensuring reliable gas composition measurements.

4 EXPERIMENTAL RESULTS AND DISCUSSION

The main objectives of the pilot scale experiments was to demonstrate the feasibility of Calcium Looping CO₂ capture from cement production due to stable operation and high CO₂ capture rates for two different reactor configurations. Secondly, the calcination performance under high specific make-up rates of fresh sorbent, and limestone performance (attrition, deposition behavior, and CO₂ carrying capacity) were investigated.

The investigated range of operation conditions are summarized in Table 4.1.

Table 4.1 Range of operation condition and characteristic Calcium Looping variables of the conducted experiments.

| | Process Variable | Symbol | Unit | Value |
|------------|--|----------------------------------|--------------------------------|------------------------------|
| Carbonator | Temperature | T _{Carb} | °C | 600 ... 710 |
| | Velocity | u _{Carb} | m/s | 0.6... 1.2* 3.5 ... 5.0** |
| | Volume fraction CO ₂ inlet | y _{CO₂,Carb} | m ³ /m ³ | 11 ... 37 |
| | Volume fraction H ₂ O inlet | y _{H₂O,Carb} | m ³ /m ³ | 15 |
| | Bed inventory | W _{Carb} | kg/m ² | 800 ... 1200 |
| Calciner | Temperature | T _{Calc} | °C | 880 ... 940 |
| | Velocity | u _{Calc} | m/s | 3.5 ... 4.5 |
| | Volume fraction O ₂ | y _{O₂,Calc} | m ³ /m ³ | 0.39 ... 0.57 |
| | Bed inventory | W _{Calc} | kg/m ² | 200 ... 600 |
| CaL | Circulation rate | m _{Circ} | kg/h | 250 ... 850 |
| | CO ₂ capture efficiency | E _{CO₂} | % | 50 ... 98 |
| | Average particle size | d ₅₀ | µm | 150 µm ± 2 µm |
| | Make up ratio | $\dot{N}_{CaO,0}/\dot{N}_{CO_2}$ | kmol/kmol | 0.8 ... 1.2 |
| | Looping ratio | $\dot{N}_{CaO}/\dot{N}_{CO_2}$ | kmol/kmol | 4 ... 20 |
| | Space time | $\dot{N}_{CaO}/\dot{N}_{CO_2}$ | kmol/(kmol·h) | 0.5 ... 2.5 |

*BFB carbonator; ** CFB carbonator

4.1 Calcium Looping CO₂ capture performance

The CO₂ capture performance of the Calcium Looping process can be characterized by three specific process values (make-up ratio, looping ratio, space time) and the carbonation calcination equilibrium (eq. 2.1). The carbonation equilibrium defines the maximum achievable CO₂ capture at a certain temperature and given CO₂ partial pressure. This so called equilibrium CO₂ capture can be calculated as follows:

$$E_{CO_2,eq}(T) = \frac{\dot{V}_{CO_2,Carb,in} - \dot{V}_{Carb,out} \cdot y_{CO_2,eq}(T)}{\dot{V}_{CO_2,Carb,in}} \quad 4.1$$

Here $\dot{V}_{CO_2,Carb,in}$ represent the volume flow of CO₂ entering the carbonator, $\dot{V}_{Carb,out}$ the total volume flow exiting the carbonator and $y_{CO_2,eq}(T)$ the equilibrium CO₂ concentration at a given temperature (T). Assuming that only CO₂ is captured in the carbonator and no side reaction occurs the equilibrium CO₂ capture can be expressed by the CO₂ inlet concentration and the equilibrium partial pressure (eq. 4.2).

$$E_{CO_2,eq}(T) = \frac{y_{CO_2,Carb,in} - y_{CO_2,eq}(T) \cdot \frac{1 - y_{CO_2,Carb,in}}{1 - y_{CO_2,eq}(T)}}{y_{CO_2,Carb,in}} \quad 4.2$$

The equation to describe the CO₂ equilibrium partial pressure was derived from the work of Baker [2] and Hills & Winter [3].

$$p_{CO_2,eq}(atm) = 2.11 \cdot 10^7 \cdot \exp\left(\frac{-164.96 \frac{kJ}{mol}}{8.314 \frac{J}{mol \cdot K} \cdot T}\right) \quad 4.3$$

In order to describe the CO₂ capture independently from the boundary conditions of the carbonator the so called normalized CO₂ is usually used. It is defined as follows:

$$E_{CO_2,normalized} = \frac{E_{CO_2}}{E_{CO_2,eq}} \quad 4.4$$

The **make-up ratio** is a measure for the sorbent's CO₂ capture capacity. With increasing make-up ratio the sorbent's CO₂ capture activity increases since the particle undergo less number of cycles before being purged from the system. The make-up ratio is calculated by the molar flow of Ca entering the Calcium Looping system divided by the molar flow of CO₂ entering the carbonator. Since molar flows are not accessible directly it was calculated using mass flow of limestone ($\dot{M}_{Limestone}$), the limestone's CaO content ($x_{CaO,0}$), the volume flow of flue gas ($\dot{V}_{Flue Gas}$), the CO₂ content of the flue gas ($y_{CO_2,Carb,in}$) and the molar weight of calcium oxide (\tilde{M}_{CaO}) and the molar volume (\tilde{V}).

$$\frac{\dot{N}_{CaCO_3,0}}{\dot{N}_{CO_2,in}} = \frac{\dot{M}_{Limestone} \cdot \frac{x_{CaO,0}}{\tilde{M}_{CaO}}}{\frac{\dot{V}_{Flue Gas} \cdot y_{CO_2,Carb,in}}{\tilde{V}}} \quad 4.5$$

At a given sorbent activity the material flow circulating between the carbonator and the calciner can be adjusted to meet a desired CO₂ capture in the carbonator. This fact is described by the **looping ratio** which is defined as ratio of the molar flow of CaO entering the carbonator and the molar flow of CaO entering the carbonator.

$$\frac{\dot{N}_{CaO}}{\dot{N}_{CO_2,in}} = \frac{\dot{M}_{Transfer} \cdot \frac{x_{CaO}}{\tilde{M}_{CaO}}}{\frac{\dot{V}_{Flue Gas} \cdot y_{CO_2,Carb,in}}{\tilde{V}}} \quad 4.6$$

The last parameter to describe the CO₂ capture is the so called **space time**. It describes a measure of the possible time of a CO₂ molecule to react in the carbonation reactor with a CaO.

$$\frac{N_{CaO}}{\dot{N}_{CO_2,in}} = \frac{M_{Carb} \cdot \frac{x_{CaO}}{\tilde{M}_{CaO}}}{\frac{\dot{V}_{Flue Gas} \cdot y_{CO_2,Carb,in}}{\tilde{V}}} \quad 4.7$$

In order to describe the CO₂ capture by one design parameter the above mentioned parameters are usually combined in the so called active space time. The expected CO₂ capture performance of an existing facility can be derived from the active space time at given carbonator operation conditions (e.g. CO₂ partial pressure, temperature or equilibrium CO₂ partial pressure respectively) and sorbent properties (eq. 4.8)

$$E_{CO_2} = k_s \cdot \varphi \cdot \tau_{active} \cdot (\bar{y}_{CO_2} - y_{CO_2,eq}) \quad 4.8$$

Key assumption of this theory is that particles react in the fast reaction regime until the average carbonation conversion is reached. A detailed explanation can be found in Charitos et al. [4]. In eq. 4.8 k_s represents the reaction constant of the sorbent in the fast reaction regime, φ the gas solid contact in the carbonation reactor, $y_{CO_2,eq}$ the equilibrium CO_2 concentration and \bar{y}_{CO_2} the average CO_2 concentration in the carbonator. It has to be considered that only a fraction of the particle react in the fast reaction. This fraction is described by equation 4.10. The characteristic reaction time t^* can be obtained by dividing the sorbents' molar CO_2 uptake by the effective reaction rate of the carbonation reaction (eq. 4.11).

$$\tau_{active} = f_{active} \cdot \tau \cdot X_{ave} \quad 4.9$$

$$f_{active} = 1 - e^{\left(\frac{-t^*}{\frac{N_{Ca}}{N_{CO_2}}}\right)} \quad 4.10$$

$$t^* = \frac{X_{avg} - X_{calc}}{k_s \cdot \varphi \cdot (\bar{y}_{CO_2} - y_{CO_2,eq})} \quad 4.11$$

4.2 Demonstration of Calcium Looping CO_2 capture under cement specific operation conditions

Within the CEMCAP project 5 experimental campaigns were conducted yielding 65 experimental points. Throughout all experimental campaigns the respective dual fluidized reactors system (CFB-CFB, TFB-CFB) of the 200 kW_{th} Calcium Looping pilot facility was operated in a very robust manner.

Usually experimental campaigns are conducted in 24 hour 3 shift mode with 3 to 4 employees per shift. An experimental campaign starts with the heat up of the reactors' refractory lining using a natural gas burner. Approximately 18 hours after the start of the heat up burner, the reactor walls are sufficiently heated, bed masses are adjusted and calcined and preliminary Calcium Looping operation can start. Stable, stationary operation conditions can be obtained after a period of approx. 30 h after start of the heat up burner. The transition from one experimental point to another ranges usually from 1 hour to several hours depending on influence of the change on the hydrodynamics and/or sorbent behavior. To ensure proper stationarity measurement points last several hours. After crucial incidents such as malfunctions of essential equipment the facility needs time to reestablish steady conditions reducing the scientific exploitable operation time.

An overview of all experimental points conducted during the CEMCAP project is given in Figure 4.1 and Figure 4.2. It should be noted that generally experimental points with low CO_2 capture rates correspond to smaller looping ratios and/or make-up ratios. Consequently, the amount of sorbent entering the carbonator is insufficient to capture adequate amount of CO_2 . This can be easily counteracted by increasing the solid circulation between the reactors or the looping ratio respectively.

Figure 4.1 includes all measurement points from the two experimental campaigns dedicated to the investigation of the integrated Calcium Looping option utilizing fluidized bed reactors. These points were run with a constant CO_2 inlet concentration of 15 %_{wet}. Since all experimental points have the same inlet concentration the following visualization was chosen. The CO_2 capture efficiency is plotted vs. the average carbonator riser carbonation temperature. For high CO_2 make-up rate of $CaCO_3$ the CO_2 capture was clearly limited by the equilibrium CO_2 capture. CO_2 capture

above the physical possible equilibrium capture are not possible. However due to uncertainties in various measurement devices, mainly the gas analyzers, which effect the calculation of the CO₂ capture particularly for low CO₂ concentrations or high CO₂ capture rates respectively, CO₂ capture rates slightly above the equilibrium were calculated .

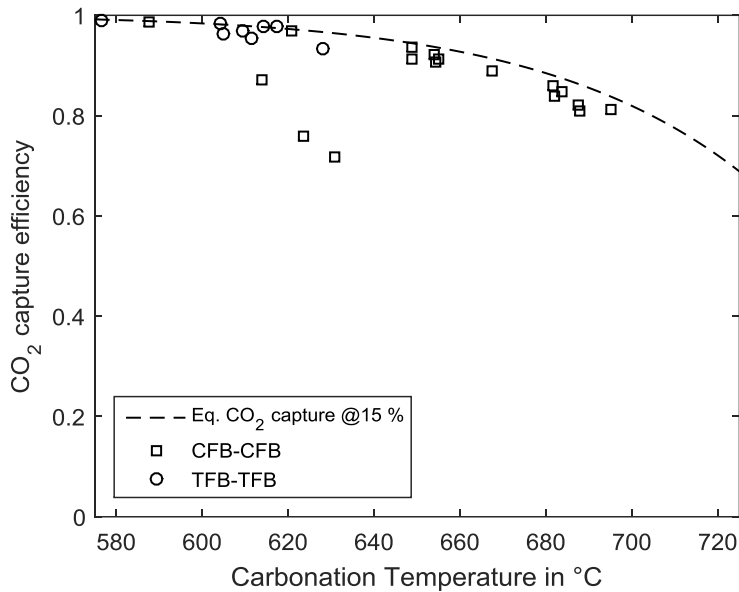


Figure 4.1 CO₂ capture efficiency vs carbonation temperature for all experimental points investigating the integrated fluidized bed CaL option.

Another approach was chosen for the visualization for the results of the investigation of the tail-end CaL option since the inlet CO₂ capture varies and consequently the achievable equilibrium CO₂ capture varies. Therefore, in Figure 4.2 the normalized CO₂ capture is plotted vs. the carbonator's CO₂ inlet concentration. The normalized CO₂ capture is defined as ratio of the obtained and the equilibrium CO₂ capture rate (cf. eq. 2.1).

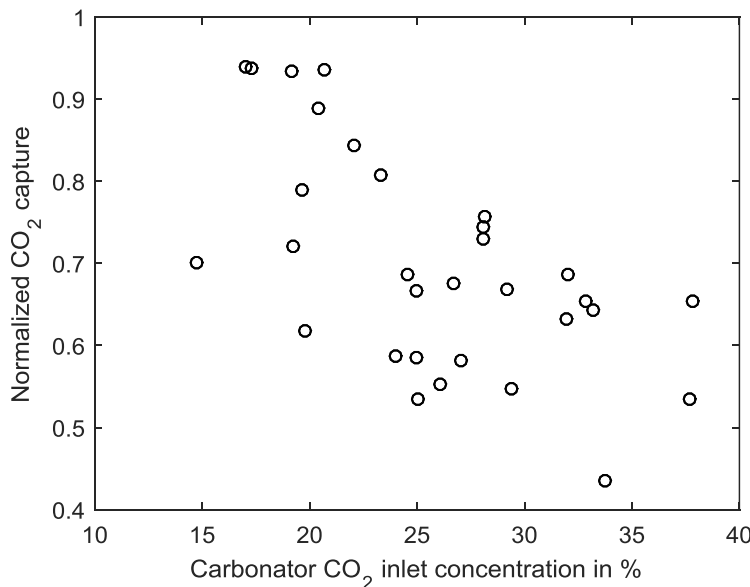


Figure 4.2 Normalized CO₂ capture efficiency vs carbonator inlet CO₂ concentration for all experimental points investigating the tail-end CaL option.

Generally it can be stated that CO₂ capture improves with decreasing CO₂ inlet concentration due to the limitation of the experimental facility. However, high CO₂ concentration favor high CO₂ capture rates since higher CO₂ partial pressures enhance the carbonation reaction while the equilibrium CO₂ concentration is only influenced by the carbonation temperature.

Detailed explanation of the respective tail-end investigation will be given in the subsequent sections.

4.2.1 Hydrodynamics

The hydrodynamic of the system is an essential parameter to operate a coupled fluidized bed system stably. During stable operation fluidization gas (synthetic flue gas or recirculation gas mixed with oxygen) is fed at the bottom of the reactor to fluidize the bed material and entrain solids in case of CFB operation. Solids and gas are separated in a cyclone while the solids fall down in the standpipe of the loop seal and the gas leaves the cyclone through the vortex finder. The loop seal undertake two key functions it seals the reactor internally and it seals both reactors against one another. While internal sealing is essential to ensure proper gas flow towards the reactor's riser the external sealing is crucial to control the solid inventory and circulating flow of the dual fluidized bed system.

Exemplary hydrodynamic profile of both reactor configuration are shown in Figure 4.3. The operating principle of a CFB reactor system can be derived from this figure. Solids entering the reactor at the bottom (a, A), are entrained in to the riser and separated by a cyclone (b-c, B-C) from the gas stream. Via a downcomer and standpipe (c-d, C-D) solids are fed in to the loop seal. The pressure difference over the loop seal (d-e, D-E) ensures that fluidization gas cannot flow reversely through the CFB's solid recycle. From the loop seals solids flow internally (e-a, E-A) or externally (d-A, D-a) into the respective reactor. In case of CFB-BFB configuration (Figure 4.3 right) the circulation between the reactors is realized by a conveyer screw from the calciner to the carbonator (c-M) and via a bottom loop seal from the carbonator to the calciner (K-a). Simplified, the carbonator behaves like a large loop seal standpipe. In this configuration necessitating adequate operation since the pressure of the two reactors are not decoupled fully by a loop seal compared to the CFB-CFB configuration.

Stable and proper designed pressured difference are key for stable operation of dual fluidized bed systems. Generally, the pressure difference between the reactors defines the proportion of bed inventory of the reactors. Conversely, the bed inventory distribution between the reactors can be adjusted by their outlet pressure. The calciner or regenerator pressure profile shows a sharp increase in the bottom region and rises almost linear along the riser stating that the solids are distributed evenly over the whole height leading to favorable calcination conditions for the sorbent. As can be seen by the large pressure difference at the bottom of CFB carbonator's most of the solids are located at the carbonator's bottom and only a small share of the total reactor inventory is accounted to the riser (A-B). In case of the bubbling bed carbonator there is hardly pressure loss along the riser (M-N) indicating that solids are barely present in the carbonator's freeboard. Additional hydrodynamic profiles for different make-up rates and CO₂ concentrations are presented in the appendix A.1.

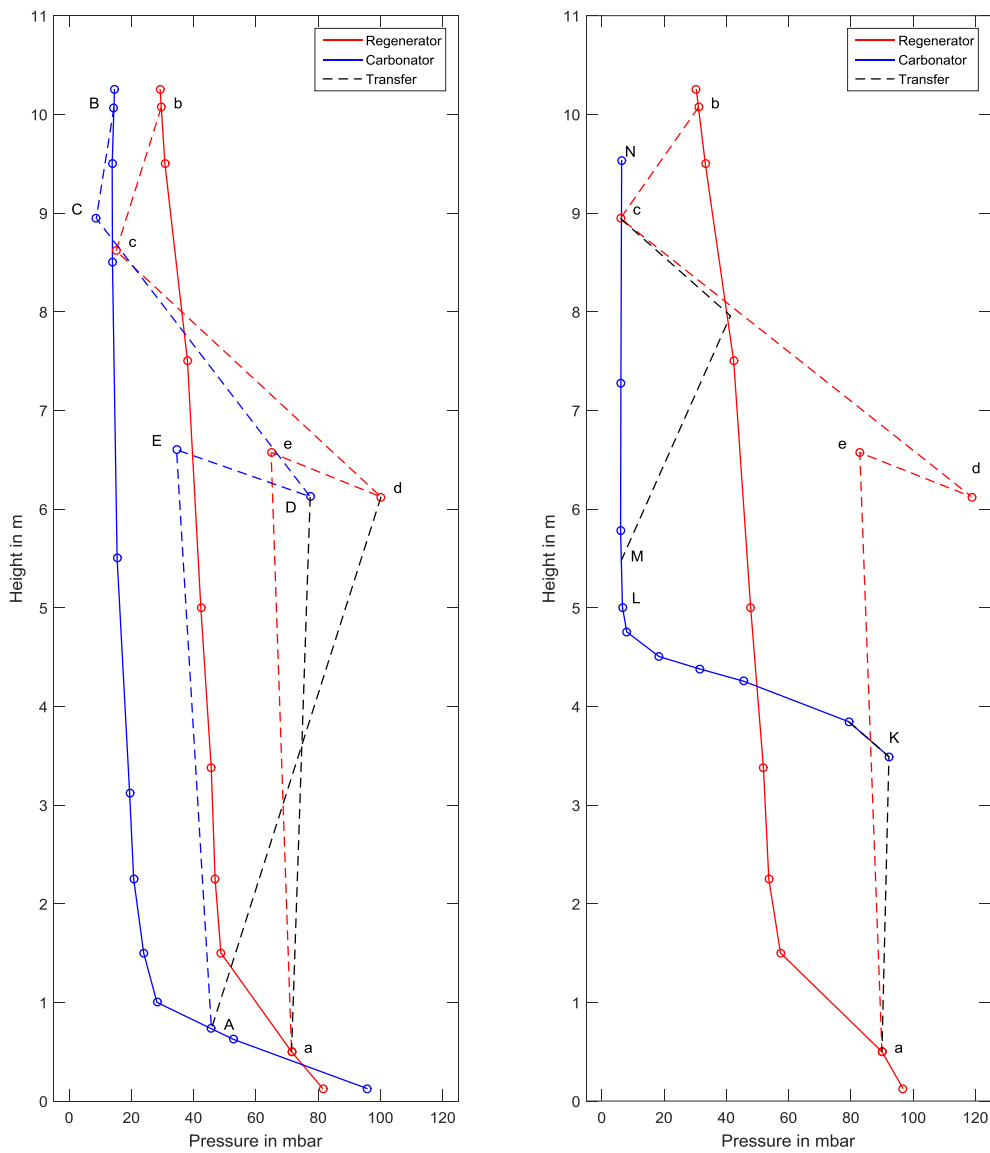


Figure 4.3 Hydrodynamic profile of (left) CFB-CFB configuration and (right) BFB-CFB configuration.

During all experimental campaigns the respective dual fluidized bed system was operated in a robust manner without major complications. Changes in pressure difference between the reactors was compensated by system and the initial situation was reestablished (cf. Figure 4.4).

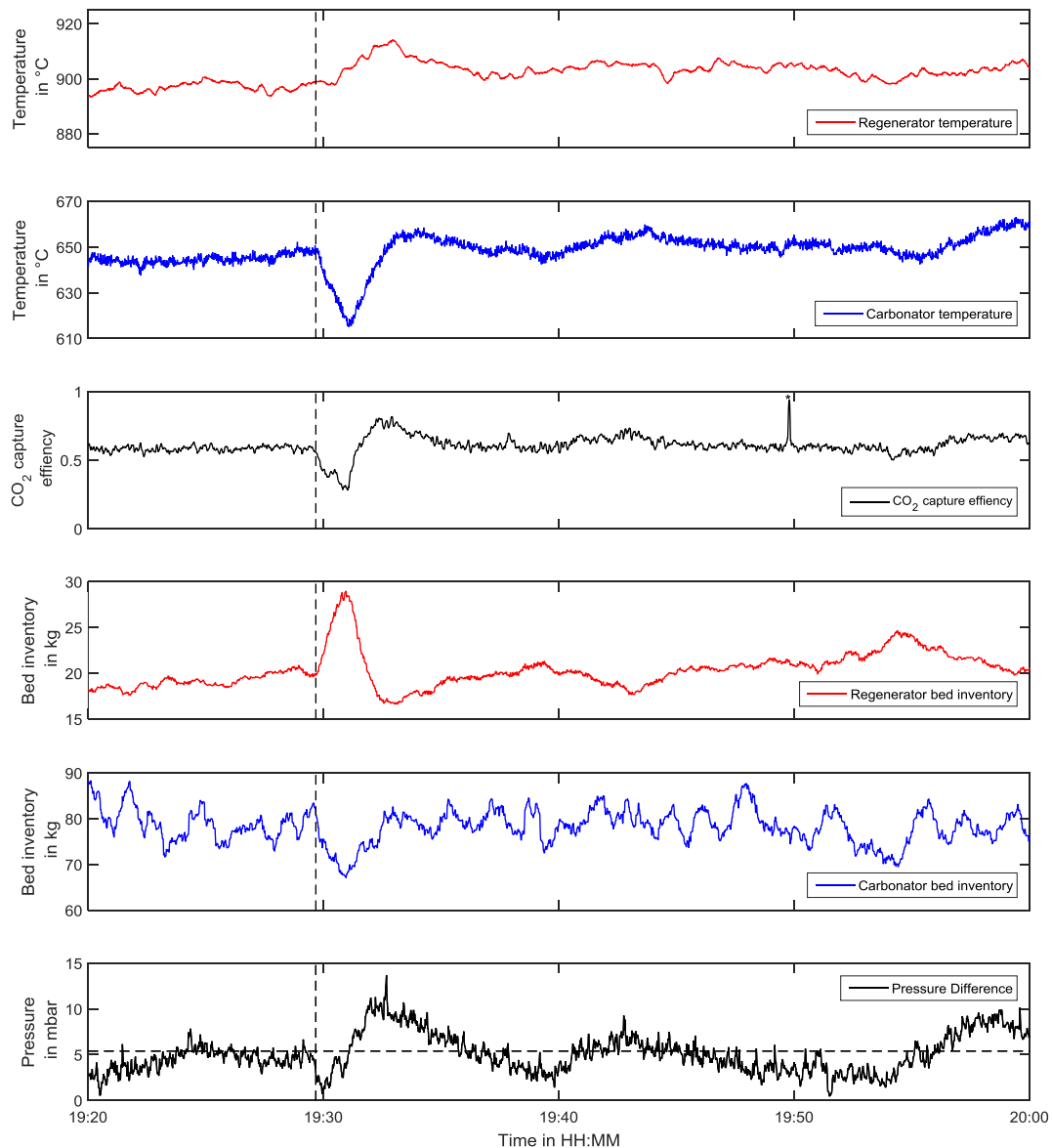


Figure 4.4 Trend showing self-stabilizing effect of the dual fluidized bed system.

An exemplary excerpt of the self-stabilizing effect of the dual fluidized bed system is presented in Figure 4.4. A drop in the pressure difference between the reactors (approx. 19:30) results in a shift of bed materials between the reactors due to the difference in hydrostatic pressure. Less hot, regenerated sorbent can enter the carbonator, simultaneously the mass transfer from carbonator to regenerator is increased. Consequently, CO₂ capture decreases, the regenerator's temperature increases while the carbonator's temperature decreases. The peak in the CO₂ capture efficiency at 19:50 (highlighted by an *) results from filter cleansing. Gas sample lines filters are periodically cleaned to avoid measurement inaccuracies caused by solid accumulation at the filters.

4.2.2 Calciner operation

In case of Calcium Looping for CO₂ capture from cement manufacturing the make-up flow of fresh CaCO₃ is rather maximized than minimized since high amount of make-up increase the sorbent performance and the purge from the Calcium Looping system can be reutilized as feedstock in the clinker manufacturing process. The high amounts of fresh, non-calcined material entering the calciner represents a notable energy sink due to the endothermic calcination reaction. Hence, the fuel input or heating duty of the calciner must be adapted according to the make-up stream. Since the amount of oxygen entering the calciner has to meet the fuel input either the fluidizing gas or the oxygen content in the fluidizing agent needs to be increased. While the first aspect can be addressed by adapting the calciner design/sizing the latter option will lead to reduced sizing of the calciner and it's recycle line as well as reduced energy consumptions by the recycle fan.

In order to stay within the design conditions of USTUTT's Calcium Looping pilot facility the fluidization agent's oxygen content was adjusted by replacing recycled flue gas with pure oxygen. Recirculation rates below 30 % were achieved at a maximum oxygen content of 55 % on a dry bases what represents the safety limitation of the pilot facility (see Figure 4.5). During the operation with these comparatively high oxygen concentration no operational issued occurred.

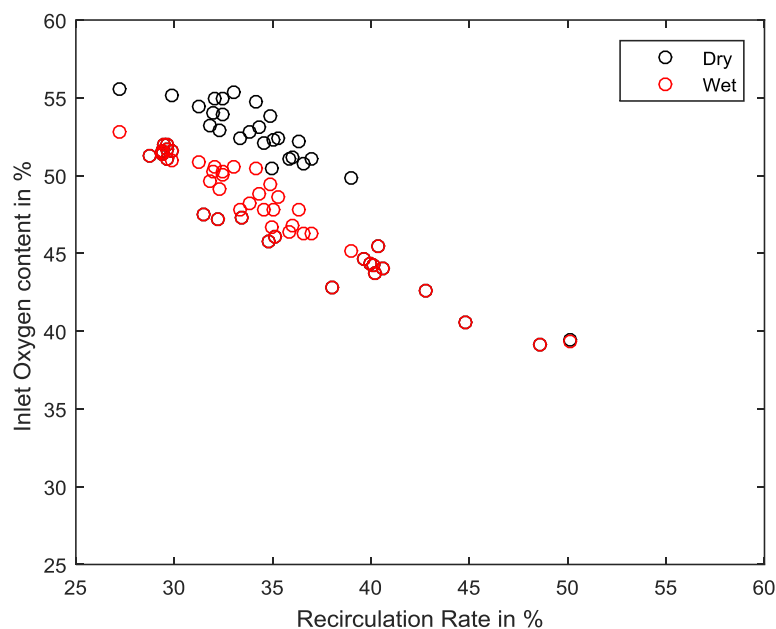


Figure 4.5 Calciner operation conditions - Oxygen content in flue gas vs recirculation rate.

Another beneficial aspect of the high make-up rates is that the temperature moderating effect of the calcination reaction is very pronounced. Combustion agent staging combined with the moderating effect of the endothermic calcination reaction leads to a very isothermal temperature profile along the calciner height. Four exemplary calciner temperature profiles for four different make up rates are shown in Figure 4.6. A uniform temperature profile in the calciner is beneficial for sorbent CO₂ carrying capacity since local temperature peaks that enhance sorbent sintering and may result in additional calcination/carbonation cycles of the sorbent are avoided.

The relatively sharp temperature decrease at the bottom of the calciner reactor results from (i) comparatively cold solid particles leaving the carbonator and entering the calciner, (ii) ambient make-up stream of limestone, (iii) fluidization gas entering the calciner and (iv) not yet completed combustion of the auxiliary fuel providing the necessary calcination energy. The calcination

degree of the solid leaving the calciner were more or less constant at a value of approx. 98 % if an average temperature above 910 °C was ensured.

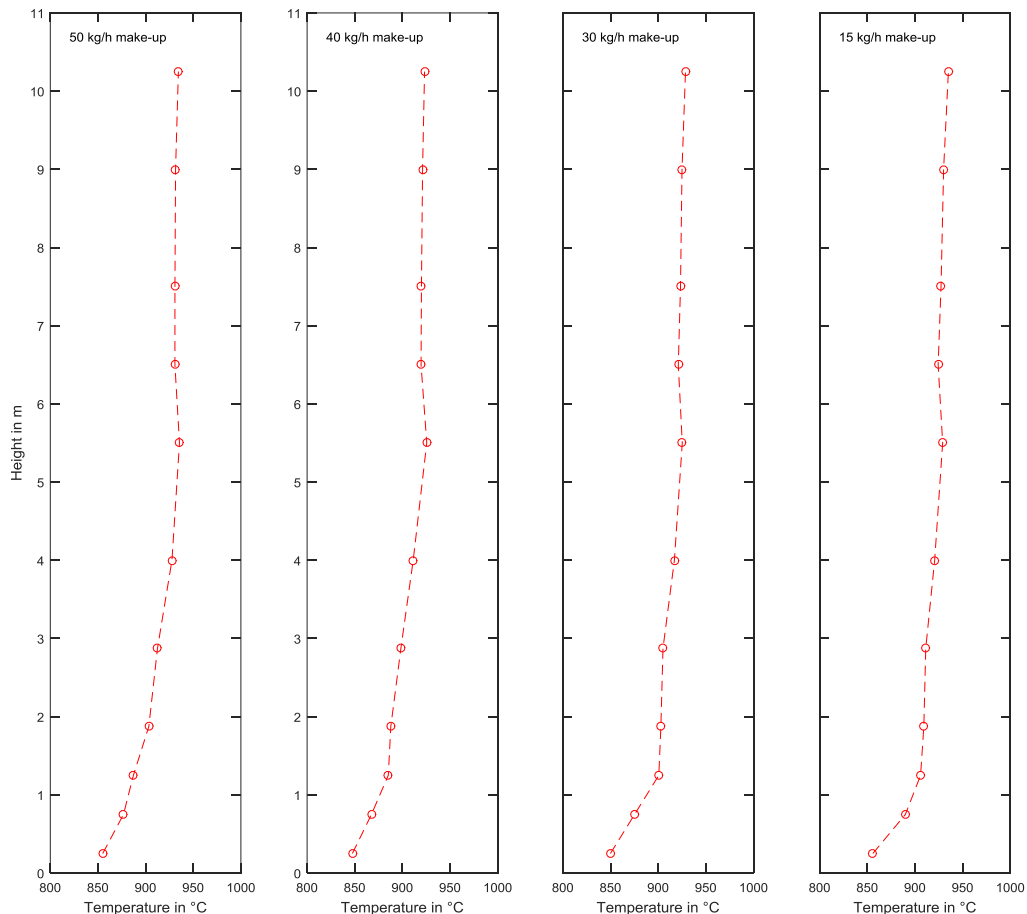


Figure 4.6 Temperature profile in the calciner for four different make-up flows of make up.

4.2.3 Carbonator operation

Throughout all experimental campaigns the carbonator operation was uncomplicated. The high sorbent activity resulting from the comparatively high make-up flows of fresh sorbent lead to high sorbent activity and thus to good CO₂ capture performances in the carbonator.

However, investigations with higher CO₂ flue gas concentrations reveal the problem that solids might not be sufficiently entrained since a large quantity of fluidization gas is removed by CO₂ capture. Therefore, the total volume of fluidization gas needed to be increased during the experimental campaigns investigating higher CO₂ flue gas concentrations. Consequently, the total amount of CO₂ entering the carbonator was also increased leading to poorer CaL operation conditions (reduced looping ratio, make-up ratio and space time). This phenomena can be addressed by a suitable carbonator reactor design. A straight approach would be to adjust the reactors inner diameter to maintain a constant fluidization velocity. Two exemplary trends showing the carbonator performance for the beneficial and poor Calcium Looping conditions are presented in Figure 4.7 and Figure 4.8.

Nonetheless it could be shown that the CaL design criteria are coherent for the cement and power plant application. For high make-up ratios (above $0.5 \text{ mol}_{\text{CaCO}_3}/\text{mol}_{\text{CO}_2}$) and looping ratios around $8 \text{ mol}_{\text{CaO}}/\text{mol}_{\text{CO}_2}$ the CO_2 capture in the carbonator was limited by the carbonation equilibrium while for lower looping ratios the CO_2 capture was limited by the incoming amount of active CaO . For lower make-up ratios ($0.17 \text{ mol}_{\text{CaCO}_3}/\text{mol}_{\text{CO}_2}$) a looping ratio of $10.5 \text{ mol}_{\text{CaCO}_3}/\text{mol}_{\text{CO}_2}$ was estimated to achieve CO_2 capture rates of 90 %.

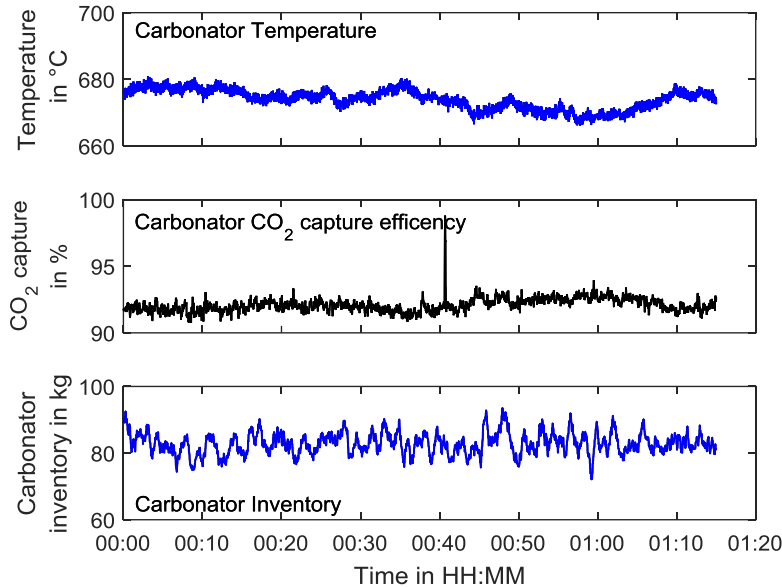


Figure 4.7 Exemplary trend showing carbonator performance for the investigation of the integrated Calcium Looping option ($MR= 0.7 \text{ mol}_{\text{CaCO}_3}/\text{mol}_{\text{CO}_2}$; $LR= 10.6 \text{ mol}_{\text{CaO}}/\text{mol}_{\text{CO}_2}$).

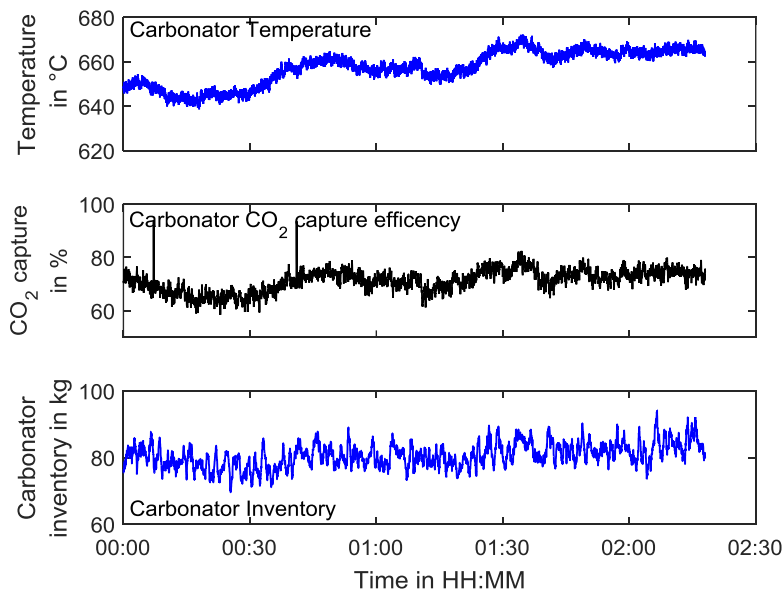


Figure 4.8 Exemplary trend showing carbonator performance for the investigation of the integrated Calcium Looping option ($MR=0.2 \text{ mol}_{\text{CaCO}_3}/\text{mol}_{\text{CO}_2}$; $LR=4.6 \text{ mol}_{\text{CaO}}/\text{mol}_{\text{CO}_2}$).

4.3 Characterization of Calcium Looping CO₂ capture

4.3.1 Influence of make-up rate

Experimental campaigns were dedicated to investigate the tail-end calcium looping configuration with different integration depths. The term integration depth was used to describe the molar amount of Ca being fed to the Calcium Looping CO₂ capture process in proportion to the molar amount of Ca used for the clinker production. Thus representing the make-up ratio of the Calcium Looping system. The make-up ratios for the so called tail-end Calcium Looping configuration are reduced compared to the integrated Calcium Looping option. The integrated Calcium Looping option was investigated within two experimental campaigns for the CFB-CFB and BFB-CFB reactor configuration feeding the highest make-up rates possible.

Generally, the deactivation of the sorbent particle can be described by an exponential decrease of the CO₂ carrying capacity passing in an asymptotic residual CO₂ carrying capacity [5,6]. With increasing make-up ratio the sorbent CO₂ capture activity increases since the particle undergo less number of cycles before being purged from the system. The CO₂ carrying capacity after N cycles is commonly described by an exponential decay with asymptotic end (eq. 4.12).

$$X_N = \frac{1}{\frac{1}{1 - X_r} + kN} + X_r \quad 4.12$$

It could be observed, that the sorbent's CO₂ carrying capacity increased as expected with increasing integration depth or make-up ratio respectively since the sorbent undergoes less cycles. Consequently, the influence of the looping ratio upon the CO₂ capture increases with increasing integration level due to the fact that more active material is available for CO₂ capture. However, the influence of this improving effect decreases during the transition from the kinetically controlled regime to the equilibrium controlled regime.

The sorbent's CO₂ carrying capacity at three make-up rates obtained from TGA analysis is presented in Figure 4.9. A description of the TGA experiments can be found in the Appendix B. The samples of the carbonator and calciner are taken at the same time. After CO₂ injection a sharp increase in mass can be observed for all samples followed by a decline to a constant but much lower increase in mass. The first part can be assigned to the fast reaction regime in which the uptake of CO₂ is limited by the reaction kinetics of the carbonation reaction while the constant increase is related to the diffusion or mass transport controlled regime. In this regime the CO₂ uptake is limited by the diffusion rate of CO₂ through the formed product layer (CaCO₃) to the active CaO.

Generally, a slightly lower CO₂ carrying capacity was observed for the calciner samples compared to the carbonator samples. This might be related to a structural change occurring in the carbonator during the carbonation of the sorbent. It was further observed that the difference between the carbonator and calciner samples is decreasing with increasing make-up ratio. However, no further improvement of the bed activity was observed when increasing the make-up ratio from 0.7 mol_{CaO}/mol_{CO₂} to 1.0 mol_{CaO}/mol_{CO₂}. The average sorbent activity for the samples averaged around 0.17 kg_{CO₂}/kg_{Sorbent} for the two high make-up ratios.

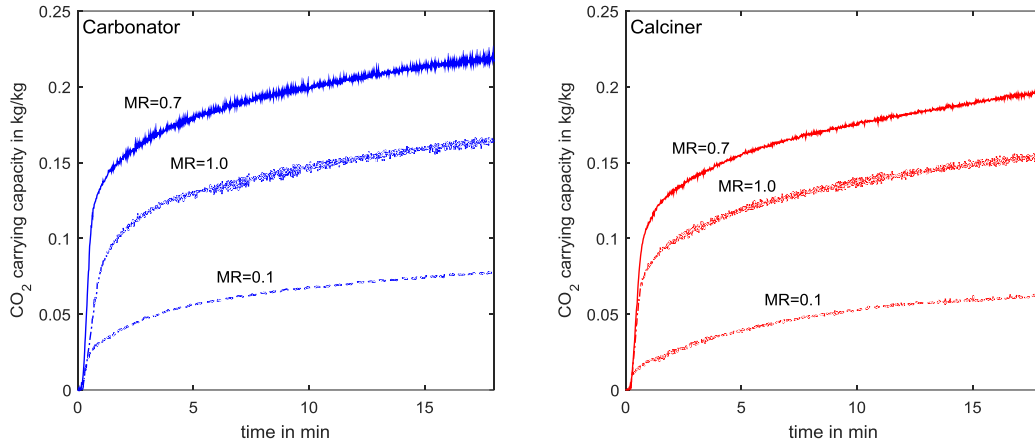


Figure 4.9 Comparison of sorbent CO₂ carrying capacity for different integration levels/make-up ratios (MR) (left) carbonator (right) calciner.

4.3.2 Influence of looping ratio

The influence of the looping ratio is closely connected to the sorbent activity. From a design point of view the looping ratio or the amount of solids being circulated between the carbonator and calciner can be utilized to achieve a desired CO₂ capture at a given sorbent activity (cf. eq 4.13).

$$E_{CO_2} = \frac{\dot{N}_{CaO} \cdot (X_{calc} - X_{avg})}{\dot{N}_{CO_2,in}} = \frac{\Delta \dot{N}_{CO_2}}{\dot{N}_{CO_2,in}} \quad 4.13$$

In equation 4.13. X_{calc} represents the molar calcination degree of the solids entering the carbonator, X_{avg} the average sorbent CO₂ carrying capacity, \dot{N}_{CaO} the molar flow of CaO entering the carbonator and \dot{N}_{CO_2} the molar flow of CO₂ entering the carbonator.

CO₂ capture is either limited by the incoming amount of CaO able to react with the CO₂ and capture it or by the calcination/carbonation equilibrium defining the minimum CO₂ partial pressure and therefore the amount of CO₂ leaving the carbonator. In case of limitation by the calcination carbonation equilibrium the effect of the looping ratio upon CO₂ capture is not pronounced. Contrary the CO₂ capture increases with increasing looping ratio if CO₂ capture is limited by the incoming amount of CaO. This effect increase with increasing sorbent activity or make-up ratio respectively.

Figure 4.10 shows the CO₂ capture performance vs. the looping ratio for three different integration levels. For better visualization the linear regression of the respective experimental data points is shown as dashed lines. For these experiments the CO₂ capture is limited by the incoming amount of active CaO. It can be clearly seen, that the influence of the looping ratio upon the CO₂ capture performance is strongly increasing with the make-up ratio or integration level respectively.

Figure 4.11 shows the CO₂ capture performance vs. the looping ratio for three make-up ratio corresponding to the integrated Calcium Looping CO₂ capture option. Little to no influence of the CO₂ capture performance on the looping ratio was observed for make-up ratios above 0.7 mol_{CaO}/mol_{CO₂} and looping ratios above 8 mol_{CaO}/mol_{CO₂}. The comparatively low CO₂ capture performance of the red data points of approx. 85 % results from a limitation in the carbonation temperature or the equilibrium CO₂ partial pressure respectively. For the red circles the carbonation temperature was kept constant at a temperature level around 700 °C while the

calcination temperature was varied. The blue circles represent a variation of the carbonation temperature at a constant calcination temperature (915 °C).

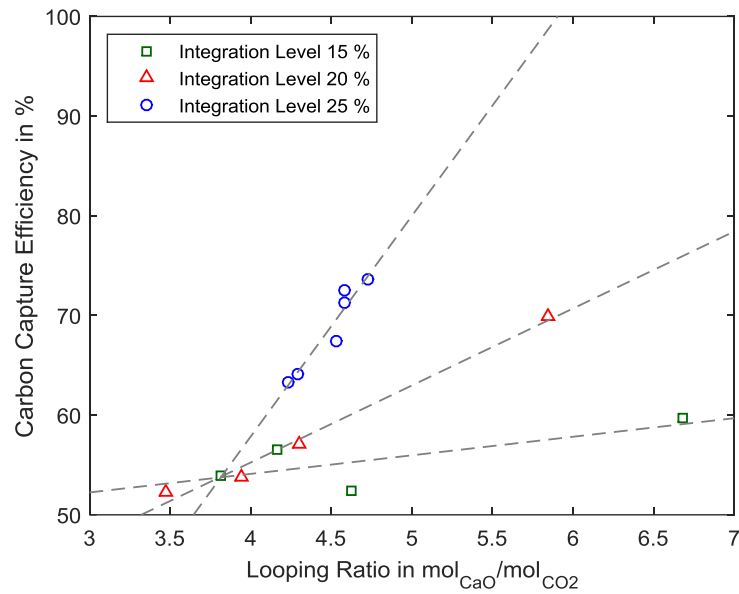


Figure 4.10 Influence of looping ratio upon CO₂ capture for three integration levels (15 %, 20 % and 25 %).

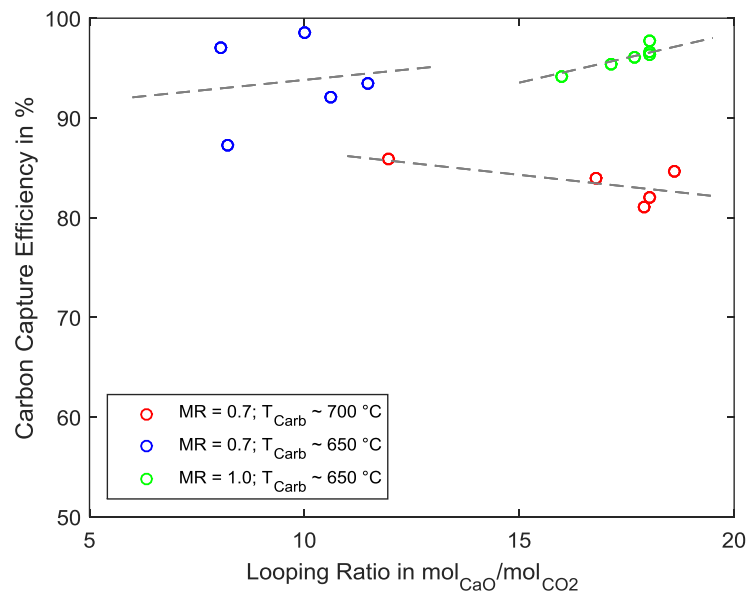


Figure 4.11 Influence of looping ratio upon CO₂ capture for the integrated Calcium Looping CO₂ capture cases.

4.3.3 Influence of CO₂ concentration in the flue gas

Generally, high CO₂ concentration in the flue gas are beneficial for the sorbents CO₂ uptake and thus for the CO₂ capture due to an increased carbonation reaction rate. The reaction rate of the carbonation reaction is commonly described by a first order reaction using a random pore model (eq. 4.14) [7,8]. In this equation k_s represents the kinetic constant, S_N the surface area, X the CaO conversion, y_{CO_2} the CO₂ concentration in the bulk phase and, $y_{CO_2,eq}$ the equilibrium CO₂ concentration. Nonetheless the amount of CO₂ able to be captured from the flue gas is also depending on the amount of CaO entering the carbonator.

$$\frac{dX}{dt} = k_s S_N \cdot (1 - X)^{2/3} \cdot (y_{CO_2} - y_{CO_2,eq}) \quad 4.14$$

Due to limitations in the experimental facility the transfer between the reactors was limiting the CO₂ capture in the carbonator. Consequently lower CO₂ capture efficiencies compared to investigations of the integrated Calcium Looping option were obtained at higher CO₂ flue gas concentrations.

The transfer rate between the reactors can be adjusted by a cone valve in each reactors loop seal. However, if not enough solids are entrained from one reactor the circulation between the reactors is constrained. During the experiments with high CO₂ concentration most of the CO₂ was captured at beginning of the carbonator leading to a reduction of the fluidization gas available to lift and entrain the solids from the carbonator. Thus, the amount of fluidization gas (flue gas mixture entering the carbonator) needed to be increase leading to a significant increase of CO₂ entering with respect to CaO which explains the comparatively low CO₂ capture rates for the experiments with higher CO₂ concentrations. For these experiments the mass transfer could not be raised above 350 kg/h stably resulting in looping ratios around 3 to 4 mol_{CaO}/mol_{CO₂}.

Appropriate design of the carbonator must be ensured if operated at high CO₂ flue gas concentration to avoid entrainment problems. A plain concept would be to adjust the carbonator's inner diameter to maintain a constant fluidization velocity.

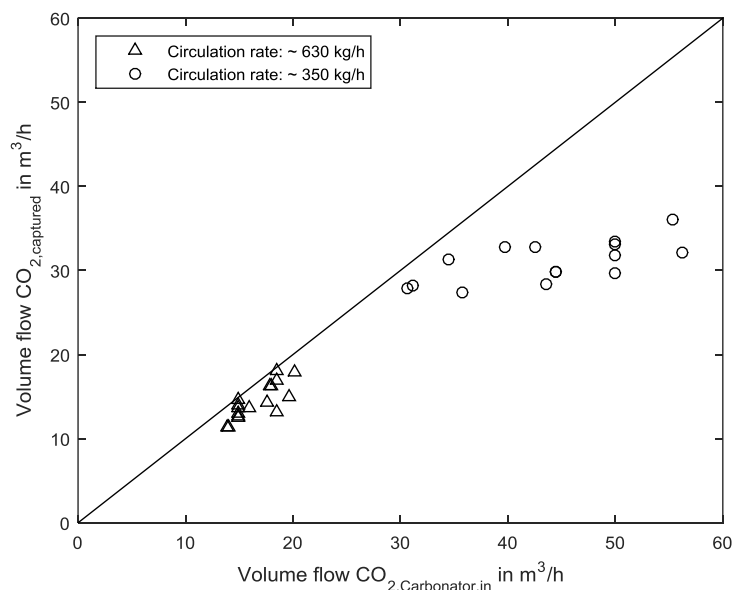


Figure 4.12 Comparison of tail-end CaL campaign and integrated CaL campaign: captured volume flow of CO₂ vs. incoming volume flow of CO₂.

respect to CO₂ capture cost. An optimum tradeoff between the amount of CO₂ captured, auxiliary fuel burnt in the Calcium Looping calciner and steam generated by carbonator cooling must be determined by simulation taken the cement plants specific requirements into account.

4.3.6 Sorbent CO₂ carrying capacity

The sorbents' CO₂ carrying capacity was determined by TGA analysis. Therefore, the solid samples taken during the pilot scale demonstration tests were first calcined under N₂ atmosphere at 860 °C for several minutes to ensure full calcination and then carbonated. A schematic carbonation phase is presented in Figure 4.14. In this figure the determination of the X_{ave} is presented. The sorbents average carrying capacity is determined by intersection of the linear fits describing the fast reaction regime (kinetically controlled) and the slow reaction regime (diffusion controlled).

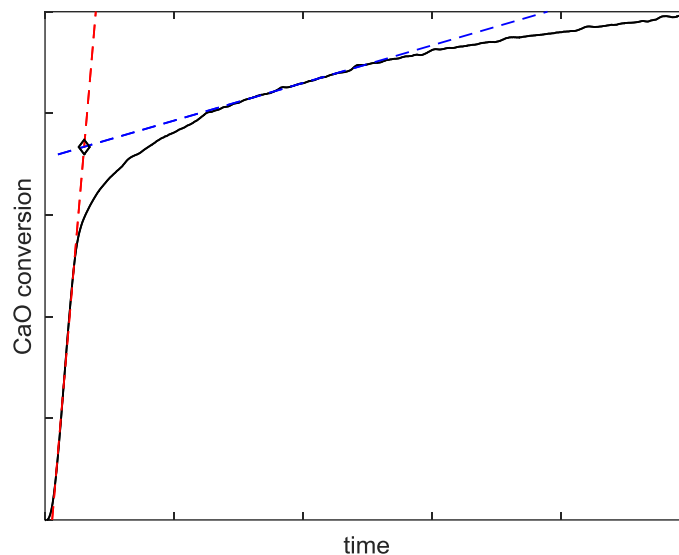


Figure 4.14 Determination of X_{avg}/X_{max} using TGA analysis. Red: fast reaction regime Blue: slow reaction regime.

It was found out that the average sorbent CO₂ carrying capacity decreased with decreasing make-up rate. For the make-up rates of 0.7 mol_{CaCO₃}/mol_{CO₂} and 1 mol_{CaCO₃}/mol_{CO₂} the average CO₂ carrying capacity was around 0.17 kg_{CO₂}/kg_{Sorbent}. There was no significant different between the evaluated samples taking from the carbonator or the calciner at elevated make up rates. However, for lower make-up ratios or increased sorbent aging the samples taken from the calciner show a slightly reduced CO₂ carrying capacity (cf. Figure 4.9). This indicates that sorbent sintering is less advanced for high make up rates. However, the sorbent's carrying capacity is strongly influenced by the calcium looping operation conditions. If the sorbent is calcined under severe calcination conditions (high temperatures, high CO₂ partial pressures, presence of H₂O) its CO₂ carrying capacity is decreased strongly.

Figure 4.15 presents the sorbent activity for a constant transfer rate of approx. 600 kg/h and at an average calcination temperature of 920 °C and carbonation temperature of 655°C and a solid carbonator inventory of 80 kg. The sorbent carrying capacity increased up to 4 time when the make-up ratio was increased from 0.2 mol_{CaCO₃}/mol_{CO₂} to 0.7 mol_{CaCO₃}/mol_{CO₂}. Similar trends were also observed for different transfer rates.

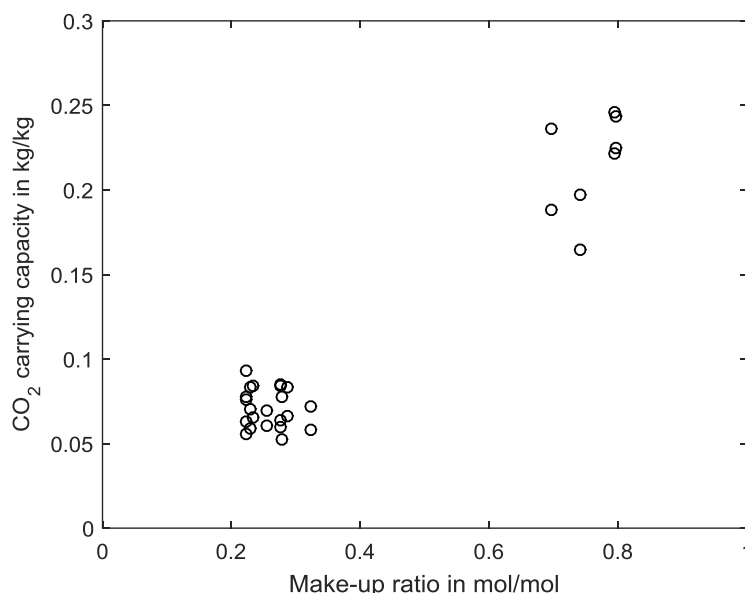


Figure 4.15 Sorbent CO₂ carrying capacity vs. make up rate for $M_{Carbonator} \sim 80$ kg;
 $M_{Transfer} \sim 600$ kg/h.

At this point it should be mentioned that make-up rates up to 4 mol_{CaCO₃}/mol_{CO₂} that represent full utilization of the cement plant's share of CaO/CaCO₃ by the Calcium Looping process could not be investigated due to restriction in calciner design. Even higher make-up ratio should lead to further increase of the sorbent's carrying capacity reducing the required looping ratio or transfer rate to achieve a target CO₂ capture rate.

4.3.7 Sorbent attrition

Two different kind of limestone qualities were used during the experimental campaigns within the CEMCAP project. The first experimental campaign was dedicated to investigate a limestone with a particle size distribution of 300-700 μm. However, due to a major damage in one of the loop seals the campaign was untimely terminated. The second campaign investigating a limestone with a smaller particle size distribution of 100-300 μm that is more suitable for cement application has shown a good CO₂ capture performance and was therefore used in the subsequent campaigns.

Loss of sorbent by attrition did not affect the Calcium Looping operation. However, enhanced sorbent attrition shall easily be compensated by an increase in make-up and the utilization of the attrited fines in the clinker manufacturing process.

A representative particle size distribution of the two used limestone is shown in Figure 4.16 and Figure 4.17. The average mass-median particle diameter (dp_{50}) decreases from 637 μm to 340 μm and from 213 μm to approx. 150 μm respectively. The fraction of larger particles larger than 1 mm can be accounted to smaller stones originating from stones present in the coal burnt in the calciner.

For both limestone qualities a shift of the mass distribution density to smaller particle classes can be observed evincing sorbent attrition. Comparing the two investigated limestones, both originating from western Germany, it can be seen that the particle size distribution of the coarser limestone is more affected by attrition than the finer limestone. This might be related to the reduced fluidization velocities required for finer particles. Since the shear forces decrease with decreasing velocity.

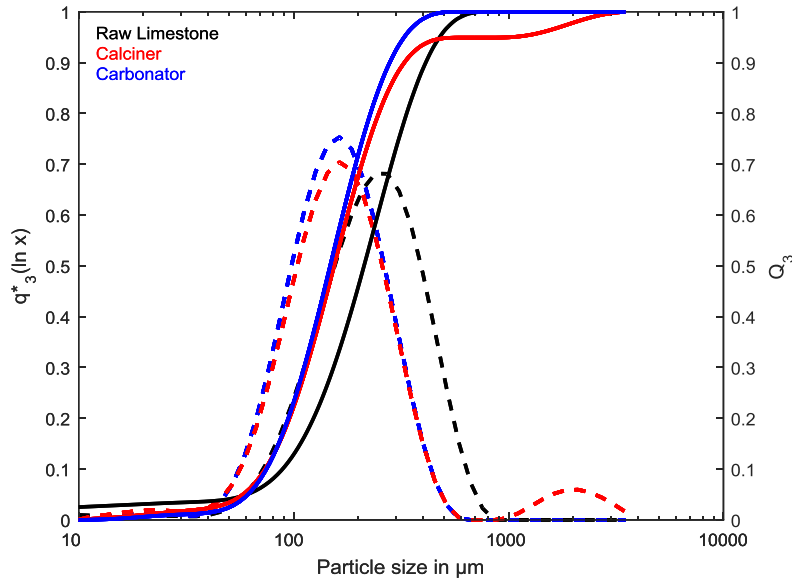


Figure 4.16 Particle size distribution of finer raw limestone and bed material taken from the calciner and carbonator loop seals.

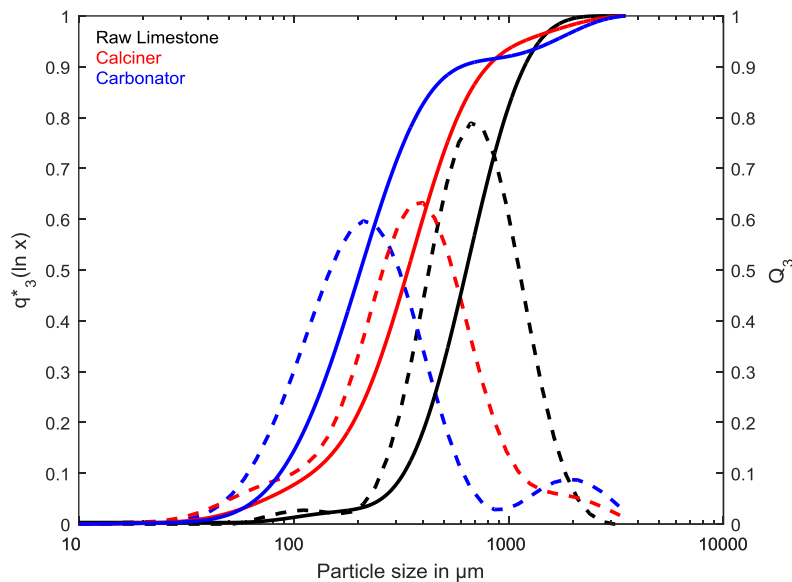


Figure 4.17 Particle size distribution of coarser raw limestone and bed material taken from the calciner and carbonator loop seals.

4.3.8 Sorbent deposition

During the five conducted experimental campaigns rarely problems accounted to deposition or difficult limestone behavior occurred. Depositions of sorbent that influenced the operation of the pilot facility occurred only after minor malfunctions that result in a temperature drop below 600 °C in humid gas atmosphere. The deposition lead to fluctuations in the hydrodynamic of the two coupled reactors. Solids circulated batch wise between the reactors and internally. The formation of deposits may be related to the formation of calcium hydroxide (Ca(OH)₂) that coated the particles since it is formed at temperatures around 580 °C.

A measure to avoid the formation of these deposition during the experiments was to stop the steam feeding to the synthetic flue gas if severe problems in the pilot plant operation occurred. After several cycles within the calciner it appeared that the calcium hydroxide was decomposed and the hydrodynamic behavior of the facility equalized back to stable conditions.

4.4 Results on entrained flow carbonation conducted at CSIC

The experimental results from the entrained bed carbonation test (drop tube experiments) were interpreted with a simple reaction model described in a previous deliverable D12.2 and briefly outlined here with the necessary changes to account for the additional measurements of gas concentrations in an intermediate point in the reactor length. On one hand, the extent of the carbonation reaction between two points in the reactor was calculated using the measurements of the CO₂ concentration in the gas phase by means of the following CO₂ mass balance:

$$\left(\begin{array}{c} \text{CO}_2 \text{ removed from} \\ \text{the gas phase} \end{array} \right) = \left(\begin{array}{c} \text{CaCO}_3 \text{ formed in the} \\ \text{stream of CaO} \end{array} \right) \quad 4.15$$

or

$$F_{\text{CO}_2\text{in}} - F_{\text{CO}_2\text{out}} = F_{\text{Ca}}(X_{\text{carb}} - X_{\text{calc}}) \quad 4.16$$

which can be written as follows to calculate the increment of carbonate content:

$$\text{Increment of carbonate conversion} = (X_{\text{carb}} - X_{\text{calc}}) = \frac{F_{\text{CO}_2\text{in}} - F_{\text{CO}_2\text{out}}}{F_{\text{Ca}}} \quad 4.17$$

To interpret the experimental results, a simple particle reaction model consistent with results from thermogravimetric tests [12] has been used. This model considers that the particle reacts at a constant rate up to the maximum CO₂ carrying capacity (X_{ave}) when the reaction rate becomes zero [13]:

$$\left(\frac{dX}{dt} \right)_{\text{reactor}} = k_s \varphi X_{\text{ave}} (\overline{v_{\text{CO}_2} - v_{\text{CO}_2\text{eq}}}) \quad 4.18$$

where k_s is the sorbent constant reaction rate and the term φ is a gas-solid contacting factor as defined in previous works [14]. From this equation it is possible to calculate the increment of carbonate content of the sorbent in the entrained carbonator as function of the reaction time (t_r):

$$(\text{Increment of CaCO}_3) = \left(\frac{dX}{dt} \right)_{\text{reactor}} t_r \quad 4.19$$

By combining equation 4.19 with the CO₂ mass balance (equation 4.17), the following expression can be obtained:

$$\left(\frac{F_{\text{CO}_2\text{in}} - F_{\text{CO}_2\text{out}}}{F_{\text{Ca}}} \right) = k_s \varphi X_{\text{ave}} (\overline{v_{\text{CO}_2} - v_{\text{CO}_2\text{eq}}}) t_r \quad 4.20$$

New experiments under different experimental conditions were carried out in order to validate the kinetic model proposed under reaction conditions in the entrained carbonator. The main operation variables tested in this deliverable and in the previous D12.2 are summarized in Table 4.2.

Table 4.2 Operating conditions and main variables during entrained carbonation test.

| | | |
|--|--------------------------|-----------|
| Carbonator temperature (°C) | T_{carb} | 590-720 |
| Carbonator inlet velocity (m/s) | u_{carb} | 0.5-2.0 |
| Inlet CO ₂ volume fraction to the carbonator | v_{CO_2} | 0.05-0.30 |
| Inlet Steam volume fraction to the carbonator | $v_{\text{H}_2\text{O}}$ | 0-0.25 |
| Maximum CO ₂ carrying capacity | X_{ave} | 0-0.70 |
| Solids flowrate (kg/h) | | 0.3-8.0 |
| Average particle size of the sorbents used (μm) | $d_{\text{p}50}$ | 35-60 |

According to the particle reaction model (eq. 4.18) one of the most relevant parameters is the maximum CO₂ carrying capacity. Therefore, total of five sorbents derived from high purity limestones and raw meals with X_{ave} from 0 up to 0.7 have been tested. The characteristics of the samples used are shown in Table 4.3. The average CO₂ carrying capacity was measured using a thermogravimetric analyzer following the standard procedure (carbonation conditions: $T_{\text{carb}}=650$ °C, $p_{\text{CO}_2}=0.10$, mass of sample=20 mg, reaction time=10 min). Most of the tests have been carried out using a sorbent named Lime Brec. X_{n} . This was obtained in the 30 kW_{th} pilot facility by calcining a high purity limestone under air firing conditions. CaL Mix X_{ave} corresponds to mixture of different purges obtained from CO₂ capture tests carried out in the 30 kW_{th} pilot facility.

Table 4.3 Main properties of the sorbents used during the entrained carbonator tests.

| Material | X_{ave} | Average particle diameter (μm) |
|---------------------------|------------------|--|
| Lime Comp. X_{r} | 0.17 | 53 |
| Lime Brec. X_{n} | 0.42 | 50 |
| Lime Brec. X_{l} | 0.67 | 50 |
| CaL Mix X_{ave} | 0.32 | 48 |
| Raw meal X_{ave} | 0.19 | 51 |

Lime Comp. X_{r} was produced by calcination of a deactivated sorbent in a heating muffle at 700 °C in order to obtain a low-activated material. Lime Brec. X_{l} was produced by calcination of a high purity limestone in a muffle at low temperature (700 °C) during 48h in order to obtain a high-activated material. Finally, Raw meal 1 X_{ave} and Raw meal 2 X_{ave} correspond to calcined raw meals supplied to CSIC from a cement plant. There was a second sample “Raw meal 2” that was overburned (as indicated by the lack of free CaO and $X_{\text{ave}} < 0.02$ during standard TG analysis and relevant fraction of Alite and other silicates determined by DRX) that was not possible to test in entrained mode as such low activity was below the detection limits.

Moreover, the particle size distribution of these samples was also measured. As can be seen in Table 4.3 and Figure 4.18, the sorbents used present a similar particle size distribution with average particle diameters around 50 μm .

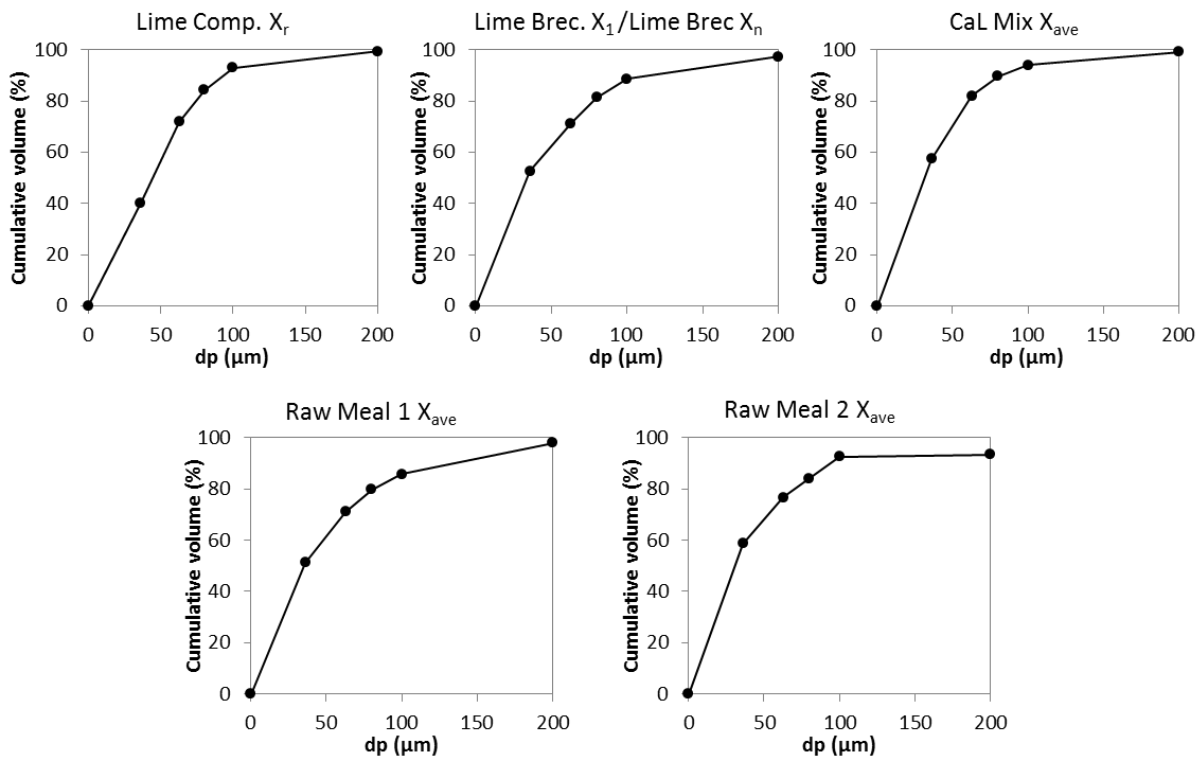


Figure 4.18 Particle size distribution the CaO sorbents used during entrained bed test.

Calcined raw meal samples which have been taken during the entrained flow calcination experiments conducted by USTUTT in WP8 have been analyzed with respect to their CO₂ carrying capacity at USTUTT and CSIC. The samples show a significant CO₂ carrying capacity concluding that CO₂ capture using flash calcined raw meal is suitable. Further assessment will follow up in a future open access publication. Carbonation experiments under entrained flow condition using flash calcined raw meal generated within WP8 were not possible since only small amounts of samples in the range of a few grams are generated during the entrained flow calcination experiments.

4.4.1 Effect of average CO₂ carrying capacity

Figure 4.19 shows the increment of the carbonate conversion as a function of the CO₂ carrying capacity, X_{ave} , under a reaction atmosphere with 15 vol% CO₂. Two sets of experimental results corresponding to two different residence times (3 and 6 s) respectively, are shown. As can be seen, the carbonate conversion follows a linear dependency with X_{ave} . This is in agreement with the particle reaction model (equation 4.20) which considers that the reaction rate is proportional to the CO₂ carrying capacity. This is an important result as indicates that the key variable on the reaction rate is the CO₂ carrying capacity irrespective of the nature of the calcined material.

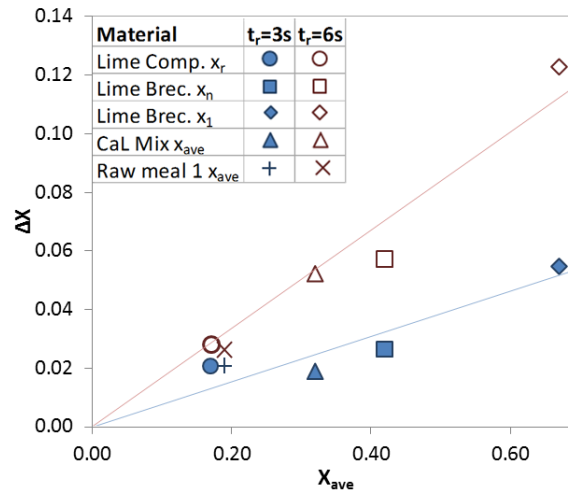


Figure 4.19 Evolution of the sorbents conversion for a fixed reaction time with the CO₂ carrying capacity under a reaction atmosphere with a 15 vol% CO₂. Solid lines correspond to trend lines of the experimental data.

4.4.2 Effect of steam

Several authors have reported in the literature a positive effect of the presence of water vapor on the CaO conversion from experimental results obtained thermogravimetric tests and bubbling beds [15–21].

In D12.2, a preliminary attempt to study the effect of water on the entrained carbonator reactor was carried out. To expand the experimental data base, additional tests were carried out with the presence of steam in the synthetic flue gas. Figure 4.20 shows the increment of carbonate conversion of the CaO sorbent as a function of the reaction time for two reaction atmospheres: 15 vol% CO₂ with (red dots) and 15 vol% CO₂ with 25 vol% H₂O (blue dots). As can be seen, slightly higher values of carbonate conversion were obtained in the entrained carbonator during the experiments carried out with the presence of steam in the synthetic flue gas.

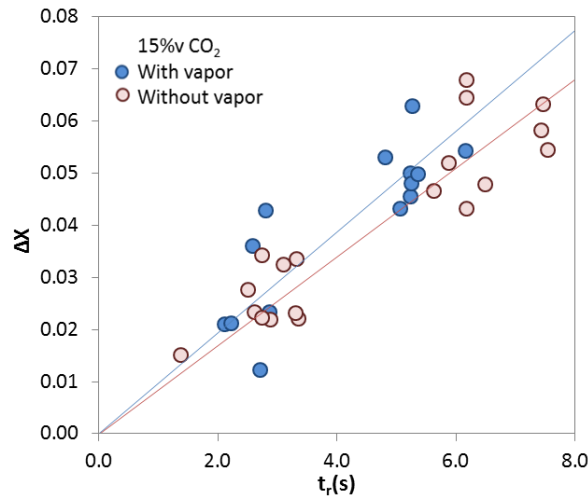


Figure 4.20 Evolution of the sorbent conversion with the reaction time under a reaction atmosphere with a 15 vol% CO_2 (red dots) and under a reaction atmosphere with a 15 vol% CO_2 and 25 vol% H_2O (blue dots). Solid lines correspond to tendency lines of the experimental data.

4.4.3 Effect of CO_2 concentration.

During the preliminary analysis of the results presented in D12.2, it was not possible to confirm the reaction order of the carbonation reaction under the short reaction times measured in the entrained bed test. Therefore, the new experiments have been used to elucidate on this important aspect on reaction kinetics.

Figure 4.21 shows the increment of carbonate conversion of the sorbent as a function of the particle reaction time for three different CO_2 flue gas concentrations plotting all experiments available for a particular material with a fixed $X_{\text{ave}}=0.42$. In this case, the residence time is calculated assuming a reactor length of 4.4 m. As can be seen, despite the increase of the carbonate conversion with the CO_2 concentration, the best fit trend lines do not follow a first reaction order.

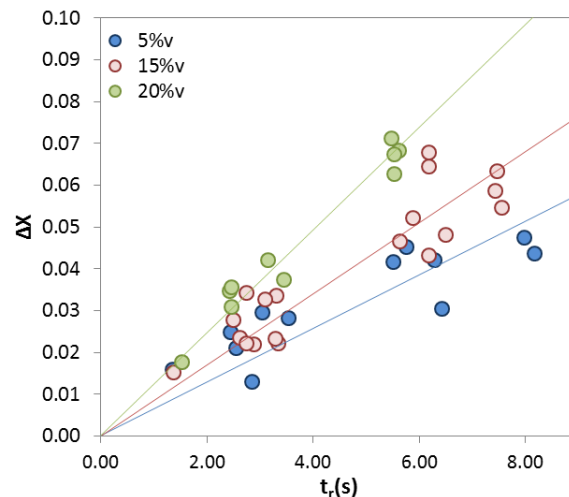


Figure 4.21 Effect of CO_2 concentration on sorbent conversion for three CO_2 concentrations. Solid lines correspond to trend lines of the experimental data.

However, there is an overwhelming level of scientific literature (see for example a recent review by Martinez et al. [22]) reporting a first reaction order for the carbonation reaction in the temperature ranges and partial pressures used in this work. Therefore, the methodology to interpret

the experimental results of Figure 4.21 should be revised. One possible limitation of the experimental set-up as used in D12.2, was linked to the existence of a zone in the upper part of the riser with a relatively low temperature, while the solids are not fully dispersed in the flue gas. An effective reactor length of 4.4 meters was assumed in the preliminary analysis of results of D12.2. To avoid the need of this assumption on effective reactor length, we have used in the new test campaigns the signal of an additional gas analyzer available in the middle of the reactor (see Fig 3.5.1) so that the effective reaction zone can be considered the length between both gas sampling ports (i.e. 3 m). At this particular point, the gas and solids are assumed to be fully mixed. There is also a relatively flat temperature profile (less than 30 °C difference respects to the average values) within this reactor length. Using the signal of the analyzer at this point reduces the uncertainty on effective reactor length but it also reduces the precision of the measurement of the difference in CO₂ concentration at the inlet and at the outlet of the reactor (see raw experimental results reported in Appendix C).

Figure 4.22 shows the increment of carbonate conversion of the sorbent calculated using the new methodology to estimate solid conversions from the decrease in CO₂ concentration in the reactor. In this case, the solid lines correspond to those calculated using the first order assumption in equation 4.4.6. It can be seen that there is a more reasonable agreement between the experimental and calculated values, which may indicate that a first reaction order reaction is still prevailing under the experimental conditions tested in this work. Clearly, the dispersion of the experimental results is substantial. More precise experimental set ups, avoiding gas-solid contact model uncertainties, would be necessary in the future to elucidate with more precision the kinetic parameters derived from these experiments, obtained under short gas-solid contact as relevant for entrained bed reactors.

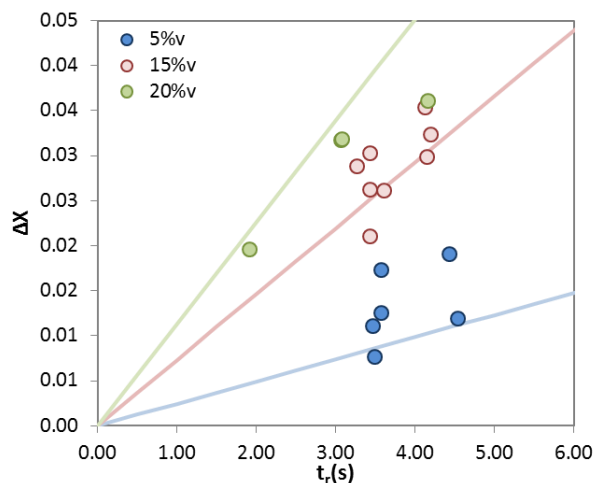


Figure 4.22 Effect of CO₂ concentration on sorbent conversion (solid lines calculated with eq. 4.4.6 and a $k_s\phi$ of 0.14 s⁻¹ for the three CO₂ concentrations)

Using this new approach and the new set of experimental results, the apparent reaction rate constant ($k_s\phi$) has been calculated as a fitting parameter by comparing both terms of equation 4.20. An average value of 0.14 s⁻¹ has been obtained for all the experiments (referred to the fraction X_{ave}) which is slightly lower than that reported in the previous report (D12.2) but still consistent with the lower range of those obtained by other authors (Charitos, Rodríguez et al. 2011, Rodríguez, Alonso et al. 2011, Arias, Diego et al. 2013, Arias, Alonso et al. 2017). We can only speculate at this stage on the reasons to derive this lower than expected kinetic parameter: shorter gas-solid contact times of the solids (due to a still un-efficient dispersion of the solids in the gas

phase and/or a departure from plug flow assumed for gas and solids) could explain the result. In future kinetic characterization of other materials for CaL applications it may be necessary to combine kinetic information from this set up operating under very short gas-solid contact times with information accessible with from TG testing, that are in principle more precise (for example when it comes to determine order of reactions) but that can only access experimental information at much longer times scales (10s of seconds to minutes).

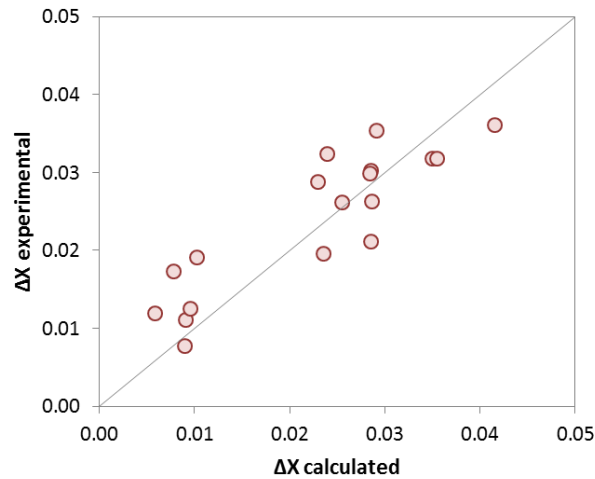


Figure 4.23 Comparison between the experimental increment of conversion and the calculated by applying equation 4.20 and $ks\phi=0.14s^{-1}$.

Finally, Figure 4.23 shows the comparison between the experimental increment of carbonate conversion and the calculated values using equation 4.20 for tests using the material with $X_{ave}=0.44$. As can be seen, there is a reasonable agreement between experimental and calculated values. This confirms a reasonable validity of the simple homogeneous kinetic model in the experimental conditions tested in the entrained carbonator used in this work. A PhD work is ongoing to complete and refine the data interpretation provided in this deliverable and one scientific journal publication with the final results and data analysis will be attempted.

5 SUMMARY AND CONCLUSIONS

USTUTT investigated the Calcium Looping CO₂ capture process under operational conditions expected for application at a clinker production plant. USTUTT's 200 kW_{th} fluidized bed pilot facility has been modified to be able to operate under cement specific conditions. In total five experimental campaigns were conducted at this facility. These test campaigns covered the field of operational conditions relevant to the Calcium Looping technology's application in the clinker production process comprehensively, investigating parameters such as high make-up ratios up to 1 mol_{CaCO₃}/mol_{CO₂}, CO₂ concentrations up to 33 vol%_{wet}, carbonator temperatures between 600 to 710 °C, and looping ratios up to 20 mol_{CaO}/mol_{CO₂}. Two different reactor configurations, a CFB carbonator coupled with a CFB calciner as well as a BFB carbonator coupled with a CFB calciner were tested. All pilot scale experiments by USTUTT were conducted using limestone as Calcium Looping sorbent. Two different limestone qualities were utilized within the experiments. No major problems regarding the applicability of the Calcium Looping for CO₂ capture from clinker production have arisen from these experimental investigations.

CO₂ capture has been demonstrated during the five experimental campaigns with stable operation yielding in total 65 representative experimental points. Robust hydrodynamic behavior of both dual fluidized bed systems (CFB-CFB and BFB-CFB) was observed during the entire operation of the pilot plant.

High CO₂ capture rates in the carbonator (up to 98 %) were demonstrated. The good capture performance results mostly form a highly active sorbent due to the high make-up ratios that are feasible when applying the Calcium Looping technology to the cement industry. Operating with increased make-up ratios (0.7 mol_{CaCO₃}/mol_{CO₂}), the sorbent activity increased up to 4 times compared to low make-up cases (0.25 mol_{CaCO₃}/mol_{CO₂}). The carbonator reactor design should be tailored precisely to the flue gases' CO₂ content since the reduction of fluidization gas due to CO₂ capture effects the entrainment of solids especially if operating at high CO₂ concentrations as in clinker manufacturing flue gases.

The high make-up feed rates of uncalcined material require the provision of an increased thermal power in the Calcium Looping calciner compared to Calcium Looping systems for power plant application. This needs to be considered for the calciner design and its operation. It can be addressed by a suitable calciner design allowing for higher thermal power of this unit or when the calciner geometry is fixed, by adjusting the calciner operation conditions (mainly adjusting the staged fluidization gas feed and increasing its oxygen content). In USTUTT's pilot scale experiments, the calciner was operated with an oxygen concentration of up to 53 vol%_{wet}. Under these conditions, the plant could be operated without temperature peaks along the calciner height, which would cause excessive sorbent deactivation and without other operational problems. However, operation with even higher oxygen concentrations may be feasible. An increase of the share of oxygen in the calciner's fluidization gas will reduce the recycle line's size and energy consumption.

Sorbent attrition has been assessed using two different limestone qualities. Reduction in particle size distribution have been observed for both qualities. The observed reduction was more pronounced for the coarser limestone. Loss of sorbent by attrition did not affect the Calcium Looping process operation (process stability, CO₂ capture efficiency). Moreover, increased sorbent attrition would be tolerable or in certain limits even beneficial to a Calcium Looping system applied to a clinker manufacturing process, since the loss of sorbent can be compensated by an increase in the make-up feed rate and the utilization of the attrited fines in the clinker production.

CSIC has completed test campaigns in 30 kW_{th} scale measuring the extent of carbonation conversion in gas-solid contact time scales between 1-6 seconds at different concentrations of CO₂, carbonation temperatures, initial sorbent activity and with different types of CaO precursors.

Several CaO precursors (high purity limestones and raw meals) with different carrying capacities (up to 0.7) have been tested. The experimental results obtained, demonstrated that the carbonation reaction rate is proportional to the X_{ave} irrespective of the nature of the calcined material. It has been confirmed that the carbonation reaction at such short time scales follows a pseudo-homogeneous kinetic model consistent with a first reaction order in respect to CO_2 . A small positive effect of steam in the gas has been detected. Apparent constant reaction rates have been calculated (referred to the active fraction of the material only) which are consistent with the lower range of others reported in the literature for other Calcium Looping applications. Some inherent limitations in the experimental technique and lab scale facility used to access kinetic information at low gas-contact times may be the main issues responsible for these deviations.

Calcium Looping CO_2 capture using fluidized bed systems has been demonstrated in industrially relevant conditions (TRL 6) by extensive experimental investigations and can be considered to be ready to be applied for CO_2 capture in the cement industry in industrial demonstration activities (i.e.: TRL 7). The less mature Calcium Looping concept using entrained flow reactors proved to be a promising technology. However, further research is required (e.g. in respect to the CO_2 capture activity of calcined raw meal based sorbent materials) to increase the maturity level of this technology before its commercial application for CO_2 capture from clinker manufacturing.

6 REFERENCES

- [1] Spinelli M, Martínez I, Lena E de, Cinti G, Hornberger M, Spörl R, Abanades JC, Becker S, Mathai R, Fleiger K, Hoenig V, Gatti M, Scaccabarozzi R, Campanari S, Consonni S, Romano MC. Integration of Ca-Looping Systems for CO₂ Capture in Cement Plants. *Energy Procedia* 2017;114:6206–14, doi:10.1016/j.egypro.2017.03.1758.
- [2] Baker EH. The calcium oxide–carbon dioxide system in the pressure range 1—300 atmospheres. *J. Chem. Soc.* 1962;0:464–70, doi:10.1039/JR9620000464.
- [3] K. J. Hill and E. R. S. Winter. Thermal Dissociation Pressure of Calcium Carbonate.
- [4] Charitos A, Rodríguez N, Hawthorne C, Alonso M, Zieba M, Arias B, Kopanakis G, Scheffknecht G, Abanades JC. Experimental Validation of the Calcium Looping CO₂ Capture Process with Two Circulating Fluidized Bed Carbonator Reactors. *Ind. Eng. Chem. Res.* 2011;50:9685–95, doi:10.1021/ie200579f.
- [5] Ortiz C, Chacartegui R, Valverde JM, Becerra JA, Perez-Maqueda LA. A new model of the carbonator reactor in the calcium looping technology for post-combustion CO₂ capture. *Fuel* 2015;160:328–38, doi:10.1016/j.fuel.2015.07.095.
- [6] Abanades JC, Alvarez D. Conversion Limits in the Reaction of CO₂ with Lime. *Energy Fuels* 2003;17:308–15, doi:10.1021/ef020152a.
- [7] Grasa G, Murillo R, Alonso M, Abanades JC. Application of the random pore model to the carbonation cyclic reaction. *AIChE J.* 2009;55:1246–55, doi:10.1002/aic.11746.
- [8] Bhatia SK, Perlmutter DD. Effect of the product layer on the kinetics of the CO₂-lime reaction. *AIChE J.* 1983;29:79–86, doi:10.1002/aic.690290111.
- [9] Blamey J, Anthony JE, Wang J, Fennell SP. The calcium looping cycle for large-scale CO₂ capture. *Progress in Energy and Combustion Science* 2010;36:260–79, doi:10.1016/j.pecs.2009.10.001.
- [10] Perejón A, Romeo LM, Lara Y, Lisbona P, Martínez A, Valverde JM. The Calcium-Looping technology for CO₂ capture: On the important roles of energy integration and sorbent behavior. *Applied Energy* 2016;162:787–807, doi:10.1016/j.apenergy.2015.10.121.
- [11] Dieter H, Bidwe AR, Varela-Duelli G, Charitos A, Hawthorne C, Scheffknecht G. Development of the calcium looping CO₂ capture technology from lab to pilot scale at IFK, University of Stuttgart. *Fuel* 2014;127:23–37, doi:10.1016/j.fuel.2014.01.063.
- [12] Grasa G, ABANADES J, Alonso M, GONZALEZ B. Reactivity of highly cycled particles of CaO in a carbonation/calcination loop. *Chemical Engineering Journal* 2008;137:561–7, doi:10.1016/j.cej.2007.05.017.
- [13] Alonso M, Rodríguez N, Grasa G, Abanades JC. Modelling of a fluidized bed carbonator reactor to capture CO₂ from a combustion flue gas. *Chemical Engineering Science* 2009;64:883–91, doi:10.1016/j.ces.2008.10.044.
- [14] Rodríguez N, Alonso M, Abanades JC. Experimental investigation of a circulating fluidized-bed reactor to capture CO₂ with CaO. *AIChE J.* 2011;57:1356–66, doi:10.1002/aic.12337.
- [15] Dieter H, Bidwe AR, Varela-Duelli G, Charitos A, Hawthorne C, Scheffknecht G. Development of the calcium looping CO₂ capture technology from lab to pilot scale at IFK, University of Stuttgart. *Fuel* 2014;127:23–37, doi:10.1016/j.fuel.2014.01.063.
- [16] Donat F, Florin NH, Anthony EJ, Fennell PS. Influence of high-temperature steam on the reactivity of CaO sorbent for CO₂ capture. *Environ Sci Technol* 2012;46:1262–9, doi:10.1021/es202679w.
- [17] Arias B, Grasa G, Abanades JC, Manovic V, Anthony EJ. The Effect of Steam on the Fast Carbonation Reaction Rates of CaO. *Ind. Eng. Chem. Res.* 2012;51:2478–82, doi:10.1021/ie202648p.

- [18] Manovic V, Anthony EJ. Carbonation of CaO-Based Sorbents Enhanced by Steam Addition. *Ind. Eng. Chem. Res.* 2010;49:9105–10, doi:10.1021/ie101352s.
- [19] Symonds RT, Lu DY, Hughes RW, Anthony EJ, Macchi A. CO₂ Capture from Simulated Syngas via Cyclic Carbonation/Calcination for a Naturally Occurring Limestone: Pilot-Plant Testing. *Ind. Eng. Chem. Res.* 2009;48:8431–40, doi:10.1021/ie900645x.
- [20] Yang S, Xiao Y. Steam Catalysis in CaO Carbonation under Low Steam Partial Pressure. *Ind. Eng. Chem. Res.* 2008;47:4043–8, doi:10.1021/ie8000265.
- [21] Sun P, Grace JR, Lim CJ, Anthony EJ. Investigation of Attempts to Improve Cyclic CO₂ Capture by Sorbent Hydration and Modification. *Ind. Eng. Chem. Res.* 2008;47:2024–32, doi:10.1021/ie070335q.
- [22] Martínez I, Grasa G, Parkkinen J, Tynjälä T, Hyppänen T, Murillo R, Romano MC. Review and research needs of Ca-Looping systems modelling for post-combustion CO₂ capture applications. *International Journal of Greenhouse Gas Control* 2016;50:271–304, doi:10.1016/j.ijggc.2016.04.002.

APPENDIX

A PROCESS OPERATION

In this section additional information/graphs corresponding to the operation of USTUTT's Calcium Looping pilot facility are given.

A.1 Hydrodynamics

In this section additional information about the hydrodynamics are presented for (i) different make-up flows (Figure 5.1 to Figure 5.4) of sorbent and (ii) different CO₂ concentrations (Figure 5.5 to Figure 5.8):

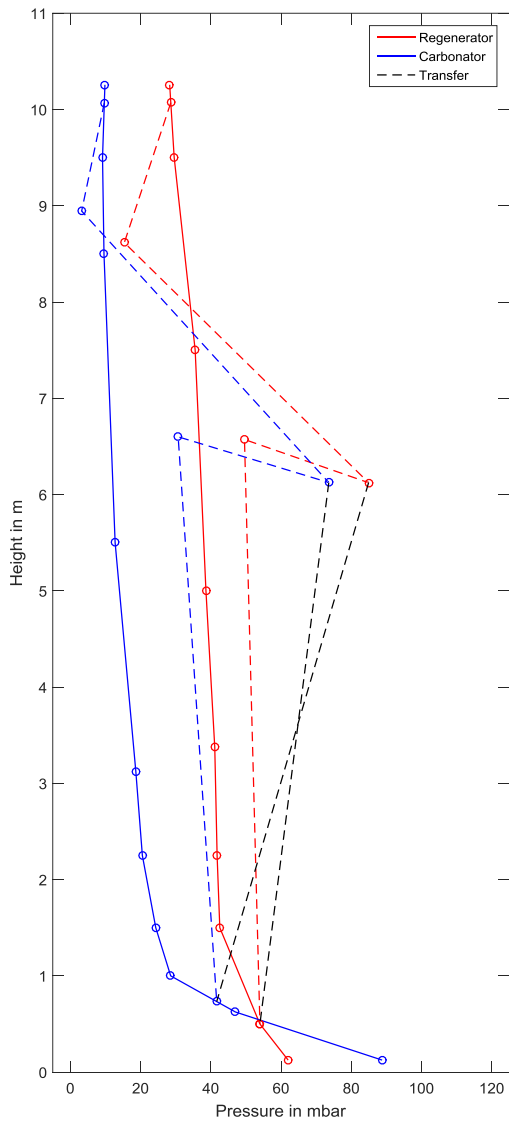


Figure 5.1 Hydrodynamic profile for a make-up flow of 50 kg/h.

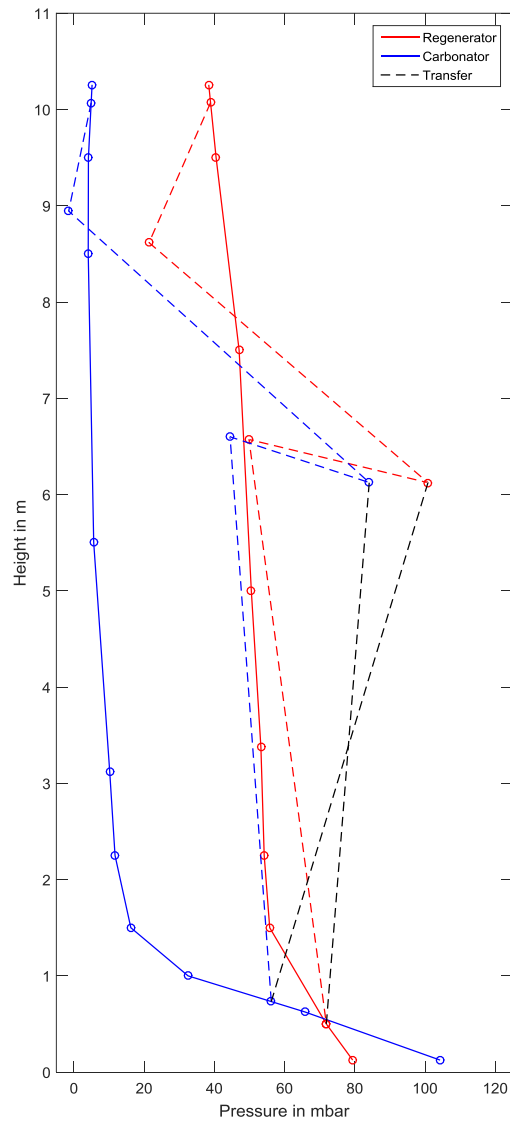


Figure 5.2 Hydrodynamic profile for a make-up flow of 40 kg/h.

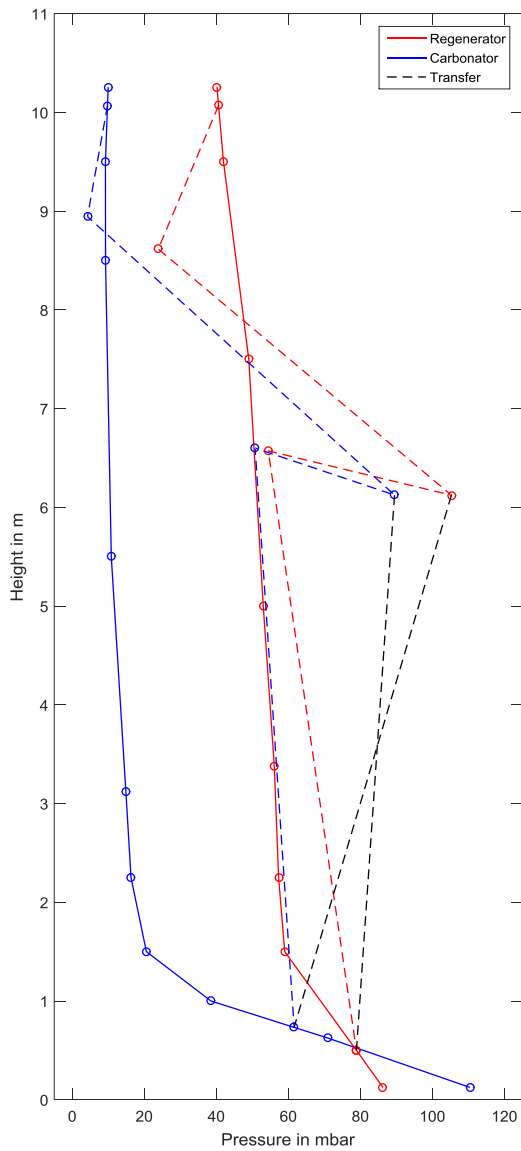


Figure 5.3 Hydrodynamic profile for a make-up flow of 30 kg/h.

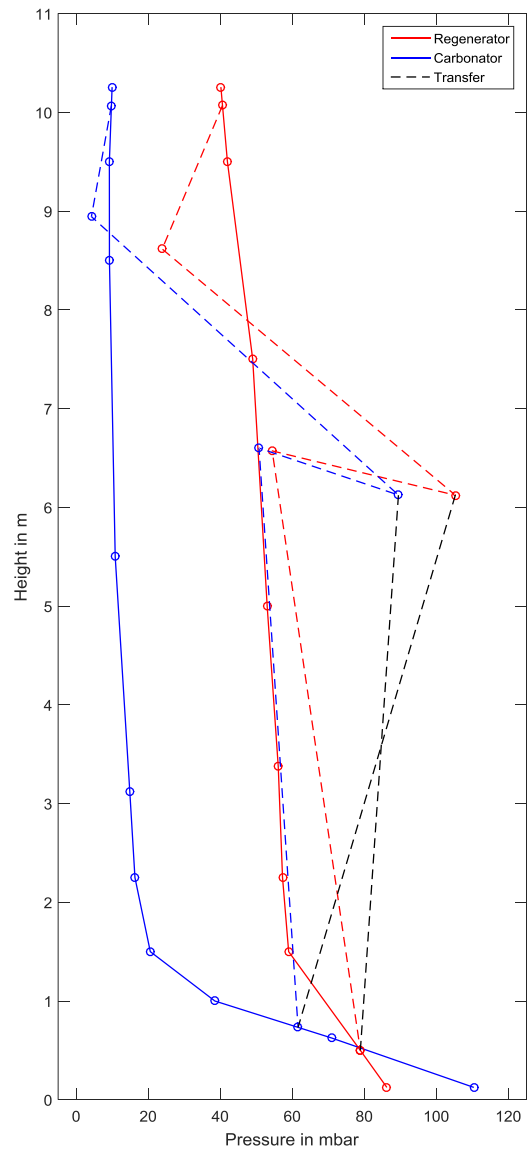


Figure 5.4 Hydrodynamic profile for a make-up flow of 15 kg/h.

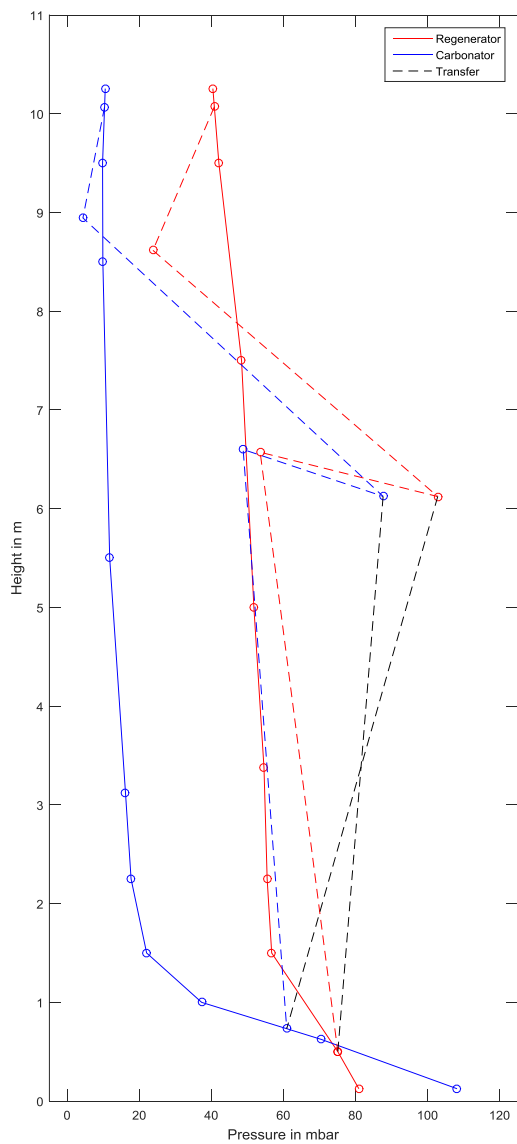


Figure 5.5 Hydrodynamic profile for a CO₂ concentration of 20 vol%.

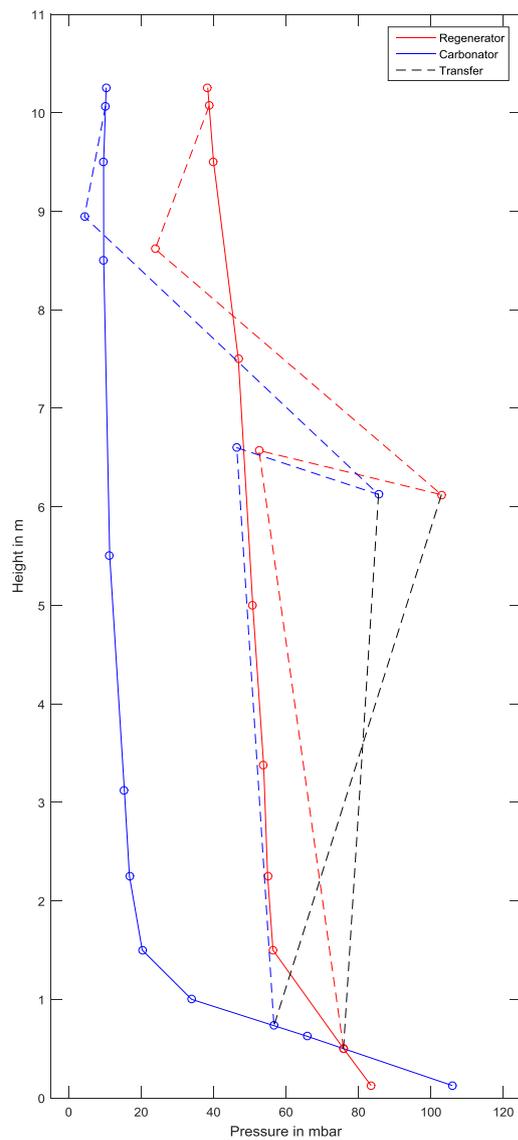


Figure 5.6 Hydrodynamic profile for a CO₂ concentration of 25 vol%.

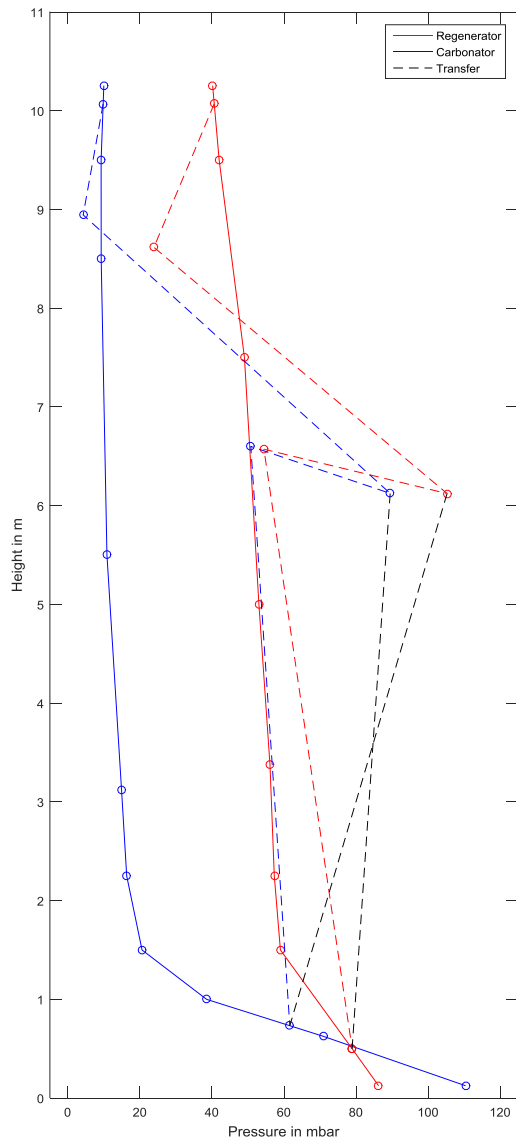


Figure 5.7 Hydrodynamic profile for a CO₂ concentration of 30 vol%.

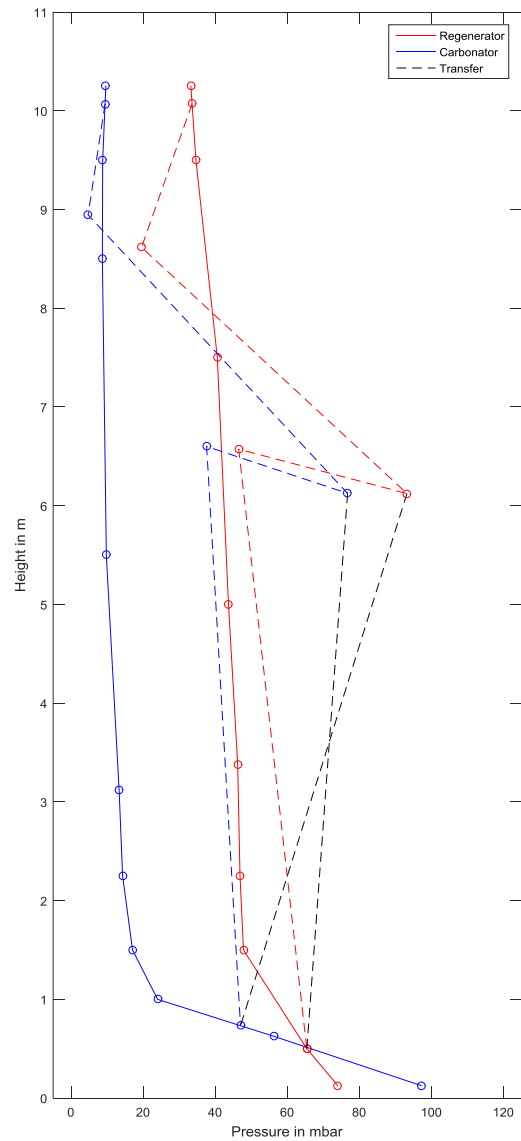


Figure 5.8 Hydrodynamic profile for a CO₂ concentration of 35 vol%.

B THERMOGRAVIMETRIC ANALYSIS (TGA) AT UNIVERSITY OF STUTTGART

The solid samples taken during the experimental campaigns were analysed using a modified TGA based on Linseis model “STA PT1600. An inductive heating was installed to realize high heating rates. The measured signal was corrected by a zero measurement in order to minimized buoyant effects. All samples were calcined under N₂ atmosphere at 850 °C for 10 minutes to ensure full calcination of the sample and then carbonated under an CO₂ atmosphere with 15 vol.% of CO₂. In Figure 5.9a zero or blank measurement is shown and in Figure 5.10 a sample measurement. While the sorbent capacity in kg_{CO2}/kg_{Sorbent} can be directly assessed form TGA analysis. Lab analysis (TIC, TOC, elemental analysis) are required to assess the molar conversion or molar sorbent CO₂ carrying capacity.

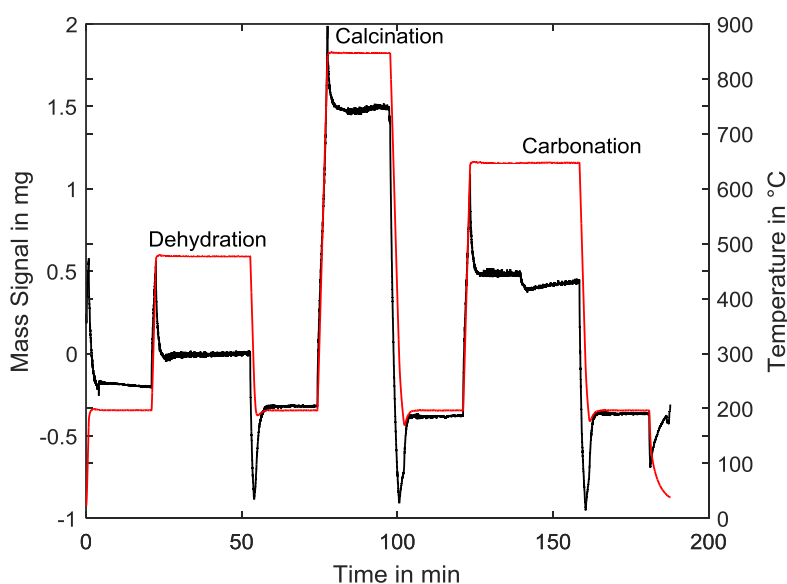


Figure 5.9 Zero measurement of for correction of sample analysis

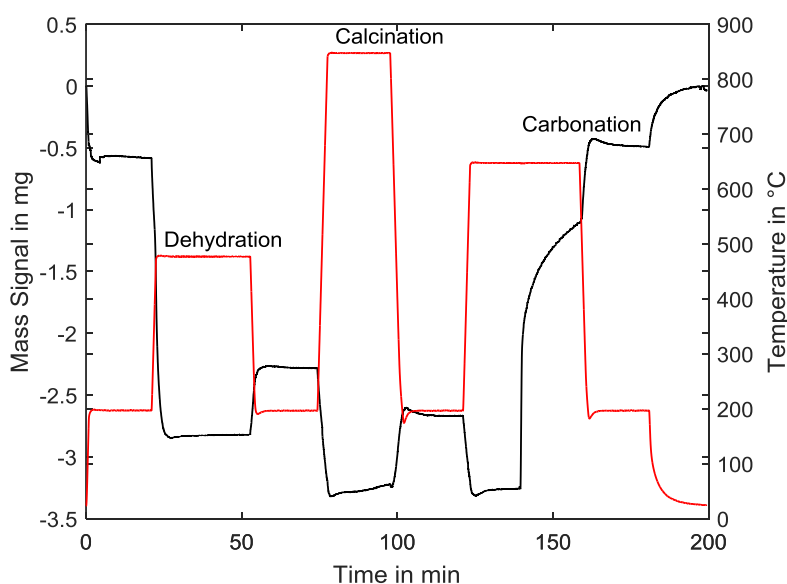


Figure 5.10 Sample analysis using inductive heated TGA STA PT 1600

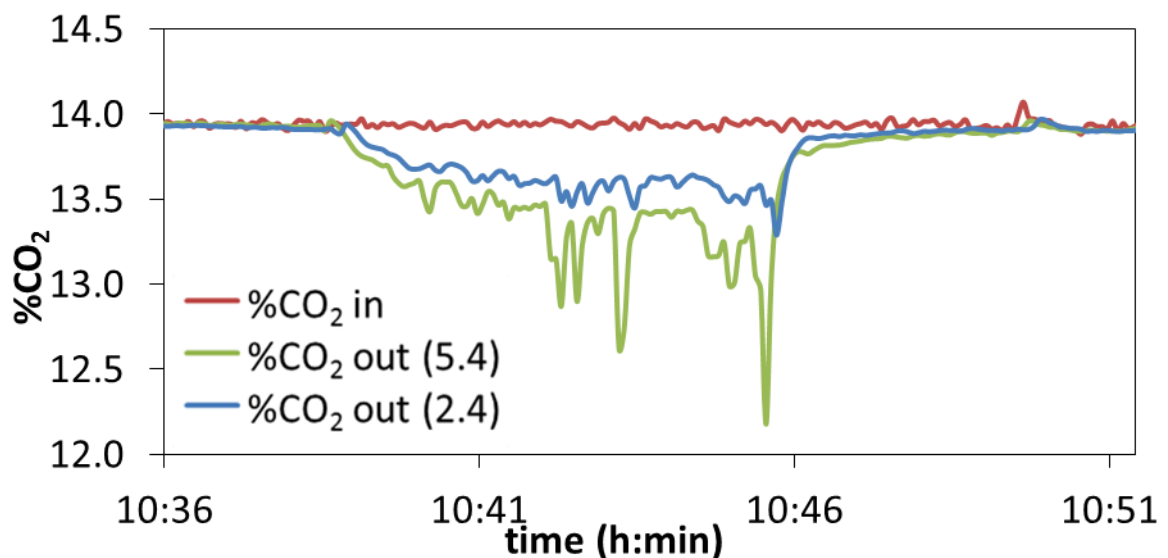
C EXPERIMENTAL CAMPAIGNS IN THE ENTRAINED ‘DOWN-FLOW’ REACTOR

C.1 Campaign 1: entrained ‘down-flow’ testing using the drain-tube solid feeding system and different calcined limestones and raw meals as sorbents: study of the CO₂ carrying capacity influence.

The objective of this campaign was to study the influence of the activity of the sorbent on the CO₂ capture. The CO₂ concentration was measured at 2.4 and 5.4 m from the injection point by using two analyzers. In this campaign, four additional sorbents with different CO₂ carrying capacities were tested in order to increase the data base of experimental results and study the influence X_{ave} on the particle reaction rate. All experiments were carried out under a reaction atmosphere of 15% v CO₂, settling the gas velocity at around 0.9 m/s and keeping the temperature constant at around 650°C.

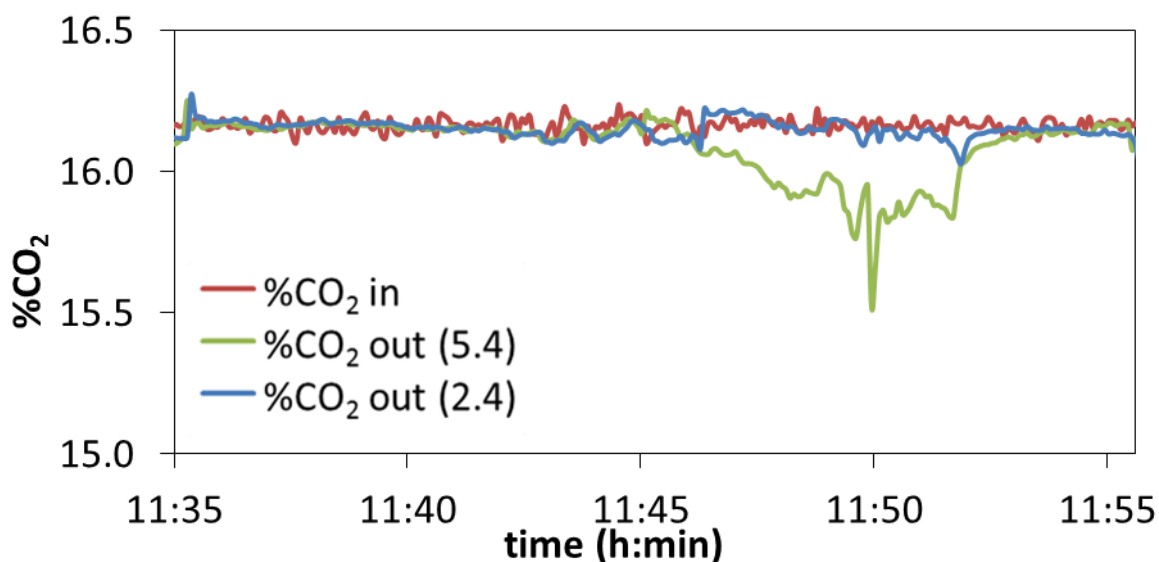
Experiment 1

| | |
|------------------------------------|------|
| Solid fed | CaO |
| X_{ave} | 0.32 |
| T (°C) | 643 |
| u_{gas} (m/s) | 0.96 |
| %CO ₂ in | 13.9 |
| Solid flow (kg/h) | 2.4 |
| Total gas flow (m ³ /h) | 8.1 |
| H ₂ O (vol%) | 0.0 |



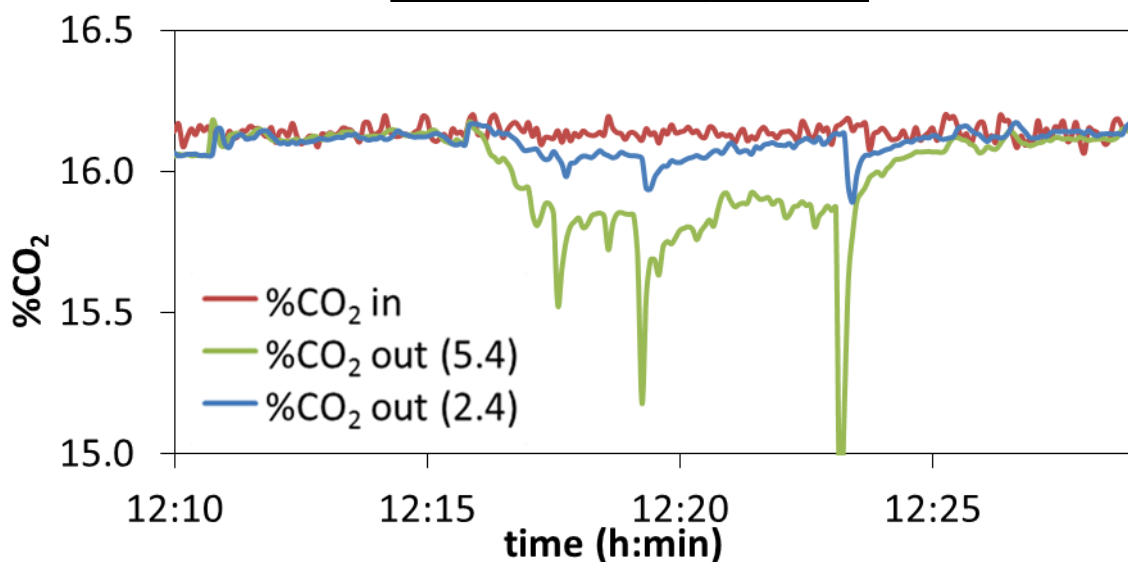
Experiment 2

| | |
|------------------------------------|------|
| Solid fed | CaO |
| X_{ave} | 0.17 |
| T (°C) | 644 |
| u_{gas} (m/s) | 0.88 |
| %CO ₂ in | 16.2 |
| Solid flow (kg/h) | 1.7 |
| Total gas flow (m ³ /h) | 7.4 |
| H ₂ O (vol%) | 0.0 |



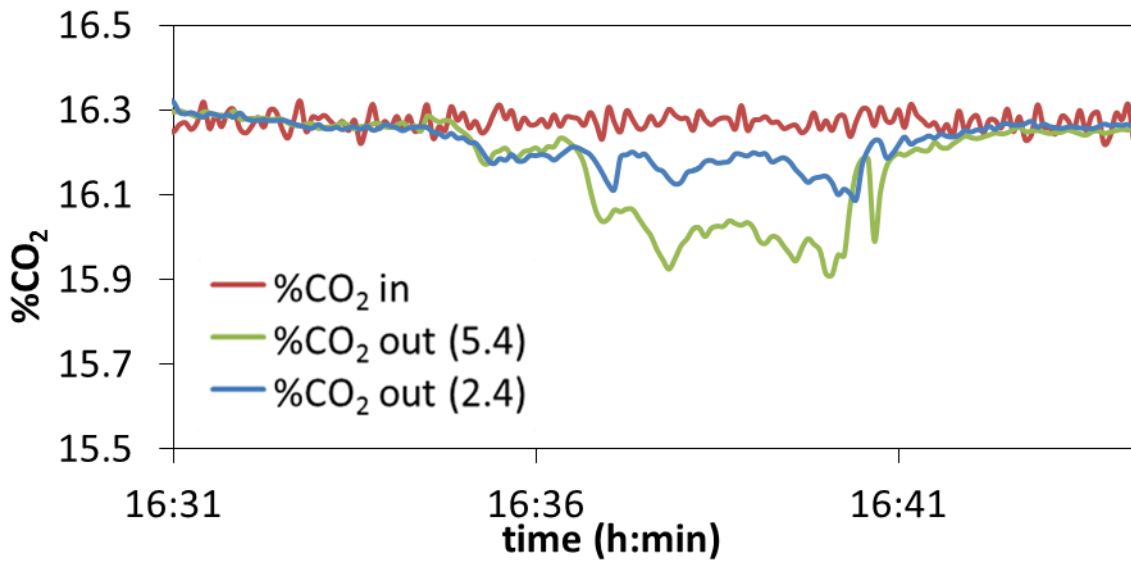
Experiment 3

| | |
|------------------------------------|------|
| Solid fed | CaO |
| Xave | 0.17 |
| T (°C) | 647 |
| u_{gas} (m/s) | 0.88 |
| %CO ₂ in | 16.1 |
| Solid flow (kg/h) | 1.9 |
| Total gas flow (m ³ /h) | 7.4 |
| H ₂ O (vol%) | 0.0 |



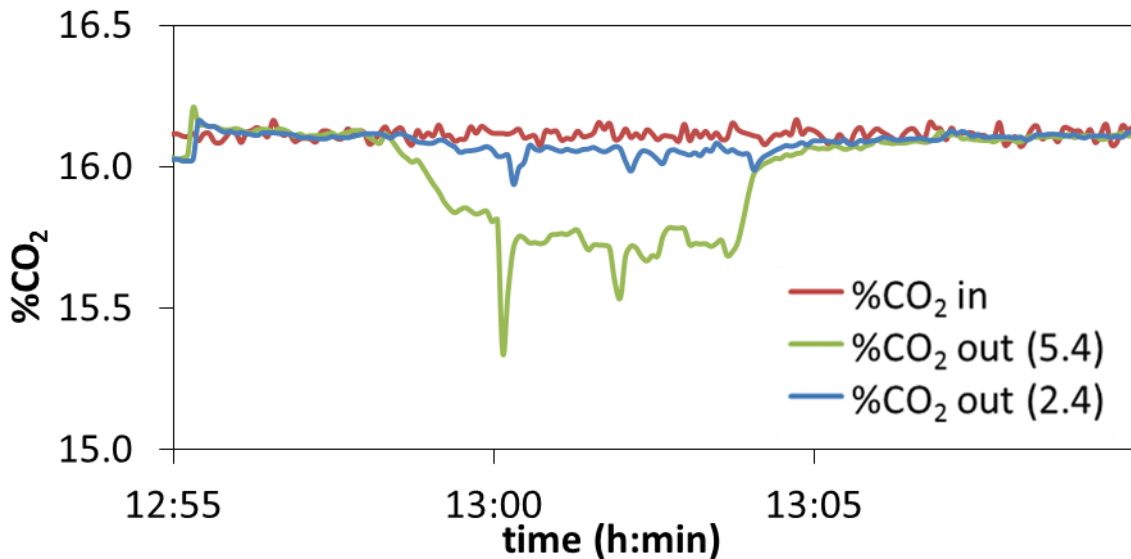
Experiment 4

| | |
|------------------------------------|------|
| Solid fed | CaO |
| Xave | 0.17 |
| T (°C) | 652 |
| u_{gas} (m/s) | 0.90 |
| %CO ₂ in | 16.3 |
| Solid flow (kg/h) | 1.6 |
| Total gas flow (m ³ /h) | 7.5 |
| H ₂ O (vol%) | 0.0 |



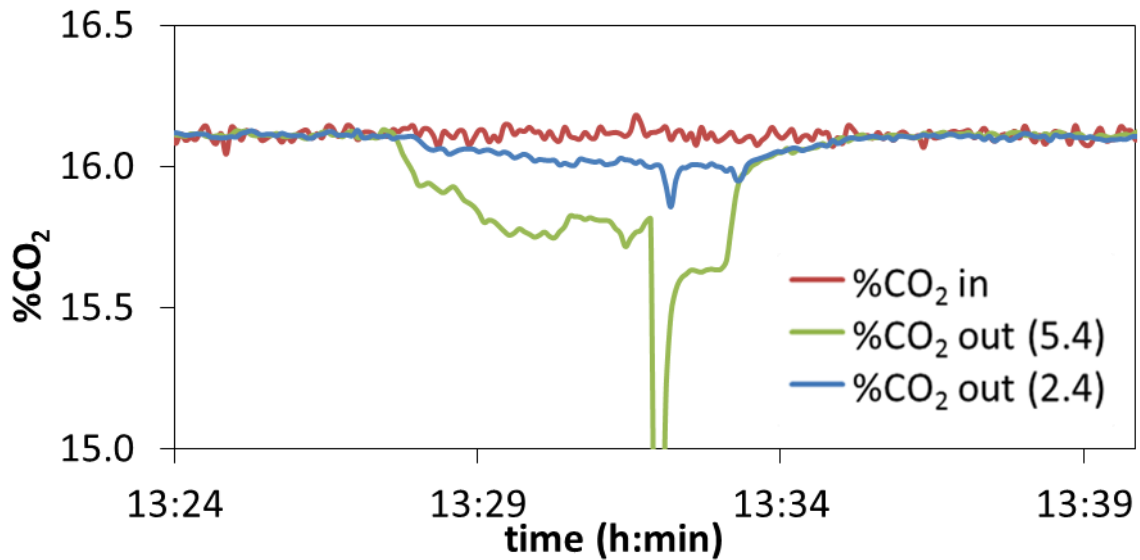
Experiment 5

| Solid fed | Raw meal |
|------------------------------------|----------|
| Xave | 0.19 |
| T (°C) | 652 |
| u_{gas} (m/s) | 0.88 |
| %CO ₂ in | 16.1 |
| Solid flow (kg/h) | 2.0 |
| Total gas flow (m ³ /h) | 7.4 |
| H ₂ O (vol%) | 0.0 |



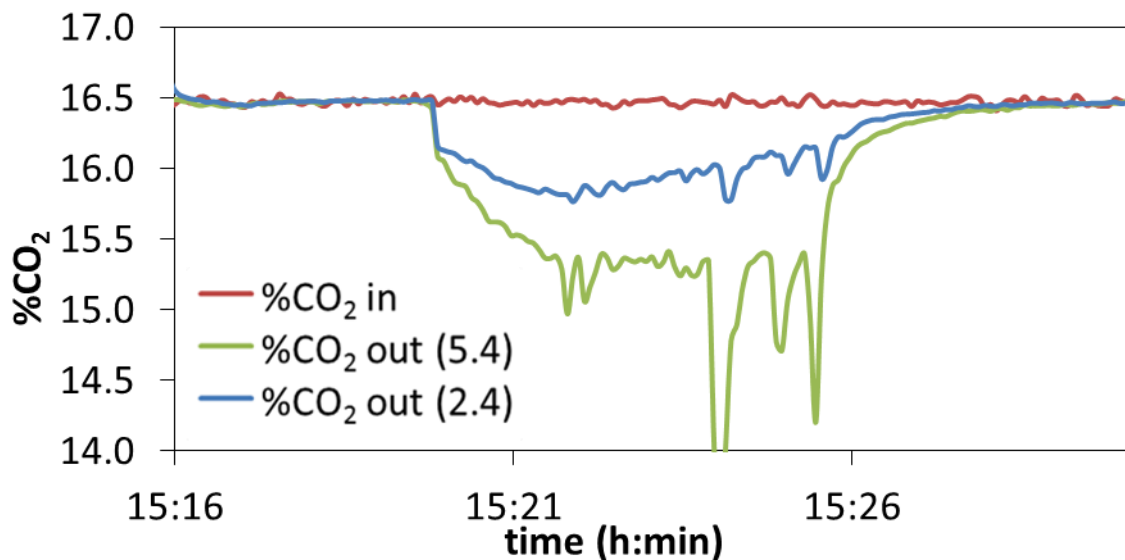
Experiment 6

| Solid fed | Raw meal |
|------------------------------------|----------|
| Xave | 0.19 |
| T (°C) | 652 |
| u_{gas} (m/s) | 0.88 |
| %CO ₂ in | 16.1 |
| Solid flow (kg/h) | 2.3 |
| Total gas flow (m ³ /h) | 7.3 |
| H ₂ O (vol%) | 0.0 |



Experiment 7

| | |
|------------------------------------|------|
| Solid fed | CaO |
| X _{ave} | 0.67 |
| T (°C) | 654 |
| u _{gas} (m/s) | 0.88 |
| %CO ₂ in | 16.5 |
| Solid flow (kg/h) | 2.0 |
| Total gas flow (m ³ /h) | 7.4 |
| H ₂ O (vol%) | 0.0 |



C.2 Campaign 2: entrained ‘down-flow’ testing using the drain-tube solid feeding system and calcined limestone as a sorbent: study of the water vapor influence.

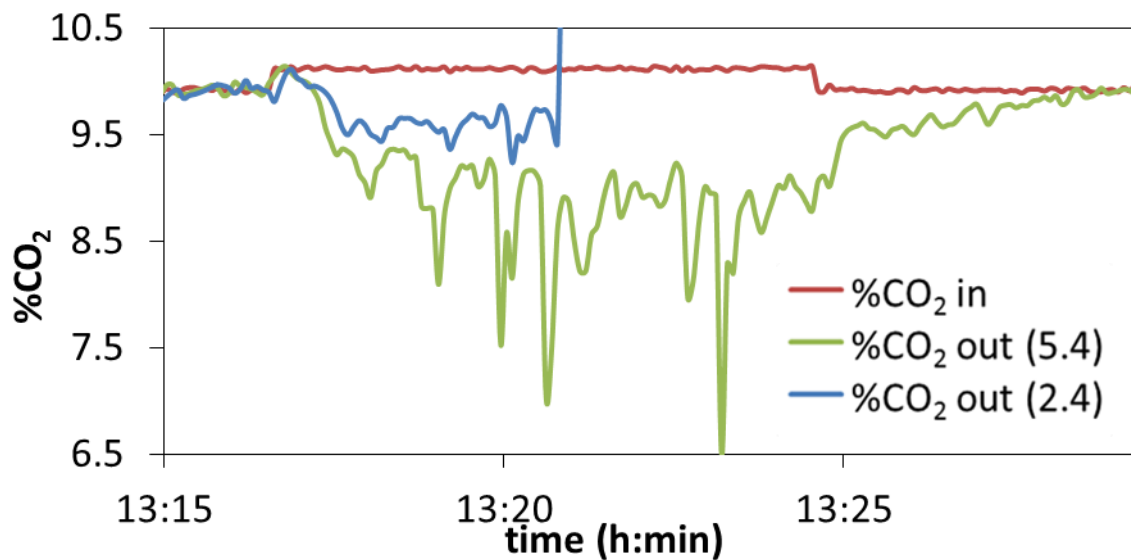
The objective of this campaign was to carry out more carbonation experiments with the presence of water vapor in the reaction atmosphere to complete the information assembled in previous campaigns and study the influence of steam on the CO₂ capture. The reactors set up and the solid feeding system, are the ones used in the previous campaign. The steam was injected in

the bottom of the gas pre-heater reactor and carried together with the CO₂ and air to the top of the carbonator reactor. The CO₂ concentration was measured at 2.4 and 5.4 m from the injection point by using two analyzers. There were some problems in experiments 3-5 with the gas sampling drying system (necessary to protect the analyzer from moisture) of the analyzer measuring at 2.4m and therefore, only the measurement at 5.4m was possible to be made.

The two sorbents used were calcined limestone with 0.32 and 0.42 of CO₂ carrying capacity, respectively. All experiments were carried out at a fixed CO₂ concentration of 15%v, while the H₂O concentration ranged from 23 to 27%v. The gas velocity was set at 1m/s and the temperature was kept constant at around 650°C.

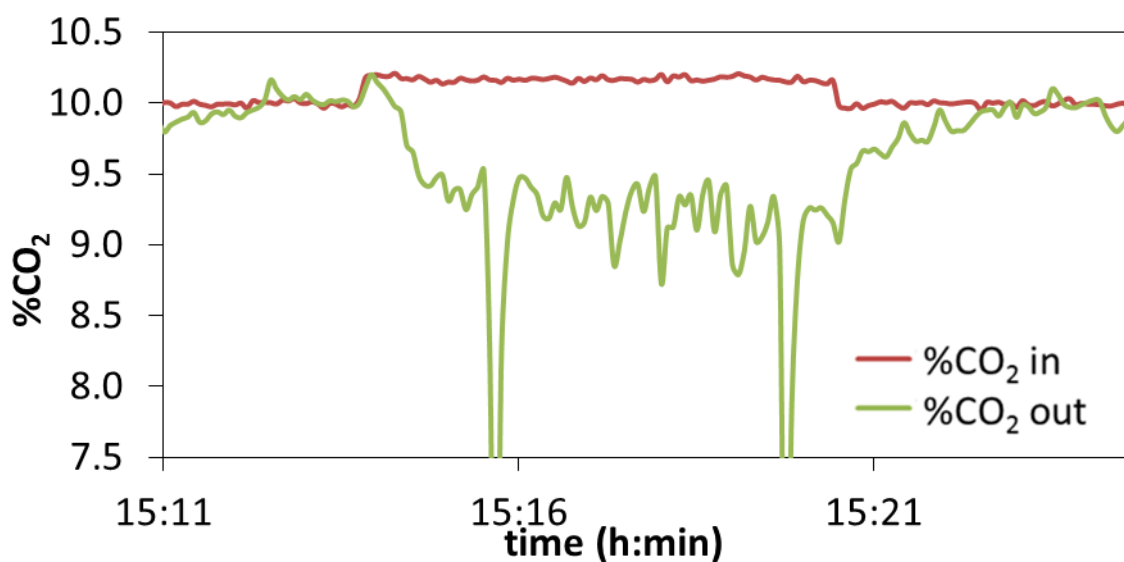
Experiment 1

| | |
|------------------------------------|------|
| Solid fed | CaO |
| Xave | 0.32 |
| T (°C) | 656 |
| u _{gas} (m/s) | 1.00 |
| %CO ₂ in | 10.1 |
| Solid flow (kg/h) | 2.4 |
| Total gas flow (m ³ /h) | 8.3 |
| H ₂ O (vol%) | 27.0 |



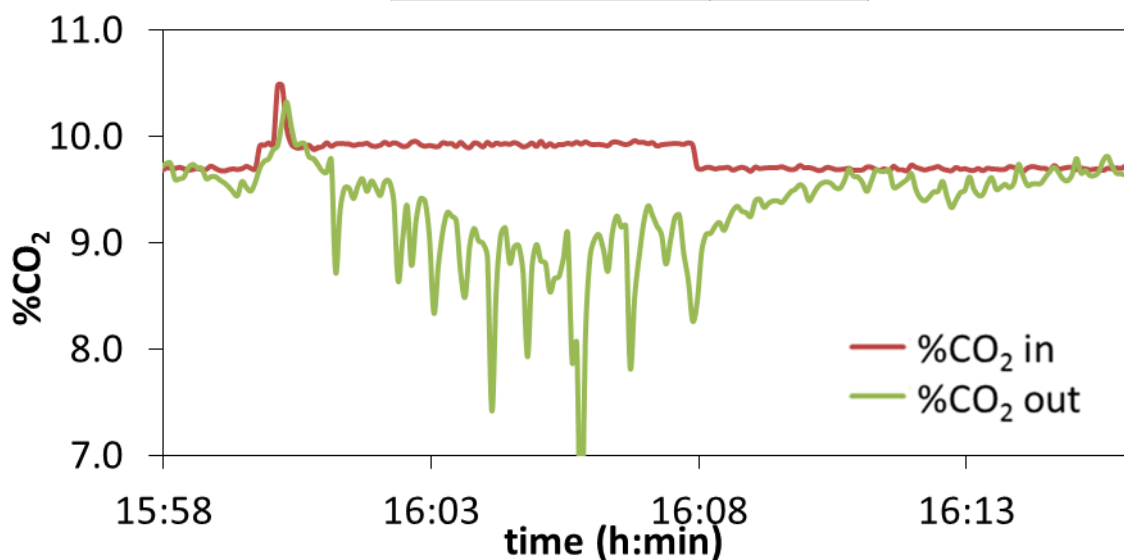
Experiment 2

| | |
|------------------------------------|------|
| Solid fed | CaO |
| Xave | 0.32 |
| T (°C) | 657 |
| u _{gas} (m/s) | 1.01 |
| %CO ₂ in | 10.2 |
| Solid flow (kg/h) | 3.2 |
| Total gas flow (m ³ /h) | 8.4 |
| H ₂ O (vol%) | 26.8 |



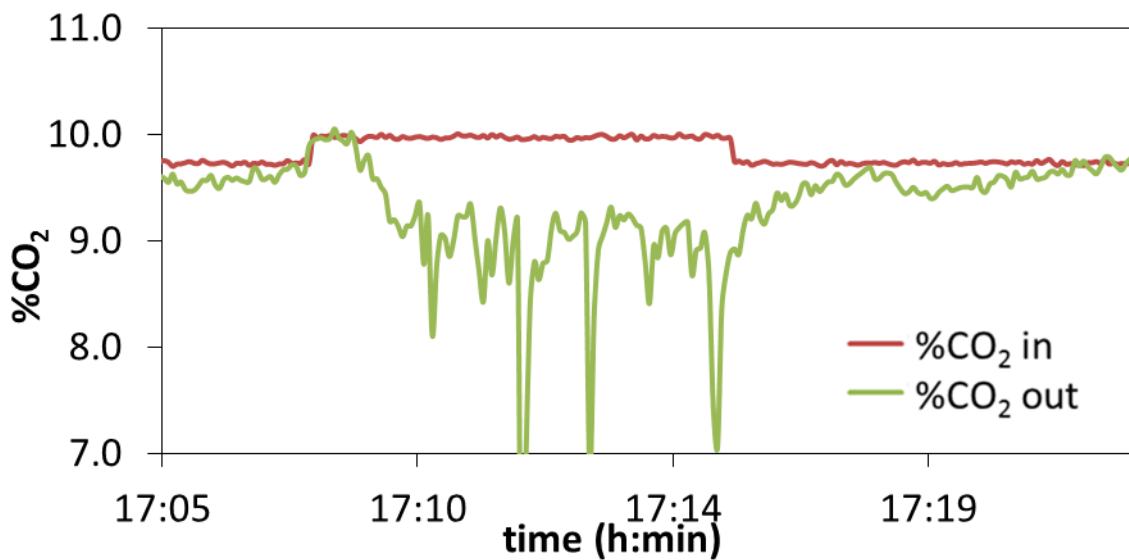
Experiment 3

| | |
|------------------------------------|------|
| Solid fed | CaO |
| Xave | 0.32 |
| T (°C) | 657 |
| u_{gas} (m/s) | 1.03 |
| %CO ₂ in | 9.9 |
| Solid flow (kg/h) | 2.6 |
| Total gas flow (m ³ /h) | 8.6 |
| H ₂ O (vol%) | 26.2 |



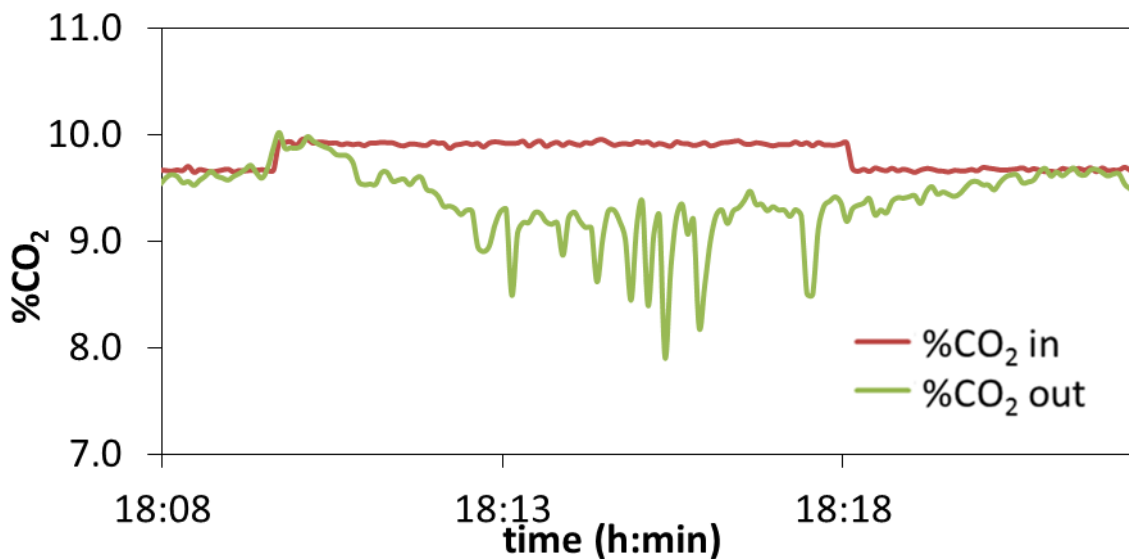
Experiment 4

| | |
|------------------------------------|------|
| Solid fed | CaO |
| Xave | 0.32 |
| T (°C) | 658 |
| u_{gas} (m/s) | 1.03 |
| %CO ₂ in | 10.0 |
| Solid flow (kg/h) | 2.6 |
| Total gas flow (m ³ /h) | 8.5 |
| H ₂ O (vol%) | 26.3 |



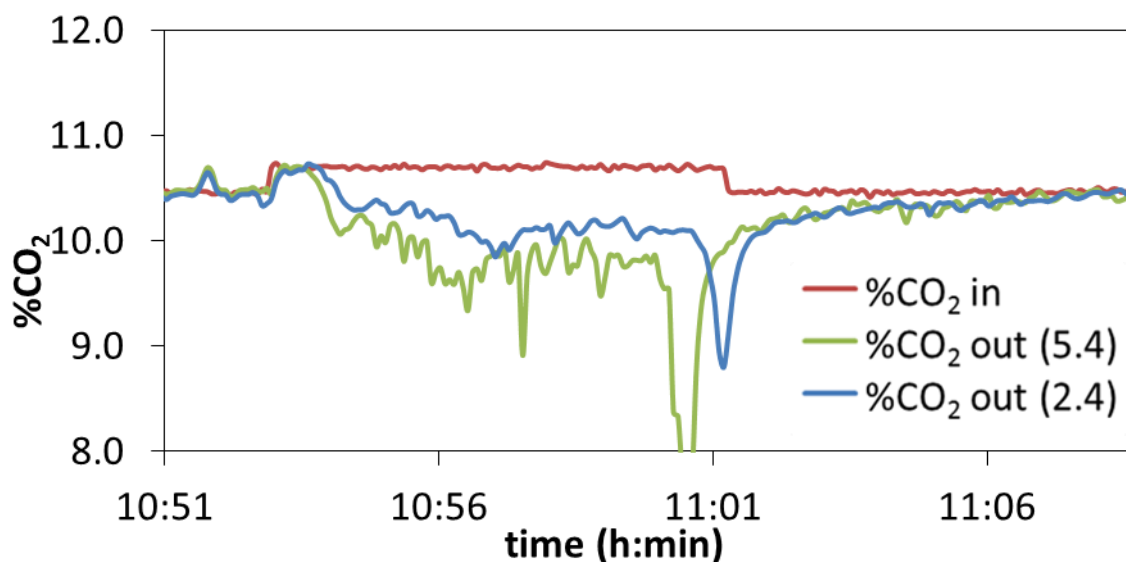
Experiment 5

| | |
|------------------------------------|------|
| Solid fed | CaO |
| Xave | 0.32 |
| T (°C) | 658 |
| u_{gas} (m/s) | 1.03 |
| %CO ₂ in | 9.9 |
| Solid flow (kg/h) | 2.5 |
| Total gas flow (m ³ /h) | 8.5 |
| H ₂ O (vol%) | 26.3 |



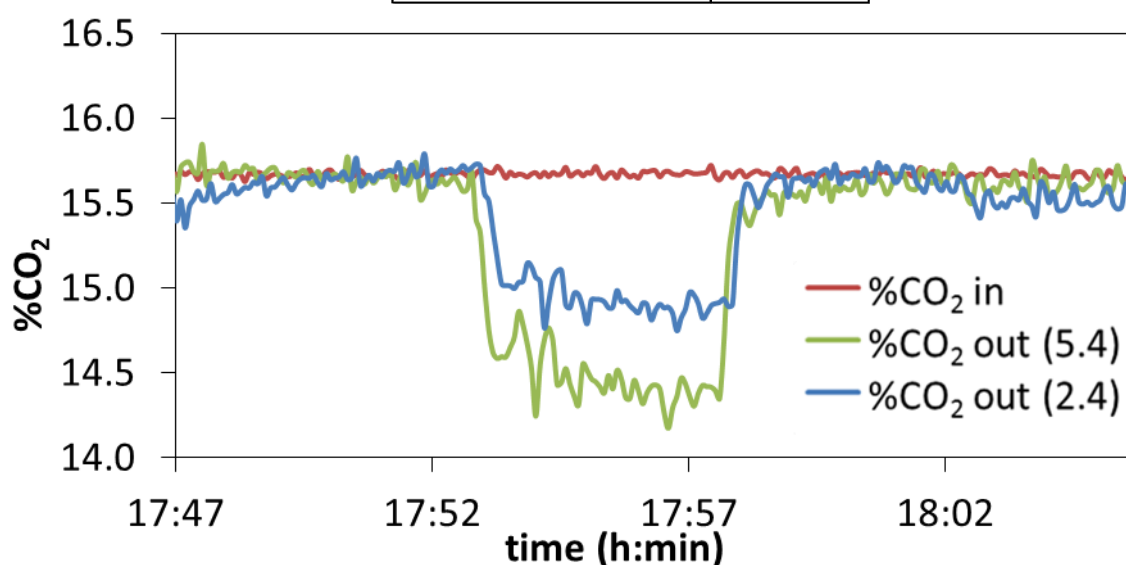
Experiment 6

| | |
|------------------------------------|------|
| Solid fed | CaO |
| Xave | 0.32 |
| T (°C) | 658 |
| u_{gas} (m/s) | 1.03 |
| %CO ₂ in | 10.7 |
| Solid flow (kg/h) | 2.7 |
| Total gas flow (m ³ /h) | 8.6 |
| H ₂ O (vol%) | 26.2 |



Experiment 7

| | |
|------------------------------------|------|
| Solid fed | CaO |
| X _{ave} | 0.42 |
| T (°C) | 655 |
| u _{gas} (m/s) | 1.15 |
| %CO ₂ in | 15.7 |
| Solid flow (kg/h) | 2.7 |
| Total gas flow (m ³ /h) | 9.6 |
| H ₂ O (vol%) | 23.4 |



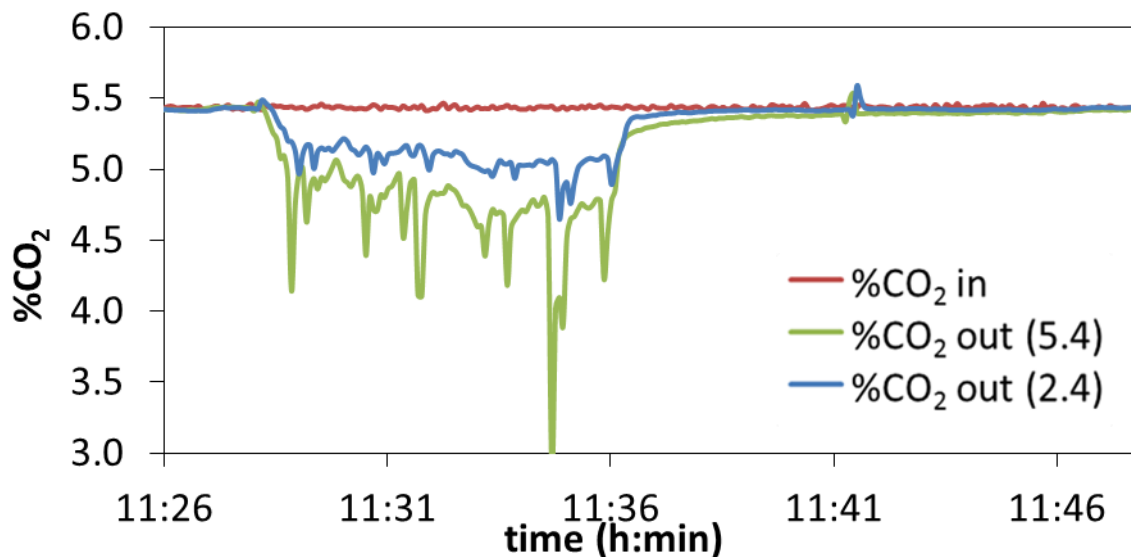
C.3 Campaign 3: entrained ‘down-flow’ testing using the drain-tube solid feeding system and calcined limestone as a sorbent: study of the CO₂ concentration influence.

The objective of this campaign was to extend the number of experiments carried out to study the influence of the CO₂ concentration of the reaction atmosphere. The CO₂ concentration was measured at 2.4 and 5.4 m from the injection point by using two analyzers.

There were made 11 experiments, three using a calcined limestone with a CO₂ carrying capacity of 0.32 and eight more using a calcined limestone with a X_{ave} of 0.42. The gas velocity was set at 0.9 m/s and the temperature was kept constant at around 650°C. The CO₂ concentration varied between 5 and 20%v in order to sweep a wide range of CO₂ concentrations.

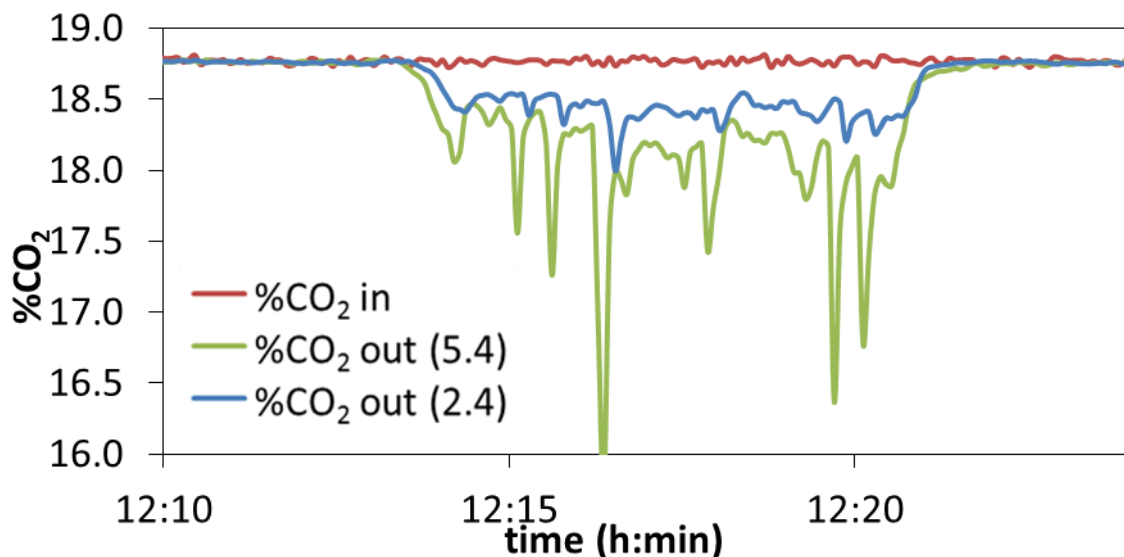
Experiment 1

| | |
|------------------------------------|------|
| Solid fed | CaO |
| X_{ave} | 0.32 |
| T (°C) | 640 |
| u_{gas} (m/s) | 0.98 |
| %CO ₂ in | 5.4 |
| Solid flow (kg/h) | 2.7 |
| Total gas flow (m ³ /h) | 8.3 |
| H ₂ O (vol%) | 0.0 |



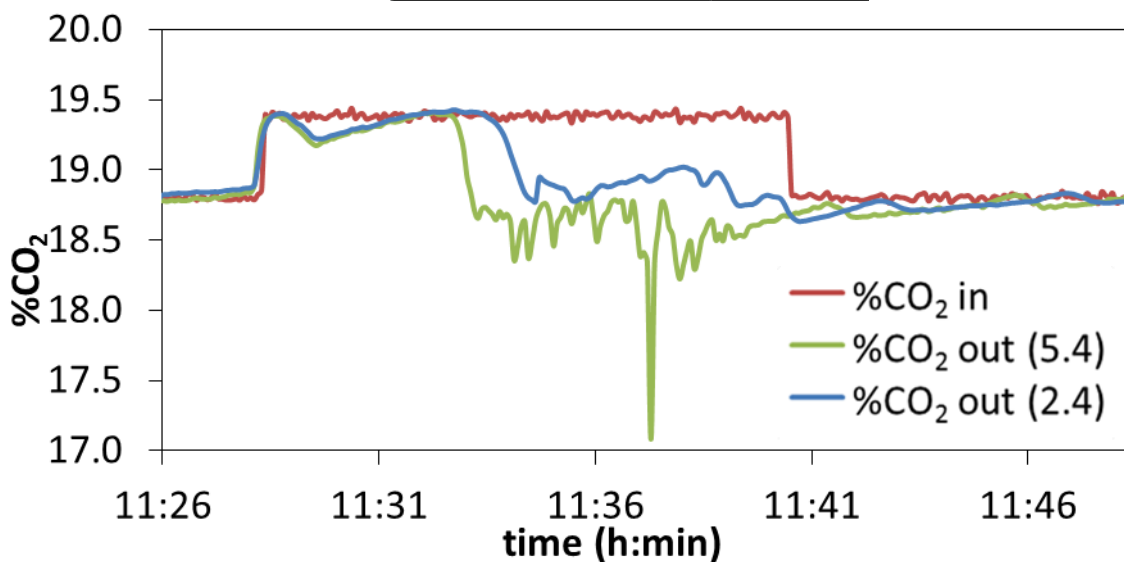
Experiment 2

| | |
|------------------------------------|------|
| Solid fed | CaO |
| Xave | 0.32 |
| T (°C) | 640 |
| u_{gas} (m/s) | 0.99 |
| %CO ₂ in | 18.8 |
| Solid flow (kg/h) | 2.5 |
| Total gas flow (m ³ /h) | 8.3 |
| H ₂ O (vol%) | 0.0 |



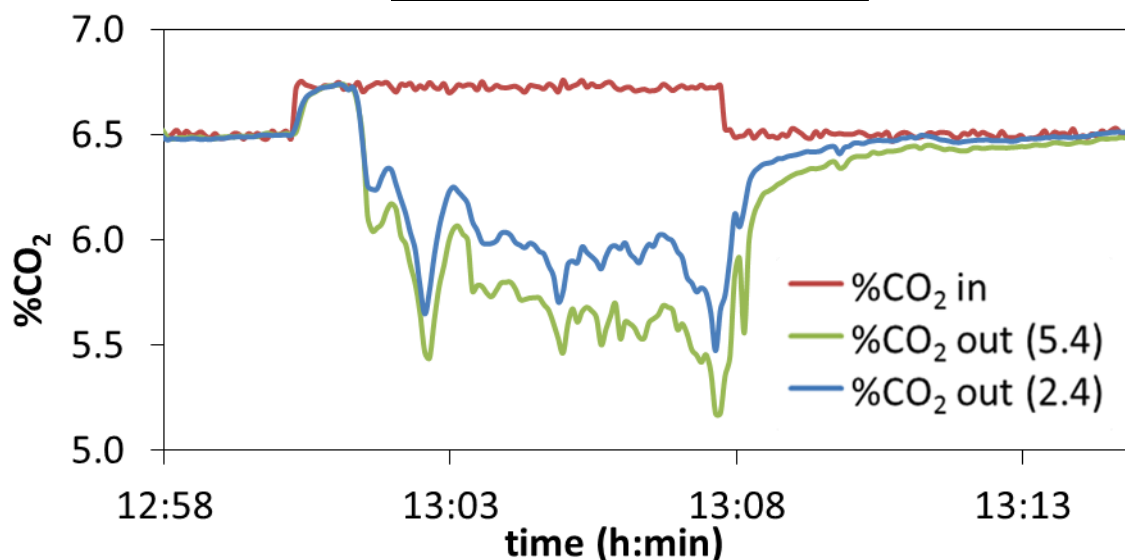
Experiment 3

| | |
|------------------------------------|------|
| Solid fed | CaO |
| Xave | 0.32 |
| T (°C) | 653 |
| u_{gas} (m/s) | 0.96 |
| %CO ₂ in | 19.4 |
| Solid flow (kg/h) | 2.6 |
| Total gas flow (m ³ /h) | 8.0 |
| H ₂ O (vol%) | 0.0 |



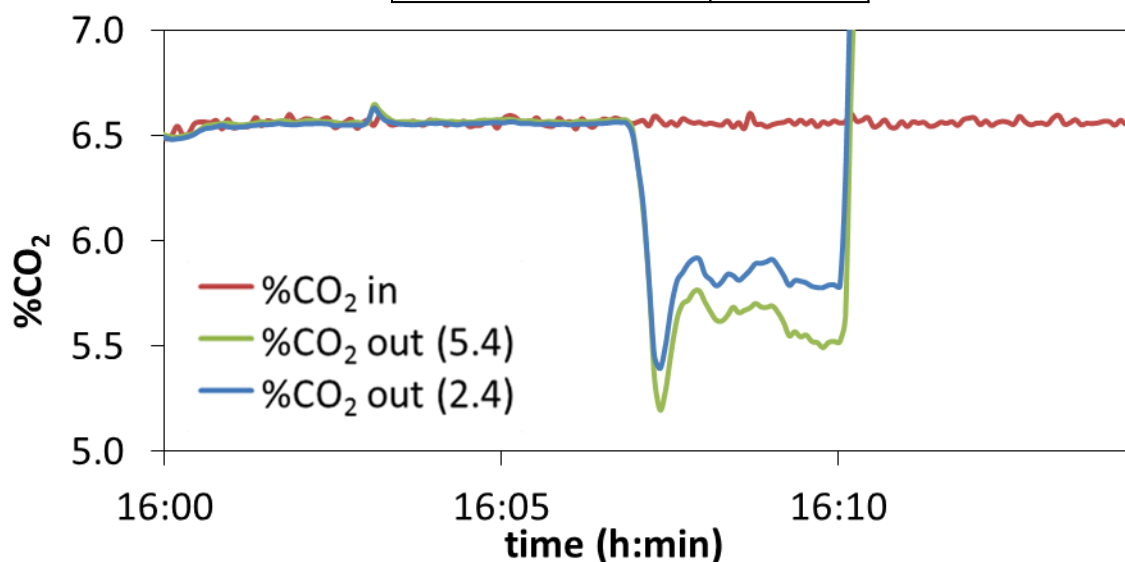
Experiment 4

| | |
|------------------------------------|------|
| Solid fed | CaO |
| Xave | 0.42 |
| T (°C) | 663 |
| u_{gas} (m/s) | 0.84 |
| %CO ₂ in | 6.7 |
| Solid flow (kg/h) | 3.1 |
| Total gas flow (m ³ /h) | 6.9 |
| H ₂ O (vol%) | 0.0 |



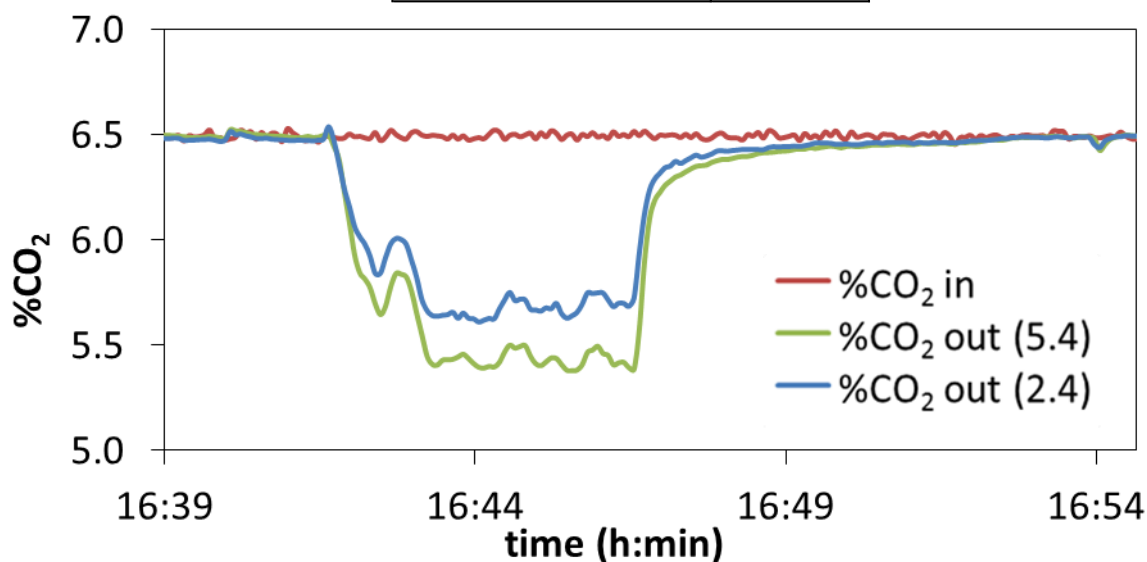
Experiment 5

| | |
|------------------------------------|------|
| Solid fed | CaO |
| Xave | 0.42 |
| T (°C) | 663 |
| u_{gas} (m/s) | 0.86 |
| %CO ₂ in | 6.6 |
| Solid flow (kg/h) | 3.9 |
| Total gas flow (m ³ /h) | 7.1 |
| H ₂ O (vol%) | 0.0 |



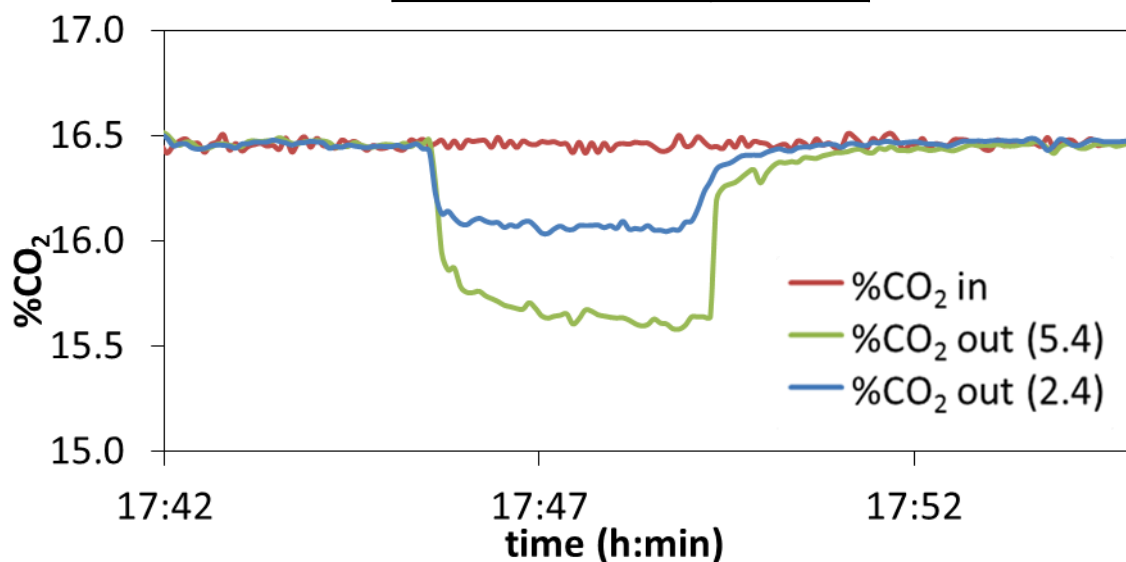
Experiment 6

| | |
|------------------------------------|------|
| Solid fed | CaO |
| Xave | 0.42 |
| T (°C) | 662 |
| u_{gas} (m/s) | 0.87 |
| %CO ₂ in | 6.5 |
| Solid flow (kg/h) | 2.9 |
| Total gas flow (m ³ /h) | 7.1 |
| H ₂ O (vol%) | 0.0 |



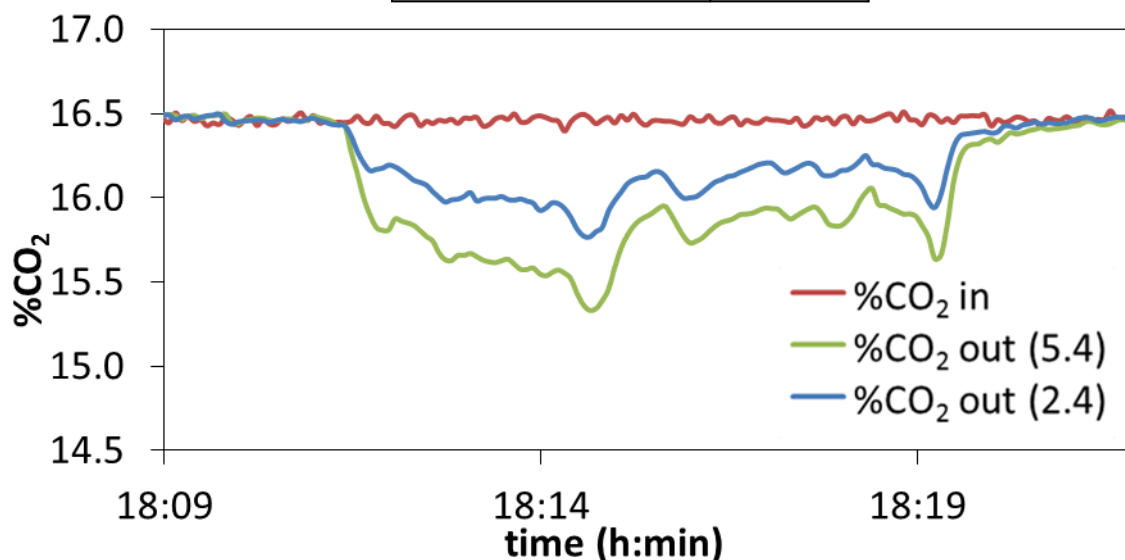
Experiment 7

| | |
|------------------------------------|------|
| Solid fed | CaO |
| Xave | 0.42 |
| T (°C) | 662 |
| u_{gas} (m/s) | 0.87 |
| %CO ₂ in | 16.5 |
| Solid flow (kg/h) | 3.4 |
| Total gas flow (m ³ /h) | 7.2 |
| H ₂ O (vol%) | 0.0 |



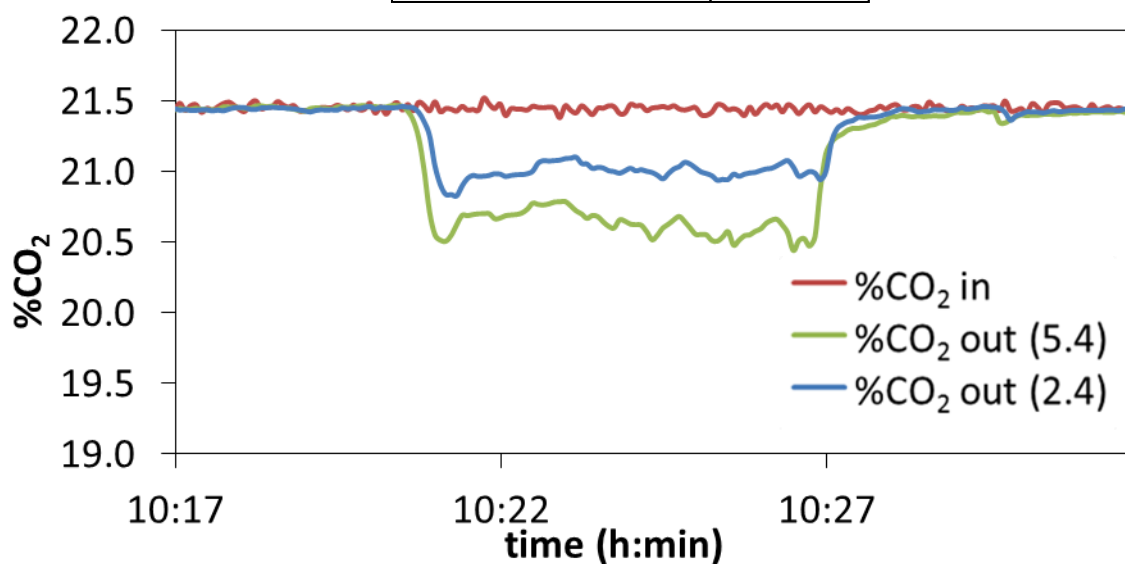
Experiment 8

| | |
|------------------------------------|------|
| Solid fed | CaO |
| Xave | 0.42 |
| T (°C) | 662 |
| u_{gas} (m/s) | 0.87 |
| %CO ₂ in | 16.5 |
| Solid flow (kg/h) | 2.2 |
| Total gas flow (m ³ /h) | 7.2 |
| H ₂ O (vol%) | 0.0 |



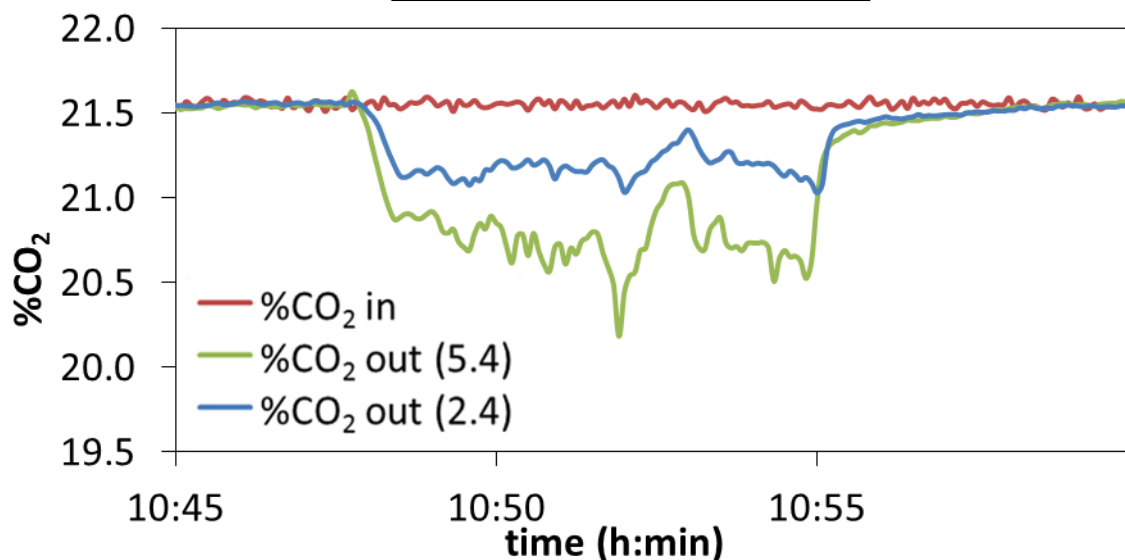
Experiment 9

| | |
|------------------------------------|------|
| Solid fed | CaO |
| Xave | 0.42 |
| T (°C) | 646 |
| u_{gas} (m/s) | 0.98 |
| %CO ₂ in | 21.5 |
| Solid flow (kg/h) | 2.9 |
| Total gas flow (m ³ /h) | 8.2 |
| H ₂ O (vol%) | 0.0 |



Experiment 10

| | |
|------------------------------------|------|
| Solid fed | CaO |
| X _{ave} | 0.42 |
| T (°C) | 641 |
| u _{gas} (m/s) | 0.98 |
| %CO ₂ in | 21.5 |
| Solid flow (kg/h) | 3.0 |
| Total gas flow (m ³ /h) | 8.2 |
| H ₂ O (vol%) | 0.0 |



Experiment 11

| | |
|------------------------------------|------|
| Solid fed | CaO |
| X _{ave} | 0.42 |
| T (°C) | 654 |
| u _{gas} (m/s) | 0.76 |
| %CO ₂ in | 21.3 |
| Solid flow (kg/h) | 3.1 |
| Total gas flow (m ³ /h) | 6.3 |
| H ₂ O (vol%) | 0.0 |

